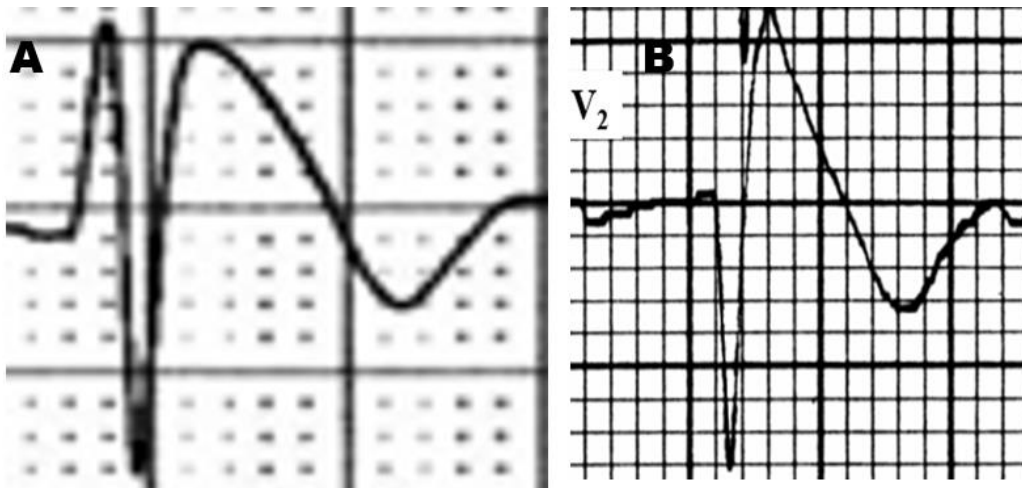


## Brugada Syndrome

The definition of the diagnosis of Brugada syndrome (BrS) has undergone a number of modifications over the years. The ECG hallmark, that is, coved type  $\geq 2$  mm ST-segment elevation followed by negative T-wave in the right precordial leads, has been key for the diagnosis in all consensus documents. However, the number of required positive leads, the position of the leads (2nd, 3rd, or 4th intercostal space) and the circumstances under which the ECG sign is evident, has changed over time.

A consensus was reached exclusively on the ECG aspects of BrS. In the new ECG criteria, only 2 ECG patterns were considered: pattern 1 that is identical to the classic type 1 (Figure 5) of the previous consensus document (coved pattern), and pattern 2 that combines patterns 2 and 3 of the previous consensus (saddleback pattern).<sup>1</sup>



**Figure.X Type 1 Brugada pattern.** J point and ST elevation  $\geq 2$  mm, with upper convexity (A) or descending oblique rectilinear (B), followed by symmetric negative T wave in the right precordial leads (V1-V2 or from V1 through V3) and/or high right precordial leads V<sub>1H</sub>, V<sub>2H</sub> and V<sub>3H</sub>.

### ECG characteristics of the type 2 Brugada pattern

The typical type 2 Brugada pattern presents saddleback appearance, which raises the suspicion of BrS, but the diagnosis depends on the type 1 pattern arising with a drug challenge. The type 2 Brugada pattern is characterized by a J point and ST segment elevation  $\geq 2$  mm (0.2 mV) with saddleback appearance, and remains at least 1 mm above the isoelectric line, followed by positive or biphasic T wave. Sometimes, J point and ST segment elevation  $< 1$  mm and with variable shape: whether coved type or saddleback appearance. The terminal section of the ST segment never exceeds 1 mm above the

isoelectric line. Following Bayés de Luna et al consensus about the ECG in the Brugada syndrome type 2 and 3 patterns are characterized by the same general shape. The high take-off ( $r'$ ) is  $\geq 2$  mm related the isoelectric line and is followed by ST elevation; concave to the top with elevation  $\geq 0.05$  mV with positive/flat T wave in V2 and T wave variable in V1. If there is some doubt, it is necessary to record the ECG in 2nd, 3rd intercostal space.<sup>1</sup>

### **Clues to differentiate Type 2 Brugada pattern from “innocent” or ordinary incomplete right bundle branch block (IRBBB)**

Differentiation of Type 2 Brugada Pattern (BP) from incomplete right bundle branch block (IRBBB) or normal triphasic pattern ( $rSr'$ ) in the right precordial leads can be a challenge. Additionally, an  $rSr'$  pattern in leads V1-V2 can be observed when ECG leads are placed in the 2<sup>nd</sup> intercostal space. Peritz et al used high lead ECGs associated with three new criteria to differentiate potential Brugada from  $rSr'$ . These accurately identified  $rSr'$  patterns V1-V2 from potential Brugada Type 2 patterns in patients with purposely placed high precordial leads.<sup>2</sup> Ohkubo et al<sup>3</sup> and Chevallier et al<sup>4</sup> described using the  $\beta$  angle, formed by the angle between the upslope of the S wave and the downslope of the  $r'$  wave, to distinguish between ordinary or “innocent” RBBB from Type 2 Br pattern. In the Chevallier research, a  $\beta$  angle cut off of  $58^\circ$  yielded a positive predictive value of 73%. Table x

The main ECG clue for the diagnosis is the angle formed by the ascending and descending ramp of the final  $r'/R'$  wave in leads V1-V2 of the QRS complex. In the type 2 Brugada pattern this angle is broad (always  $\geq 36^\circ$ ) with blunt contours. On the other hand, the “innocent”<sup>4</sup> or ordinary<sup>3</sup> IRBBB the mean angle of the final  $r'/R'$  wave has on average less than one third of the type 2 Brugada pattern ( $\approx 12^\circ$ ) and its contour is acute (Figure 6).

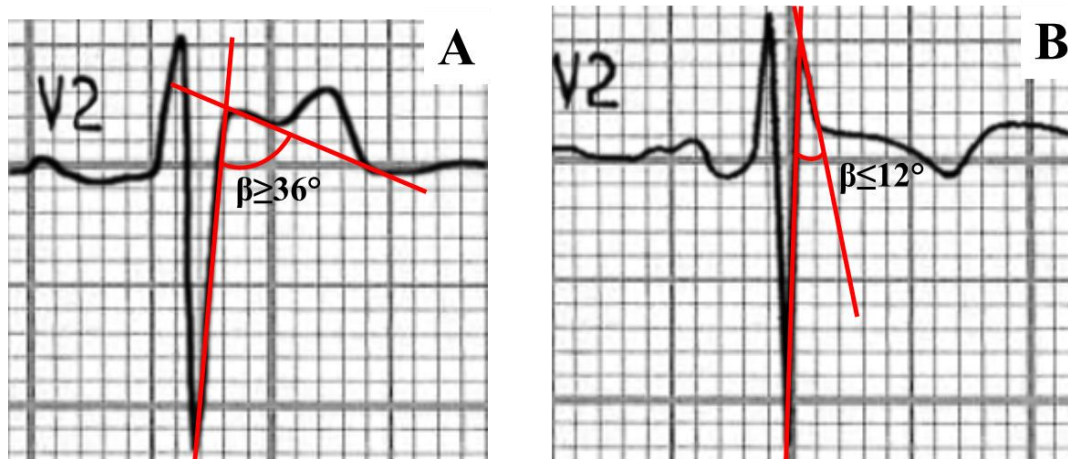


**Figure x. Type 2 Brugada pattern versus ordinary IRBBB.** A) Typical type 2 Brugada pattern in the precordial lead V2. Note the ST with saddleback appearance and followed by positive T wave in V2. The angle formed by the ascending and descending ramp of the final R' wave with blunt contours and the so-called  $\beta$  angle always is  $\geq 36.8^\circ$ . B) Typical IRBBB pattern in the precordial leads V1-V2. Note the r'/R' final wave with acute contour ("high take-off") and narrow  $\beta$  angle  $\leq 12^\circ$ .  $\beta$  angle is formed by the ascending and descending ramps of r'/R' final wave in V1-V2, and the duration of the base of the triangle formed by R'/r' at 5 mm from the high take-off is greater than 3.5 mm and there is a mismatch between V1 and V6.

Serra et al. demonstrated that by measuring the length of the base of the triangle at the isoelectric line formed by the upslope of the S wave and downslope of the r' wave either at the isoelectric point or at 5mm or 0.5mV from the r' peak they could differentiate type 2 BrP from the "innocent" ECG pattern of health athletes who had a triphasic pattern with final r' wave in V<sub>1</sub>-V<sub>2</sub> or in both. In Type 2 BrP the duration of the base of the triangle formed by ascendant and descendent arms of r' -wave at 5mm or 0.5 mV from the peak of r' or high take-off is the easiest to measure and may be useful in clinical practice. The duration  $\geq 160$  ms (4 mm) in V<sub>1</sub> and/or V<sub>2</sub> identifies patients with Type 2 Brugada pattern. This value has a Sensitivity: 85%; Specificity: 95%; Positive Predictive Value (PPV): 94.4%; and Negative Predictive Value (NPV) 87.9%. The authors considered that the measurement of the base of the triangle of r' in V<sub>1</sub>-V<sub>2</sub> taken at 5 mm from the peak or e high take-off of r' is much easier to perform than the Chevalier  $\beta$ -angle and has even greater accuracy.<sup>5</sup> Figure x

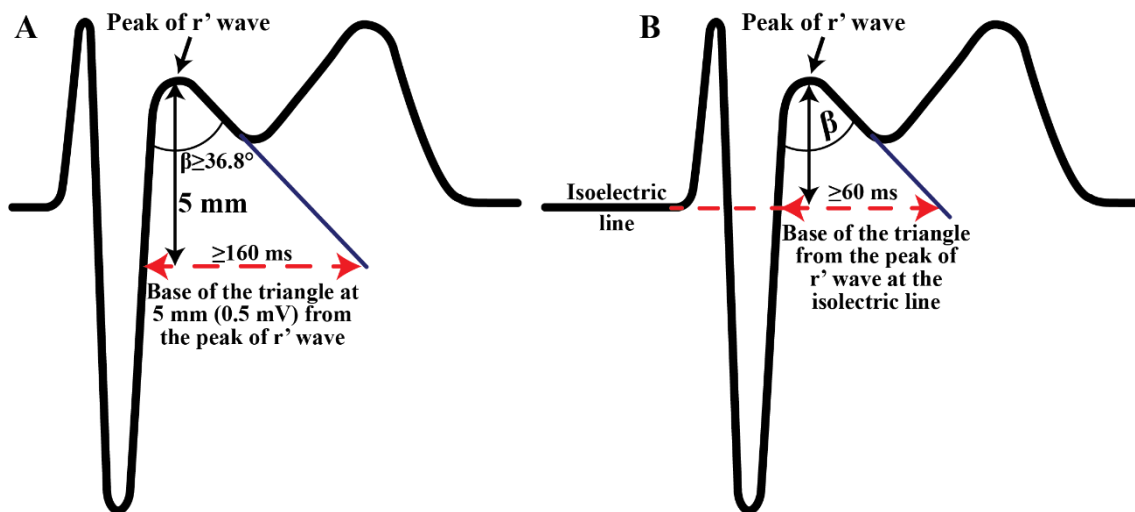


Figure x. Characteristic of type 2 Brugada pattern. The  $\beta$  angle is formed by the ascendent and descendent ramp of R'/r' wave.<sup>6</sup> This angle has a mean value of  $36.8^\circ$ . Additionally, the peak of r' wave is broad. (A) Base of the triangle at 5 mm from the peak of r' wave  $\geq 160$  ms. (B) Base of the triangle from the peak of r' wave at the isoelectric line  $\geq 60$  ms.

Differentiation of type 2 Brugada pattern from ordinary or “innocent” incomplete right bundle branch block (IRBBB) or normal rSr' pattern in the right precordial leads can be a challenge. Crea et al. collected 14 ECGs with triphasic pattern (rSr'/ rSR') of the QRS complex in leads V1 and V2 at the 4th intercostal space. The authors used the 2012 consensus conference criteria for the diagnosis of type 2 Brugada pattern and presented the ECGs to 42 participants: 14 arrhythmologists, 14 general cardiologists and 14 electrophysiology fellows. The same 14 ECGs, with a different order, were proposed fifteen days later to the same cohort to assess intra-observer variability. The authors analyzed all 14 ECGs in order to assess whether or not the 2012 Consensus Conference criteria for the Brugada pattern were fulfilled. All patients performed a provocative test with IC antiarrhythmic drug (flecainide) in order to exclude or confirm the diagnosis of BrS. The authors demonstrated, for the first time, a low inter-observer agreement in the diagnosis of the type 2 Brugada pattern in categories of cardiologists with different abilities. Reproducibility of type 2 Brugada pattern diagnosis (intra-observer agreement) was poor, even among experts. These findings highlight the difficulties in analysing ECGs with suspicion of BrS and, therefore, underscore the key role of clinical and anamnestic data.

Table x lists parameters to differentiate type 2 Brugada pattern from innocent IRBBB.

	<b>Type 2 Brugada pattern</b>	<b>Innocent IRBBB</b>
High take-off angle	Approximately 36° blunt contours	Acute narrow $\beta$ angle $\leq 12^\circ$
$\beta$ angle	$\geq 36.8^\circ$ (sensitivity: 86%, specificity: 94.7%, PPV: 93.5%, NPV: 88.5%) <sup>5</sup>	Minor $\leq 12^\circ$
ST segment	Bimodal with camel hump shape	ST depression convex upward followed by asymmetric negative T wave in the right precordial leads
T-wave	Positive or plane	Negative
Duration of the base of the triangle at 5 mm from the peak of r' wave <sup>6</sup>	$\geq 160$ ms (4 mm)	Minimal
Duration of the base of the triangle at the isoelectric line from the peak of r' wave	$\geq 60$ ms (1.5 mm)	
High take-off contour	Wide/ blunt	Acute
QRS duration	Usually $>120$ ms	QRS duration between 110 and 120 ms in adults, between 90 and 100 ms in children between 4 and 16 years of age, and between 86 and 90 ms in children less than 8 years of age.
Clinical significance	Suspected BrS	It is considered a normal variant, commonly seen in children, adolescents and healthy athletes. Sometimes an abnormality exists in the peripheral Purkinje conduction system consequence of delayed postnatal differentiation of Purkinje fibers in cases of reduced Nkx2.5 levels

Table x. Differential diagnosis between the type 2 Brugada pattern and “innocent” IRBBB. PPV: positive predictive value; NPV: negative predictive value.

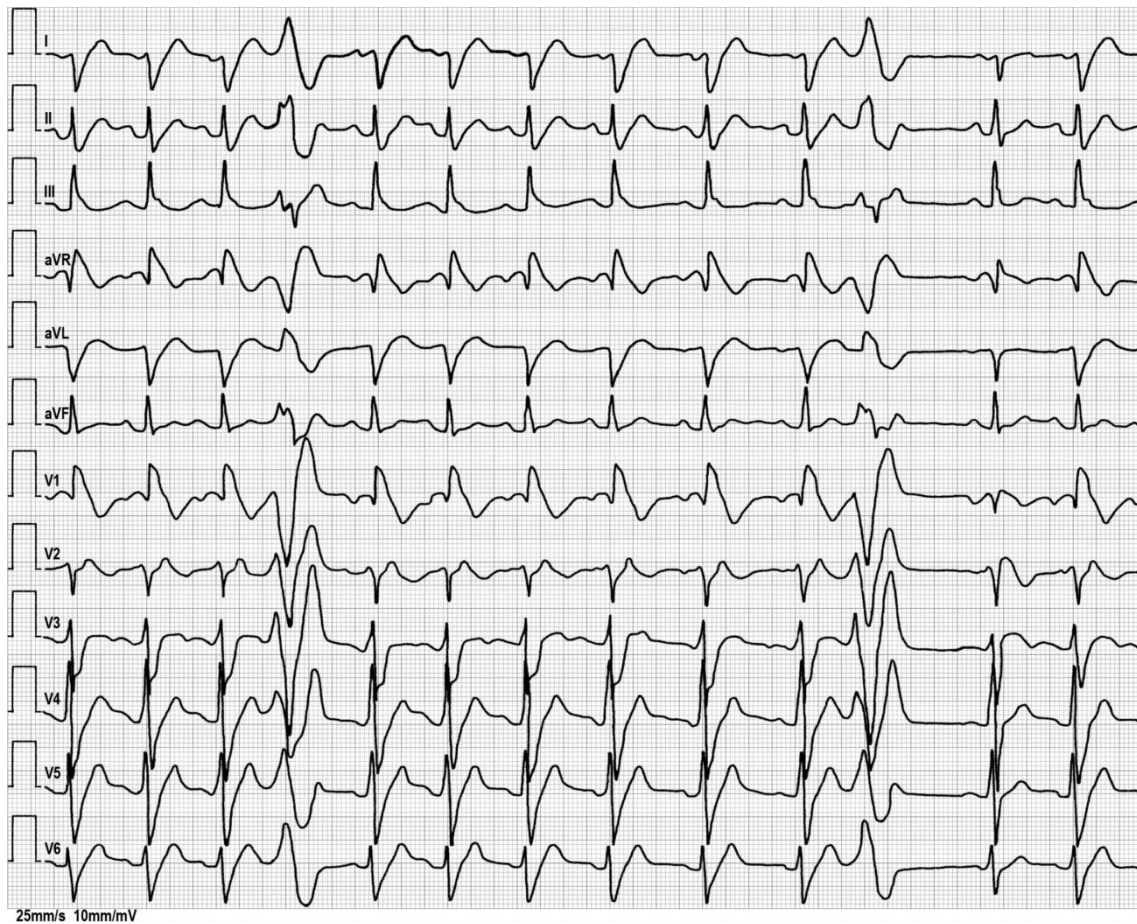
Crea et al studied the inter-observer and intra-observer agreement in the diagnosis of type 2 BP in a cohort of 14 clinical cardiologists, 14 arrhythmologists and 14 electrophysiologists. They collected 14 ECGs with a triphasic QRS complex in lead V1-

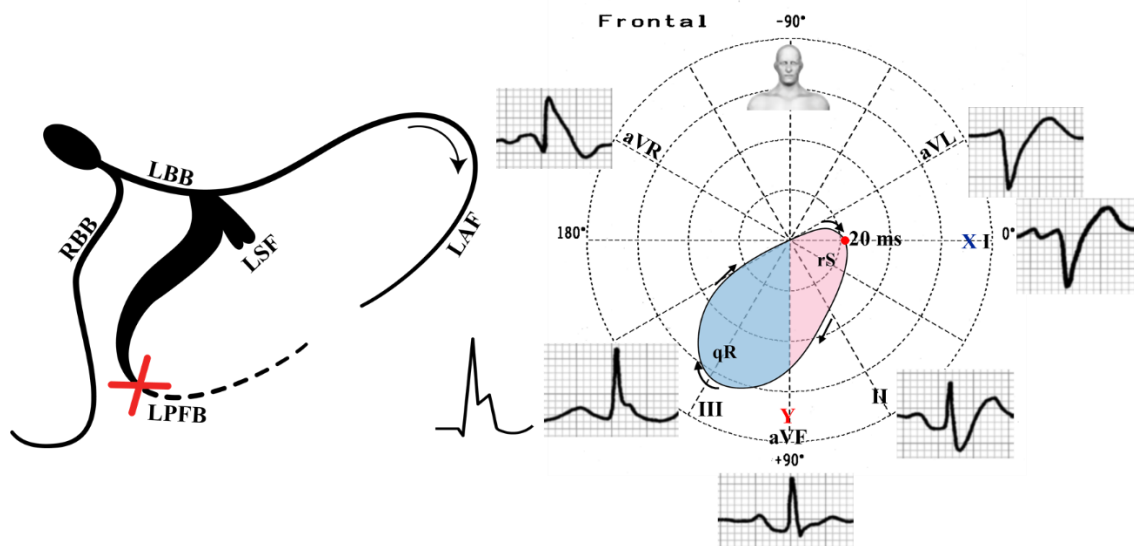
V2 at the 4th intercostal space. The authors proposed these ECGs, specifying to use 2012 Consensus conference criteria for diagnosis of type 2 BrS. The same 14 ECGs, with a different order, were proposed fifteen days later to the same cohort to assess intra-observer variability. Authors analyzed all 14 ECGs in order to assess whether or not 2012 Consensus Conference criteria for BrS were fulfilled. All patients underwent provocative test with flecainide in order to exclude or confirm the diagnosis of Brugada Syndrome (BrS). Slight inter-observer agreement (Fleiss K<0.20) in the diagnosis of type 2 BrS was observed in all three categories of cardiologists. Considering five operators per class, intra-observer agreement is variable (k ranging from 0,000 to 0,857), with a slight superiority of arrhythmologists (k minimum value 0,276; k maximum value 0,857). The authors verified a low inter-observer agreement in diagnosis of type 2 BrS in categories of cardiologists with different abilities. Reproducibility of type 2 BrS diagnosis (intra-observer agreement) is poor, even among experts. These findings show that the mere isolated electrocardiographic analysis is not enough, making personal and family questioning data essential.<sup>7, 8</sup>

**(2013) HRS/EHRA/APHRS expert consensus statement on the diagnosis and management of patients with inherited primary arrhythmia syndromes**

The 1st and the 2nd consensus report/conference (2002/2005) stated that the definitive diagnosis of BrS should only be established when the type I ECG pattern is documented in combination with at least one previously mentioned clinical criteria. The (2013) HRS/EHRA/APHRS expert consensus statement on the diagnosis and management of patients with inherited primary arrhythmia syndromes<sup>9</sup> established that the diagnosis of BrS is performed with the type 1 ECG pattern alone: J-point and ST elevation  $\geq 2$  mm in  $\geq 1$  lead in the right precordial leads V1-V2, positioned in the 2nd, 3rd or 4th intercostal space, occurring either spontaneously or after provocative drug test with IV of Class I antiarrhythmic drugs. Additionally, BrS is diagnosed in patients with type 2 in  $\geq 1$  lead among the right precordial leads V1, V2 positioned in the 2nd, 3rd or 4th intercostal space, when a provocative i.v. drug test with Class I antiarrhythmic drugs induces a type I ECG pattern, even when other clinical criteria are not fulfilled, as the finding can be associated with SCD during follow-up. Thus, all patients who present a type 1 ECG pattern, even when isolated, should be considered at risk.

**Premature ventricular contractions “unmasking” a hidden type 1 Brugada ECG pattern behind bifascicular block: Left posterior fascicular block and complete right bundle branch block**





Sinus rhythm, heart rate 94bpm, PQ interval 220ms, right axis deviation ( $+125^\circ$ ), rR in I and aVL, qR pattern with notch in the descending ramp of R in III lead, a broad fractionated QRS complex with complete right bundle branch block (RBBB) + LPFB appearance (right axis deviation ( $+125^\circ$ ), rR in I and aVL, qR pattern with notch in the descending ramp of R in III lead,), several broad monomorphic premature ventricular contractions (PVCs) Contractions without short QT coupling “R-on T phenomenon unmasking a hidden type 1 ECG Brugada pattern behind CRBBB, *Spontaneous hidden type 1 Brugada electrocardiographic pattern “unmasking” by -PVCs*, broad and deep S wave in I lead:<sup>10</sup> prominent final R wave in aVR, (R wave  $\geq 3$  mm or R/q  $\geq 0.75$  in lead aVR (aVR sign).<sup>11</sup> Slow conduction in the right ventricular outflow.

### ECG markers in identifying patients at risk in BrS

While some ECG markers of depolarisation and repolarisation abnormalities are known to be linked to increased arrhythmic risk, their sensitivity or specificity seems low, and they have not been tested in large prospective studies. The following markers are proposed:

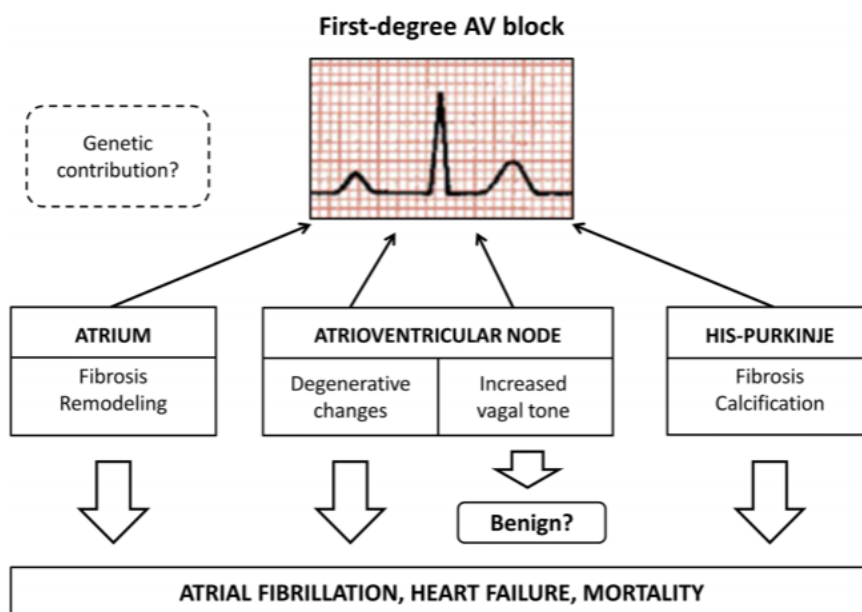
- ✓ QRS fragmentation (fQRS): defined as  $\geq 2$  notches of the R wave or in the nadir of the S wave in at least two consecutive leads. fQRS is a powerful depolarization marker for ventricular fibrillation (VF)/ sudden cardiac death (SCD). Right ventricular apical pacing (RVAP) manifested QRS fragmented spikes, which could be associated with spontaneous VF in patients with BrS. In a systematic review and meta-analysis Rattanawong et al demonstrated that baseline fQRS increased major arrhythmic events up to 3-fold. This



study suggests that fQRS could be an important tool for risk assessment in patients with BrS.<sup>12</sup>

- ✓ RVAP could enhance the conduction abnormality and predict the susceptibility to VF in patients with BrS.<sup>13</sup>
- ✓ Augmented P-wave duration in lead II / P-wave dispersion.<sup>14</sup>
- ✓ PR prolongation as a consequence of His-ventricle (HV) split or HV prolongation. Besides a history of cardiac arrest or syncope, first-degree AV block on basal ECG is an independent predictor of malignant arrhythmic event (MAEs) and a stronger marker of arrhythmic risk than a spontaneous 'coved-type' ECG pattern in patients with BrS.<sup>15</sup> First-degree AV block is associated with more frequent major arrhythmic events in BrS patients. PR interval seemed to be prolonged but is yet to be determined whether the PR interval association is still significant if it did not cross the first-degree AV block threshold.<sup>16</sup> A history of syncope or cardiac arrest, first-degree AV block on basal ECG is an independent predictor of MAEs and a stronger marker of arrhythmic risk than a spontaneous type 1 ECG pattern in patients with BrS.<sup>15</sup>

Factors associated with PR prolongation and their clinical significance<sup>17</sup> (Figure 8).



- ✓ BrS patients with Mobitz type II second-degree AVB, high-degree AVB, or third-degree AVB). Kamakura et al accompanied 223 BrS patients with a history of syncope from two centers were The clinical characteristics of patients with high-risk AVB (Mobitz type II second-degree AVB, high-degree AVB, or third-degree AVB) were investigated. During a follow-up the 99 ± 78 months, the authors identified six BrS patients (2.7%) with high-risk AVB. Three of the six patients (50%) with AVB presented with syncope

associated with prodromes or specific triggers. Four patients (67%) were found to have paroxysmal third-degree AVB during the initial evaluation for BrS and syncope, while two patients developed third-degree AVB during the follow-up period. The incidence of first-degree AVB was significantly higher in AVB patients than in non-AVB patients (83% vs. 15%). There was no significant difference in the incidence of VF between AVB and non-AVB patients.<sup>18</sup> High-risk AVB can occur in BrS patients with various clinical presentations. Although rare, the incidence is worth considering, especially in BrS patients with first-degree AVB.

- ✓ Type 1 Brugada ECG pattern in peripheral leads
- ✓ Presence of a prominent final R wave in aVR, R wave  $\geq 3$  mm or R/q  $\geq 0.75$  in lead aVR (aVR sign).<sup>11</sup> Slow conduction in the right ventricular outflow tract may contribute to the induction of VF by programmed ventricular stimulation. Positive R-wave sign in lead aVR can be used to identify patients with BrS at risk for malignant ventricular tachyarrhythmia.<sup>19</sup>
- ✓ Broad and deep S wave in I lead<sup>10</sup>
- ✓ “Northwest QRS axis”<sup>20</sup>
- ✓ The presence of a spontaneous type 1 ECG, history of syncope, ventricular effective refractory period  $< 200$  ms, and fQRS seem useful to identify candidates for prophylactic ICD.<sup>21, 22</sup>
- ✓ Inferolateral early repolarization (ER) in association with coved type Brugada ECG pattern: J-wave syndromes. The prevalence of ER in inferolateral leads was high and an especially persistent form of ER was associated with a worse outcome in BrS patients with documented VF.<sup>23</sup> The presence of a J wave in multiple leads and horizontal ST-segment morphology after J wave may indicate a highly arrhythmogenic substrate in patients with BrS.<sup>24</sup>
- ✓ fQRS, early repolarization pattern (ERP) and BrS in association are common ECG findings in high-risk BrS patients, occurring in up to 27% of cases. When combined, f-QRS and ERP confer a higher risk of appropriate ICD.<sup>25</sup> On multivariable analysis, a history of VF, syncope episodes, inferolateral ERP, and f-QRS were independent predictors of documented VF and SCD.<sup>26</sup>
- ✓ Prolonged QRS duration measured from lead II or V2  $\geq 120$  ms. Prolonged QRS duration as measured on a standard 12-lead ECG is associated with VA and could serve as a simple noninvasive marker of vulnerability to life-threatening cardiac events in patients with

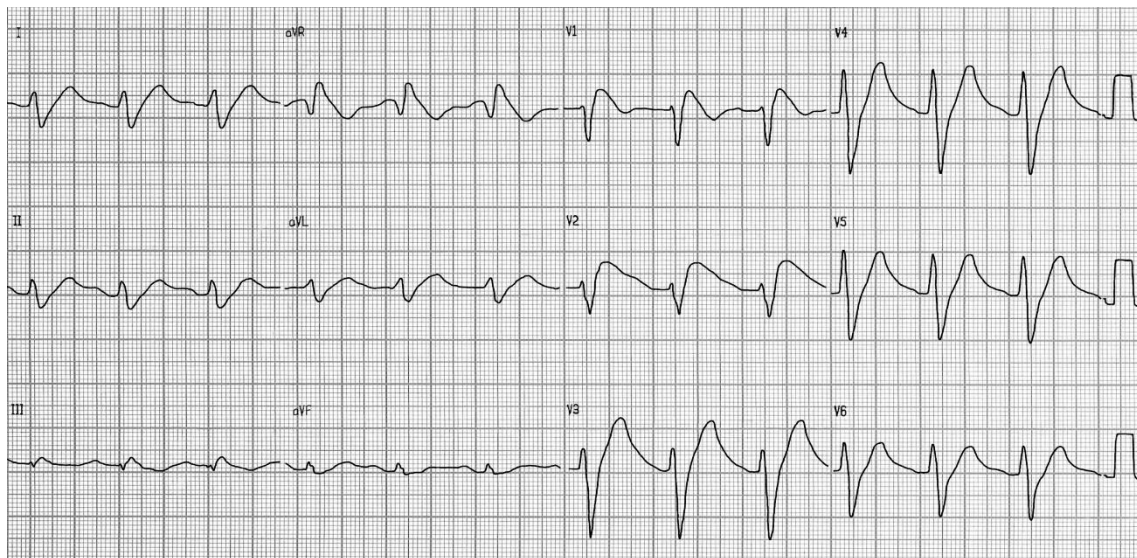
BrS.38 The duration of the QRS in leads V1 and V2 is greater than in the middle and left precordial leads.<sup>27, 28</sup>

- ✓ Low QRS amplitude. Patients with the minimum amplitude of type 1 ECG lower than or at the median value had a higher incidence of VF. In multivariate analysis, syncope, past VF episode, and minimum amplitude of type 1 ECG  $\leq 0.8$  mV are independent predictors of VF events during follow-up. Low-voltage type 1 ECG is highly and independently related to fatal ventricular tachyarrhythmia in patients with BrS.<sup>29</sup>
- ✓ QT interval prolongation in the right precordial leads is an additional ECG hallmark of BrS. QTc interval more than 460 ms in lead V2. Increase in QRS complex duration ( $>110$  ms) in the right precordial leads, in the absence of complete RBBB: parietal block.<sup>30</sup>
- ✓ Tpeak – Tend prolongation and Tpeak – Tend dispersion.<sup>31</sup>
- ✓ Dynamic alterations in the ST elevation amplitude.<sup>32</sup>
- ✓ Augmented ST elevation during the early recovery phase of exercise test.<sup>33</sup>
- ✓ Late potentials (LPs) in high-resolution ambulatory electrocardiography
- ✓ LPs and T-wave amplitude variability (TAV) in high-resolution ambulatory ECG: analysis of both LPs and TAV (taking circadian periodicity into account) is useful in identification of high-risk BrS patients.<sup>34, 35</sup>
- ✓ The presence of AF. Spontaneous AF and VF are closely linked clinically and electrophysiologically in BrS patients. Patients with spontaneous AF have more severe clinical backgrounds in BrS. SCN5A mutation is associated with electrical abnormality but not disease severity. Up to one-third of inherited heart disease patients may develop AF. While common general population risk factors are key factors in patients with hypertrophic cardiomyopathy, the genotype is independently associated with AF. Amongst inherited arrhythmia syndromes, AF is less common, though often occurring below the age of 50 years.
- ✓ Sinus Node Dysfunction (SND) in women concomitant with BrS. SND is not a rare concomitant disorder in BrS and there is a possible genetic connection. The function of both the sinus node and AV node are attenuated in patients with programmed electrical stimulation-induced VF.<sup>36</sup>

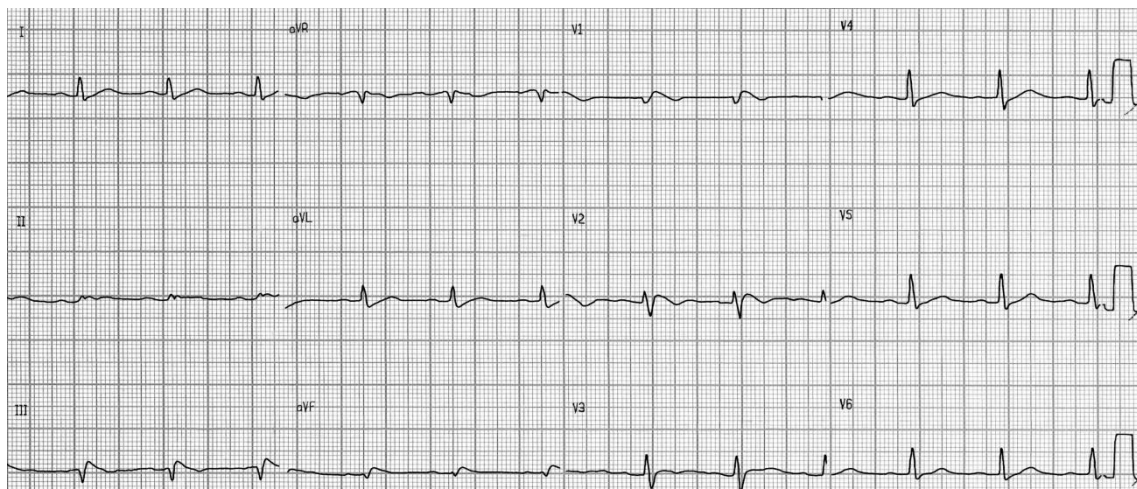
Type 1 Brugada ECG pattern in peripheral leads in patients with BrS. This ECG parameter can be seen in 10% of the patients with BrS either spontaneously or induced by drug and is an independent predictor for a MAEs. Type 1 ST elevation in the peripheral ECG leads is present in around 1 of 10 patients with BrS, This ECG pattern is associated with a higher risk for malignant arrhythmic events. Type 1 ST elevation in the peripheral

ECG leads may reflect a more diffuse arrhythmogenic substrate or a more severe phenotype, which in turn is responsible for the higher risk for MAEs. Therefore, the presence of type 1 ST elevation in the peripheral ECG leads may identify patients at higher risk of SCD in BrS and may be integrated in risk stratification.<sup>37-43</sup>

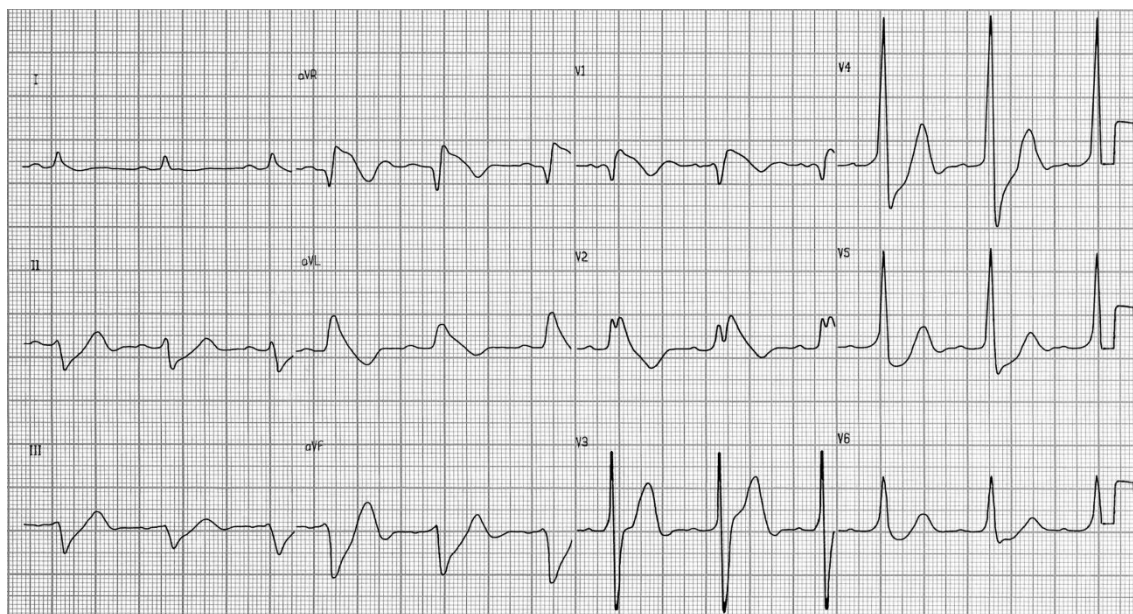
### Examples



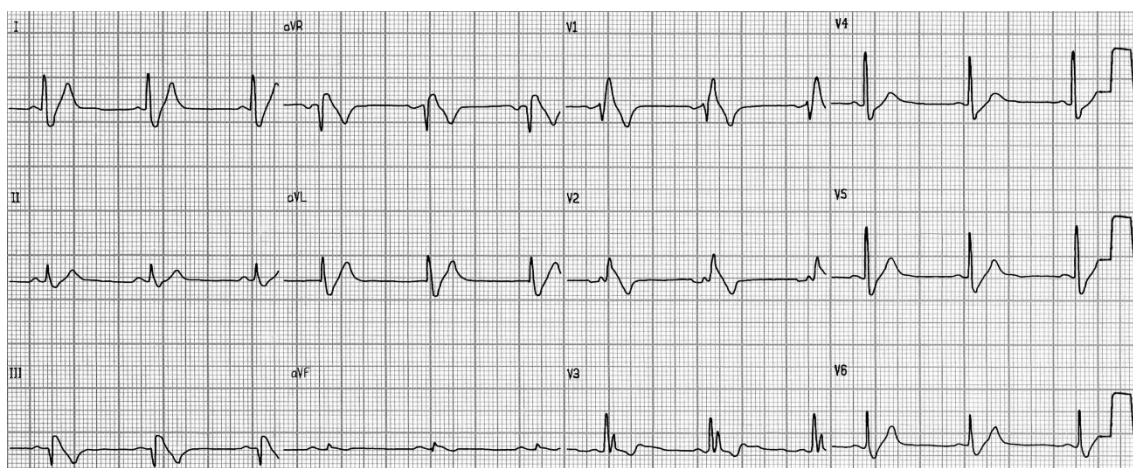
Example of type 1 ST elevation in the aVR lead. Some ST depression was also present in the inferior and lateral leads, reflecting reciprocal changes/ mirror images of the major ST elevation in the right precordial leads.



Example of type 1 ST elevation in the inferior leads.



Example of type 1 ST elevation in the aVL and aVR leads, and concomitant reciprocal changes in the inferior leads (ST depression).



Example of type 1 ST elevation in the inferior and aVR leads.

Type 1 Brugada pattern in the peripheral leads was observed in 4.2% of patients during ajmaline test (10.3% of positive tests) and was associated with wider QRS interval and greater QTc prolongation compared with the rest of the patients.<sup>37</sup>

Honarbaksh et al. developed a risk score model in a multicenter international cohort of patients with BrS, and no previous CA was used to evaluate the role of 16 proposed clinical or ECG markers in predicting VAs/ SCD during follow-up. Predictive markers were incorporated into a risk score model, and this model was validated by using out-of-sample cross-validation. A total of 1,110 patients with BrS from 16 centers in 8 countries were included (mean age 51.8 years; 71.8% male). Median follow-up was 5.33 years; 114 patients had VA/SCD (10.3%) with an annual event rate of 1.5%. Of the 16 proposed risk

factors, probable arrhythmia-related syncope, spontaneous type 1 ECG Brugada pattern, early repolarization, and a type 1 Brugada ECG pattern in peripheral leads were associated with a higher risk of VA/SCD. A risk score model incorporating these factors revealed a sensitivity of 71.2% and a specificity of 80.2% in predicting VA/SCD at 5 years. Calibration plots showed a mean prediction error of 1.2%. The model was effectively validated by using out-of-sample cross-validation according to country. Factors reviewed in the Cohort to determine if they played a role in the risk stratification of patients with BrS where Age at diagnosis, sex, probable arrhythmia-related syncope, diagnosis by family screening of SCD, spontaneous type 1 Brugada ECG pattern, SCN5A mutation, positive programmed ventricular stimulation, ventricular effective refractory period(VERP) <200 ms, inus node disfunction(SND), AF/atrial flutter, ER in peripheral leads, type 1 Brugada ECG pattern in peripheral leads, aVR sign, broad and deep S-wave in lead I, QRS duration >120 ms in V2 and QRS fragmentation. The authors concluded that this multicenter study identified 4 risk factors for VA/SCD in a primary prevention BrS population. A risk score model was generated to quantify risk of VA/SCD in BrS and inform ICD implantation.<sup>44</sup>

### **Utility of multiple risk factor combination rather than programmed electrical stimulation**

Beyond the type 1 Brugada ECG pattern, careful analysis of the surface ECG could reveal subtle electrical markers of depolarization and repolarization abnormalities, which can parallel the severity of the disease. A multicenter study taking these ECG markers into account in patients with spontaneous type 1 Brugada ECG patterns. It led to the development of a user-friendly tool for predicting the risk of VF, exclusively based on the combination of age and three ECG markers: a long corrected Tpeak-Tend interval ( $\geq 100$  ms in precordial leads), a peripheral type 1 Brugada pattern in a peripheral lead and early repolarization.<sup>45</sup> The main concern is the lack of comparison with clinical variables other than ECG findings such as cardiac syncope, a powerful predictor of CE in primary prevention patients.<sup>46</sup> Findings from the time domain analysis of the ECG are questioned as unable to provide additional criteria for risk stratification, and most of the BrS patients are indicated an ICD no matter the ECG pattern (spontaneous type I vs. others). Delinière et al reported a higher incidence of syncope in their cohort of BrS patients suffering SCA/VF. Perhaps syncope should be included in multivariate analysis,

in order to assess interaction of clinical variables and ECG findings, however syncope, like a family history of SCD, may be useful for risk stratification but lacks specificity. A high incidence of neurally mediated susceptibility in asymptomatic individuals with Brugada-type ECG pattern has been reported.<sup>47</sup> Most of the analysis performed up to date consisted in time domain description of ECG records as presented by Deliniere et al. But the time domain analysis is subjected to 'handmade' measurements over ECG records, and accuracy and reproducibility have not been evaluated. Automatization of quantitative measurements over digitalized ECG is as a potential tool able to characterize the arrhythmogenic substrate avoiding subjective interpretations and providing better reproducibility.<sup>48</sup> The signal-averaged ECG requires long time records and is highly dependent on noise. The spectral decomposition of ECG records and the analysis of the high-frequency content might be rapidly used in the clinic to increase diagnostic and predictive capabilities over clinical variables in BrS patients.<sup>49</sup>

The prognostic value of PES in BrS remains controversial. Asymptomatic BrS patients generally have a better prognosis than those with symptoms. Additionally, asymptomatic patients with a drug-induced type 1 Brugada ECG pattern have a low risk. Yasuhiro Yokoyama et al. evaluated the value of nonaggressive PES with up to two extra stimuli for predict clinical factors for risk stratification in asymptomatic BrS patients. The authors studied 193 consecutives asymptomatic BrS patients with type 1 ECG (mean age: 50 ± 13 years, 180 males) who underwent PES using a nonaggressive uniform protocol (1 or 2 extrastimuli). Cardiac events (CEs) = SCD or VT during the follow-up period were examined. During a mean follow-up of 101 ± 48 months, seven asymptomatic patients (3.6%) had a CE. The incidence of CEs was not different between patients with and without inducible ventricular tachyarrhythmia by PES coincident with previous studies.<sup>50</sup>

<sup>51</sup> The weight of available evidence suggests that PES in patients with BrS receive a Class III level recommendation (risk ≥ benefit), because of the potential for harm from both the invasive nature of the procedure and the potential for misleading information.<sup>52</sup>

The clinical significance of risk factor combinations, including spontaneous type 1 ECG, family history of SCD, QRS duration in lead V2 ≥120 ms, and presence of J wave in the inferior and or lateral leads, was evaluated. Using the Kaplan-Meier method according to the number of risk factors, the prevalence of CE in patients with three or four risk factors was determined to be significantly higher than in those with one risk factor. This study suggests that inducibility of ventricular tachyarrhythmia does not predict future CEs in

asymptomatic BrS patients. On the other hand, a poly-parametric combination analysis of the other four clinical risk parameters may be effective for risk assessment.<sup>53</sup>

BrS is diagnosed in patients with ST-segment elevation with type 1 morphology  $\geq 2$  mm in  $\geq 1$  lead among the right precordial leads V1, V2, positioned in the 2nd, 3rd or 4th intercostal space occurring either spontaneously or after provocative drug test with intravenous administration of Class I antiarrhythmic drugs. 2. BrS is diagnosed in patients with type 2 or type 3 ST-segment elevation in  $\geq 1$  lead among the right precordial leads V1, V2 positioned in the 2nd, 3rd or 4th intercostal space when a provocative drug test with intravenous administration of Class I antiarrhythmic drugs induces a type I ECG morphology

1. Absence of apparent structural heart disease
2. Absence of drugs effects, electrolyte disturbance and CHD
3. Documented PVT/VF
4. Family history of SCD at  $< 45$  years in first-degree relatives
5. Type 1 ECG Brugada pattern (coved-type) in proband and family members
6. Induction of VT/VF with Programmed Electrical Stimulation
7. Syncope, cardiac arrest or nocturnal agonal respiration.

### **BrS types, locus, OMIM, gene, channels affected and percentage**

- I. BrS-1<sup>54</sup>: Locus: 3p21-23; OMIM: 601144; Gene: SCN5A; Ion channel and effect: INa<sup>+</sup> loss-of-function; Protein: NaV1.5 -  $\alpha$  subunit of the cardiac sodium channel carrying the sodium current INa<sup>+</sup>; % of probands: 11-28%. Amin et al<sup>55</sup> hypothesized based on a study of AF in a large cohort of BrS patients, that a reduced number of potentially triggering premature atrial contractions (PACs) in the presence of a more extensive substrate in SCN5A mutation carriers may account for AF being no more prevalent in patients with SCN5A mutations than in those without. Given the polemic and complex issues underlying the



pathophysiology of BrS, one should regard this hypothesis as one potential mechanism of many that influence the prevalence of AF in BrS. Mutations in SCN5A lead to a broad spectrum of phenotypes, however the SCN5A gene is not commonly involved in the pathogenesis of BrS and associated disorders. Studies have revealed significant overlap between aberrant rhythm phenotypes, and single mutations have been identified that evoke multiple rhythm disorders with common gating lesions. Nav1.5 consists of peak and late components (INa-P and INa-L). Mutant Nav1.5 causes alterations in the peak and late Na<sup>+</sup> current and is associated with an increasingly wide range of genetic arrhythmias. More than 400 mutations have been identified in the SCN5A gene. Although the mechanisms of SCN5A mutations leading to a variety of channelopathies can be classified according to the alteration of INa-P and INa-L as gain-of-function, loss-of-function and both, few researchers have summarized the mechanisms in this way<sup>56</sup>. Gain-of-function mutations in SCN5A lead to more Na<sup>+</sup> influx into cardiomyocytes through aberrant channel gating causing LQT3. Slowed or incomplete inactivation of the NaV1.5 channel results in an additional inward current, known as the late or persistent sodium current (I<sub>pst</sub>), during the plateau phase of the ventricular action potential with ST segment prolongation and late T occurrence. Among the mutations in SCN5A associated with LQT3 is 1795insD, which is characterized by the insertion of 3 nucleotides (TGA) at position 5537 C-terminal domain of the NaV1.5 protein<sup>57</sup>. Carriers of this mutation may not only present with LQT3, but also with ECG features of sinus bradycardia, progressive cardiac conduction disease, and Brugada syndrome, thus creating the first described arrhythmic ‘overlap syndrome’<sup>58</sup>. Interestingly, 1795insD is supposed to be a gain-of-function mutation in light of the QT prolongation, but a loss-of-function mutation in light of the sinus bradycardia, progressive cardiac conduction disease, and Brugada syndrome. Additionally, and multifocal ectopic premature Purkinje-related complexes; loss-of-function mutations in SCN5A result in amplitude reduction in peak Na<sup>+</sup> current, further leading to channel protein dysfunction. i or cardiac conduction defect an entity with minor structural heart disease. In addition, both loss- and gain-of-function mutations may cause dilated cardiomyopathy and/or atrial fibrillation.<sup>59</sup> On ECG PR interval prolongation is the only parameter that predicted the presence of a SCN5A mutation in BrS, additionally, late potentials on high resolution ECG LP were

more frequently observed in SCN5A mutation carriers <sup>60</sup>. SCN5A mutation is associated with an increased risk of drug-induced ventricular arrhythmia in patients without baseline type-1 ECG. In particular, Snon-missense and Smissense-TP are at high risk <sup>61</sup>.

- II. BrS-2 <sup>62</sup>: Locus: 12p13.3; OMIM: 911778; Gene: GPDIL; Ion channel and effect: INa<sup>+</sup> loss-of-function; Protein: Glycerol-3phosphate dehydrogenase like peptide-reduced GPD1-L activity leads to phosphorylation of Nav1.5 and decreased INa<sup>+</sup>; % probands: Rare. Defects in this gene are also a cause of sudden infant death syndrome (SIDS). SIDS is the SCD of an infant younger than 1 year that remains unexplained after a thorough case investigation, including performance of a complete autopsy, examination of the death scene, and review of clinical history.
- III. BrS-3 <sup>63</sup>: Locus: 12p13.3; OMIM: 114205; Gene: CACNA1C, Cav1.2; Ion channel and effect: ICa loss-of-function; Protein: e: Cav1.2- a-subunit of the voltage-gated calcium channel carrying the L-type calcium current ICa(L); % probands: 6.6%. Chromosomal location: 12p13.33, which is the short (p) arm of chromosome 12 at position 13.33. Shared with Timothy syndrome. SN5A and CACNA1C: complex BrS <sup>64</sup>.
- IV. BrS-4 <sup>63</sup>: Locus: 10p12.33; OMIM: 600003; Gene: CACNB2b, Cavβ2b; Ion channel and effect: ICa loss-of-function; Protein: Cavβ2B- β-2 subunit of the voltage-gated calcium channel carrying the L-type calcium current ICaL.(LTCC) regulates calcium entry into cardiomyocytes. CACNB2 (β2) LTCC auxiliary subunits traffic the pore-forming CACNA subunit to the membrane and modulate channel kinetics. β2 is a membrane associated guanylate kinase (MAGUK) protein. A major role of MAGUK proteins is to scaffold cellular junctions and multiprotein complexes. β2.1 may also function in the heart as a MAGUK scaffolding unit to maintain N-cadherin-based adherens junctions and heart tube integrity <sup>65</sup>; % probands: 4.8%.
- V. BrS-5 <sup>66</sup>: Locus: 19q13,1; OMIM: 600235; Gene: SCN1B, Naβ1; Ion channel and effect: INa<sup>+</sup> loss-of-function; Protein: Nav β 1- β 1 subunit of the sodium channel carrying the sodium current: INa<sup>+</sup>; % probands: 1.1%. Loss-of-function mutations in the β-subunits (encoded by C) have also been described for AF <sup>67</sup>. # 612838 A

number sign (#) is used with this entry because of evidence that BrS-5 and a nonspecific cardiac conduction defect are caused by heterozygous mutation in the SCN1B gene on chromosome 19q13.1.

- VI. BrS-6.<sup>68</sup>: Locus: 11q13-14; OMIM: 604433; Gene: KCNE3, MiRP2; Ion channel and affect: Ito gain-of-function; Protein: MiRP2-  $\beta$  subunit to voltage potassium channels. Modulates the transient outward potassium current Ito; % probands: Rare. # 613119 A number sign (#) is used with this entry because of evidence that BrS-6 is caused by heterozygous mutation in the KCNE3 gene on chromosome 11q13.
- VII. BrS7<sup>69</sup>: Locus: 11q23.3; OMIM: 6081214; Gene: SCN3B; Ion channel and affected: INa<sup>+</sup> loss-of-function; Note: Navb-3 subunit of the cardiac sodium channel carrying the sodium current INa<sup>+</sup>; % probands: Rare. # 613120 A number sign (#) is used with this entry because of evidence that BrS-7 and AF-16 (18, 19) are caused by heterozygous mutation in the SCN3B gene on chromosome 11q24. BrS8: Locus: 12q11.23; OMIM: 600935; Gene: KCNJ8, Kir6.1; Ion channel and effect: Ik-ATP gain-of-function; Protein: Kir6., carries the inward rectifier potassium current Ikr; % probands: 2%. # 613123 A number sign (#) is used with this entry because of evidence that BrS-8 is caused by heterozygous mutation in the HCN4 gene on chromosome 15q24<sup>70</sup>.
- VIII. BrS-8 is caused by heterozygous mutation in the HCN4 gene on chromosome 15q24<sup>70</sup>. Locus: 12q11.23; OMIM: 600935; Gene: KCNJ8, Kir6.1; Ion channel and effect: Ik-ATP gain-of-function; Protein: Kir6., carries the inward rectifier potassium current Ikr; % probands: 2%. # 613123 A number sign (#) is used with this entry because of evidence that BrS-8 is caused by heterozygous mutation in the HCN4 gene on chromosome<sup>70</sup>.
- IX. BrS9: Locus: 7q21.11; OMIM: 114204; Gene: CACNA2D1, Ca,  $\alpha 2\delta$ ; Ion channel and effect: ICa loss-of-function; Protein:  $\alpha 2\delta$  subunit of the voltage-gated calcium channel carrying the L-type calcium current ICa(L); % probands: 1.8%. Rare.# 616399 A number sign (#) is used with this entry because of evidence that BrS-9 is caused by heterozygous mutation in the KCND3 gene on chromosome 1p13<sup>71</sup>.

- X. BrS10: Locus:1p13.2; OMIM:605411; Gene: KCND3, Kv4.3; Ion channel and effect: Ito gain-of-function; Protein: Kv4.3,  $\alpha$ -subunit of the transient outward potassium channel Ito; % probands: Rare. The prominent role of the Ito in BrS pathogenesis, the rare gain-of-function mutations in KCND3 serve as a pathogenic substrate for BrS. Giudicessi et al provided the first molecular and functional evidence implicating novel KCND3 gain-of-function mutations in the pathogenesis and phenotypic expression of BrS, with the potential for a lethal arrhythmia being precipitated by a genetically enhanced I(to) current gradient within the right ventricle where KCND3 expression is the highest <sup>71</sup>.
- XI. BrS11 <sup>72</sup>: Locus: 17p13.1; OMIM: 607954; Gene: RANGRF; Ion channel and effect: INa<sup>+</sup> loss-of-function; Protein: Encodes MOG1 – influences trafficking of Nav 1.5. The protein MOG1 is a cofactor of the cardiac sodium channel, Nav1.5. Overexpression of MOG1 in Nav1.5-expressing cells increases sodium current markedly. Mutations in the genes encoding Nav1.5 and its accessory proteins have been associated with cardiac arrhythmias of significant clinical impact; % Probands: Rare <sup>73</sup>. Olesen et al. screening of Nav1.5 cofactor MOG1 uncovered a novel nonsense variant that appeared to be present at a higher frequency among patients than in control subjects.
- XII. BrS12 <sup>74</sup>: Locus: 3p21.2-2-p14.3; OMIM: 602701; Gene: SLMAP; Ion channel and effect: INa<sup>+</sup> loss-of-function; Protein: Sarcolemma membrane-associated protein, a component of T-tubes and the sarcoplasmic reticulum – influences trafficking of Nav1.5; % Probands: Rare. T-tubules and sarcoplasmic reticulum are essential in excitation of cardiomyocytes, and sarcolemmal membrane-associated protein (SLMAP) is a protein of unknown function localizing at T-tubules and sarcoplasmic reticulum. The mutations in SLMAP may cause BrS via modulating the intracellular trafficking of hNav1.5 channel.
- XIII. BrS13: Locus <sup>75</sup>: 12p12.1; OMIM: 601439; Gene: ABCC9 SUR2A; Ion channel and effect: Ik(ATP) gain-of-function; Protein: SUR2A, the adenosine triphosphate (ATP) binding cassette transporter of the Ik(ATP) channel.; % Probands: Rare. The ABCC9 is an ion channels/ion channel-related AF. Adenosine triphosphate (ATP)-sensitive potassium cardiac channels consist of inward-rectifying channel subunits Kir6.1 or Kir6.2 (encoded by KCNJ8 or

KCNJ11) and the sulfonylurea receptor subunits SUR2A (encoded by ABCC9). KCNJ8 is a susceptibility gene for BrS and early repolarization syndrome (ERS and point to S422L as a possible hotspot mutation. The S422L-induced gain of function in ATP-sensitive potassium channel current is due to reduced sensitivity to intracellular ATP. ABCC9 has ERS and BrS susceptibility genes. A gain-of-function in IK-ATP when coupled with a loss-of-function in SCN5A may underlie type 3 ERS, which is associated with a severe arrhythmic phenotype <sup>76</sup>.

- XIV. BrS14 <sup>77</sup>: Locus: 11q23; OMIM: 601327; Gene: SCN2B, Nav $\beta$ 2; Ion channel and effect: INa<sup>+</sup> loss-of-function; Protein: Nav $\beta$ 2- $\beta$ -2subunit of the cardiac sodium channel carrying the sodium current INa; % Probands: Rare. Riuró et al. identified a novel missense mutation in the sodium  $\beta$ 2 subunit encoded by SCN2B, in a woman diagnosed with BrS. They studied the sodium current from cells coexpressing Nav 1.5 and wild-type ( $\beta$ 2WT) or mutant ( $\beta$ 2D211G)  $\beta$ 2 subunits. Electrophysiological analysis showed a reduction in INa density when Nav 1.5 was coexpressed with  $\beta$ 2D211G. Single channel analysis showed that the mutation did not affect the Nav 1.5 unitary channel conductance. Instead, protein membrane detection experiments suggested that  $\beta$ 2D211G decreases Nav 1.5 cell surface expression. The effect of the mutant  $\beta$ 2 subunit on the INa strongly suggests that SCN2B is a candidate gene associated with BrS.
- XV. BrS15: Locus: 12p11; OMIM: 602861; Gene: PKP2, Plakophilin-2; Ion channel and effect: INa<sup>+</sup> loss-of-function; Protein: Plakophilin-2 – interacts with INa<sup>+</sup>; % probands: Rare. Plakophilin-2 (PKP2) variants could produce a BrS phenotype, which is the same allelic disorder as some sudden unexplained nocturnal death syndromes (SUNDS). All coding regions of PKP2 gene in 119 SUNDS victims were genetically screened using PCR and direct Sanger sequencing methods. Three novel mutations (p.Ala159Thr, p.Val200Val, and p.Gly265Glu), one novel rare polymorphism (p.Thr723Thr), and 8 polymorphisms were identified. A compound mutation (p.Ala159Thr and p.Gly265Glu) and a rare polymorphism (p.Thr723Thr) were found in one SUNDS case with absence of the apparent structural heart disease. The detected compound mutation identified in this first investigation of PKP2 genetic phenotype in SUNDS is regarded as the plausible genetic cause of this SUNDS case. The rare incidence of PKP2 mutation in SUNDS (1%) supports the previous viewpoint that SUNDS is most likely an

allelic disorder as BrS <sup>78</sup>. Mutations in proteins of the desmosome are associated with arrhythmogenic cardiomyopathy (AC). Life-threatening ventricular arrhythmias (VAs) often occur in the concealed forms/phase of the AC before the onset of structural changes. Evidence indicating that loss of desmosomal integrity (including mutations or loss of expression of plakophilin-2; PKP2) leads to reduced sodium current, the PKP2-INa relation could be partly consequent to the fact that PKP2 facilitates proper trafficking of proteins to the intercalated disc, and, PKP2 mutations can be present in XV patients diagnosed with BrS, thus supporting the previously proposed notion that AC and BrS are not two completely separate entities <sup>79</sup>. Mutations on PKP2 account for the majority of AC cases, a disease characterized by high incidence of VAs and a progressive cardiomyopathy with fibrofatty infiltration involving predominantly the right ventricle. Although BrS was initially described as a purely electric condition in intact hearts, it is now recognized that structural changes occur mainly at the right ventricular outflow tract (RVOT) <sup>80</sup>. These findings support the hypothesis, suggested in the past by some clinicians, that the two conditions could be at the bookends of a phenotypical common spectrum. PKP2 is a structural protein of the desmosome whose principal role is to maintain tissue integrity and cell-to-cell stability. However, data from cellular and mouse models demonstrated that loss of PKP2 could facilitate arrhythmias by decreasing sodium current <sup>81</sup>, thus through an electrophysiological effect. Indeed, in vitro characterization of the PKP2 mutations detected in patients with a BrS phenotype showed a decreased sodium current, consistent with the clinical phenotype. Super-resolution microscopy data showed that loss of PKP2 could affect proper trafficking of the sodium channel at the membrane, thus supporting the concept that proteins could have accessory roles aside from the primary one ascribed to them. The role of the cardiac intercalated disc as a functional unit with both structural and electric regulatory functions has been opening new paths of investigations on the possible arrhythmogenic substrate in BrS <sup>82</sup>.

- XVI. BrS-16: Locus: 3q28; OMIM: 601513; Gene: FGF12, FHAF1; Ion channel and effect: INa<sup>+</sup> loss-of-function; Protein: Fibroblast growth factor homologues factor-1- mutation decreases INa<sup>+</sup>; Cytogenetic location: 3q28-q29; % Probands: Rare. Multilevel investigations strongly suggest that Q7R-FGF12 is a disease-

associated BrS mutation. FHF effects on Na(+) and Ca(2+) channels are separable. Most significantly, the Hennessey study establishes a new method to analyze effects of human arrhythmogenic mutations on cardiac ionic currents. On the basis of the recent demonstration that FGF homologous factors (FHF; FGF11-FGF14) regulate cardiac Na(+) and Ca(2+) channel currents, FHF are candidate BrS loci<sup>83</sup>. Mutation FGF12 also causes neonatal-onset epilepsy.

- XVII. BrS-17<sup>84</sup> Locus: 3p22.22; OMIM: 604427; Gene: SCN10A, Nav1.8; Ion channel and effect: INa+ loss-of-function; Protein: Nav1.8- $\alpha$ subunit of the neural sodium channel.; % Probands: 16.7%. Hu et al identified SCN10A as a major susceptibility gene for BrS, thus greatly enhancing our ability to genotype and risk stratify probands and family members. The SCN10A SNP V1073 is strongly associated with BrS. Rare variants in the screened QRS-associated genes (including SCN10A) are not responsible for a significant proportion of SCN5A mutation negative BrS. The common SNP SCN10A V1073 was strongly associated with BrS and demonstrated loss of Nav1.8 function, as did rare variants in isolated patients<sup>85</sup>. The expression of sodium channel Nav1.8 in cardiac nervous systems has been identified, and variants of SCN10A that encodes Nav1.8 contribute to the development of BrS by modifying the function of Nav1.5 or directly reducing the Na+ current. Fukuyama et al screened for the SCN10A gene using a high-resolution melting method and direct sequencing, and compared the clinical characteristics among the probands with gene mutations in SCN10A, 6 probands with CACNA1C and 17 probands with SCN5A. They identified six SCN10A variant carriers (2.5%): W189R, R844H (in two unrelated probands), N1328K, R1380Q, and R1863Q. Five were male. Four were symptomatic: one died following SCD age 35, one suffered ventricular fibrillation, and two had recurrent syncope. Compared with BrS patients carrying SCN5A or CACNA1C mutations, although there were no significant differences among them, symptomatic patients in the SCN10A group tended to be older than those in the other gene groups<sup>86</sup>.
- XVIII. BrS-18<sup>87</sup>: Locus: 6q; OMIM: 604674; Gene: HEY2 (transcriptional factor); Ion channel and effect: INa+ loss-of-function; Protein: Transcription factor identified in GWAS; % Probands: Rare. The association signals at SCN5A-SCN10A demonstrate that genetic polymorphisms modulating cardiac conduction can also

influence susceptibility to cardiac arrhythmia. The implication of association with HEY2, supported by new evidence that Hey2 regulates cardiac electrical activity, shows that BrS may originate from altered transcriptional programming during cardiac development.

- XIX. BrS-19 <sup>88</sup> Locus: 7p12.1; OMIM: 603961; Gene: SEMA3A, Semaphoring; Ion channel and effect: Ito gain-of-function; Protein: NaV1.5 -  $\alpha$  subunit of the cardiac sodium channel carrying the sodium current  $I_{Na}$ ; % of Probands: Rare. Boczek et al were the first to demonstrate SEMA3A as a naturally occurring protein that selectively inhibits Kv4.3 and SEMA3A as a possible BrS susceptibility gene through a Kv4.3 Ito gain-of-function mechanism

Some mutations associated with BrS can also cause other heart conditions. Those who show more than one cardiac condition at the same time caused by a single mutation are described as having an overlap syndrome <sup>89</sup>.

#### ECG types from first consensus report <sup>90,91</sup>

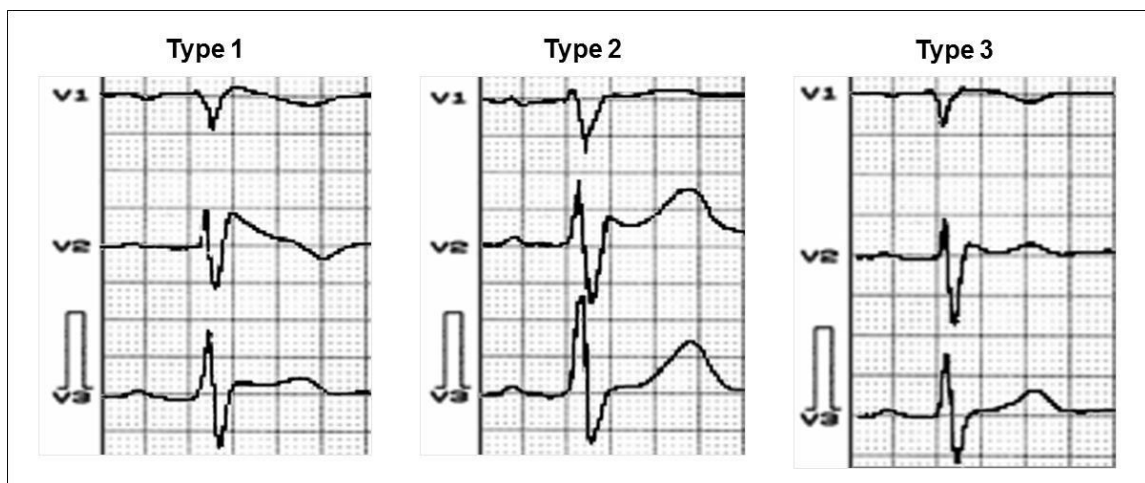


**Figure x.** Type 1: ST-segment elevation is triangular or coved to the top (“coved type”)  $\geq 2$  mm (0,2 mV) elevation in  $>1$  right precordial lead V1-V3 in the presence or absence of a sodium-channel blocker and followed by negative symmetrical T wave. Type 0 as coved-type ST elevation without a negative T wave <sup>22</sup>. Type 2: J point and ST segment elevation  $\geq 2$  mm (0,2 mV) with saddleback appearance, and remains at least 1 mm above the isoelectric line, followed by positive or biphasic T wave. Type 3: J point and ST segment elevation  $<1$  mm and with variable shape: whether coved type or saddleback



appearance. In type 3, the terminal section of the ST segment never exceeds 1 mm above the isoelectric line. Note that type 2 and 3 patterns are characterized by the same general shape of the J-ST-T wave, but the ST segment elevation in type 3 pattern is slightly less than 0.1 mV.

**New ECG classification**

Type 1 Brugada pattern: J point and ST segment elevation  $\geq 2$  mm, with upper convexity or descending oblique rectilinear followed by negative T wave on the right precordial leads ( $V_1$ - $V_2$  or from  $V_1$  through  $V_3$ ) and/or high right precordial leads  $V_{1H}$ ,  $V_{2H}$  and  $V_{3H}$ .

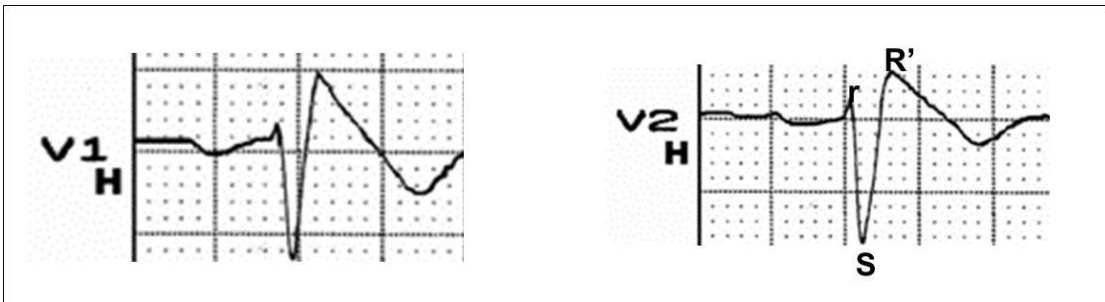


**Figure x.** Type 1 Brugada pattern.

Type 2 Brugada pattern: it has ST segment elevation with saddleback shape, high take-off angle broad,  $\beta$  angle always  $>36^\circ$  and the base of the triangle from high take-off of 5 mm.

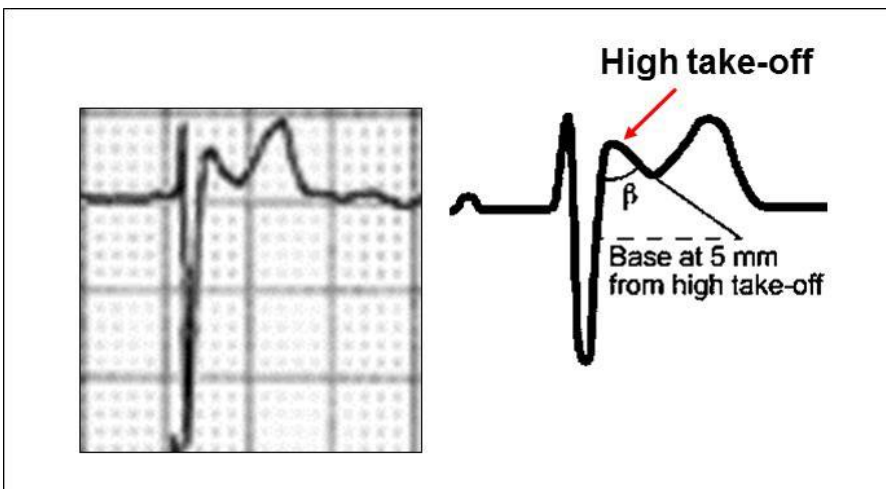


**Figure x.** Type 2 Brugada pattern.

## Proposal of classification of type 1 Brugada pattern Right precordial leads

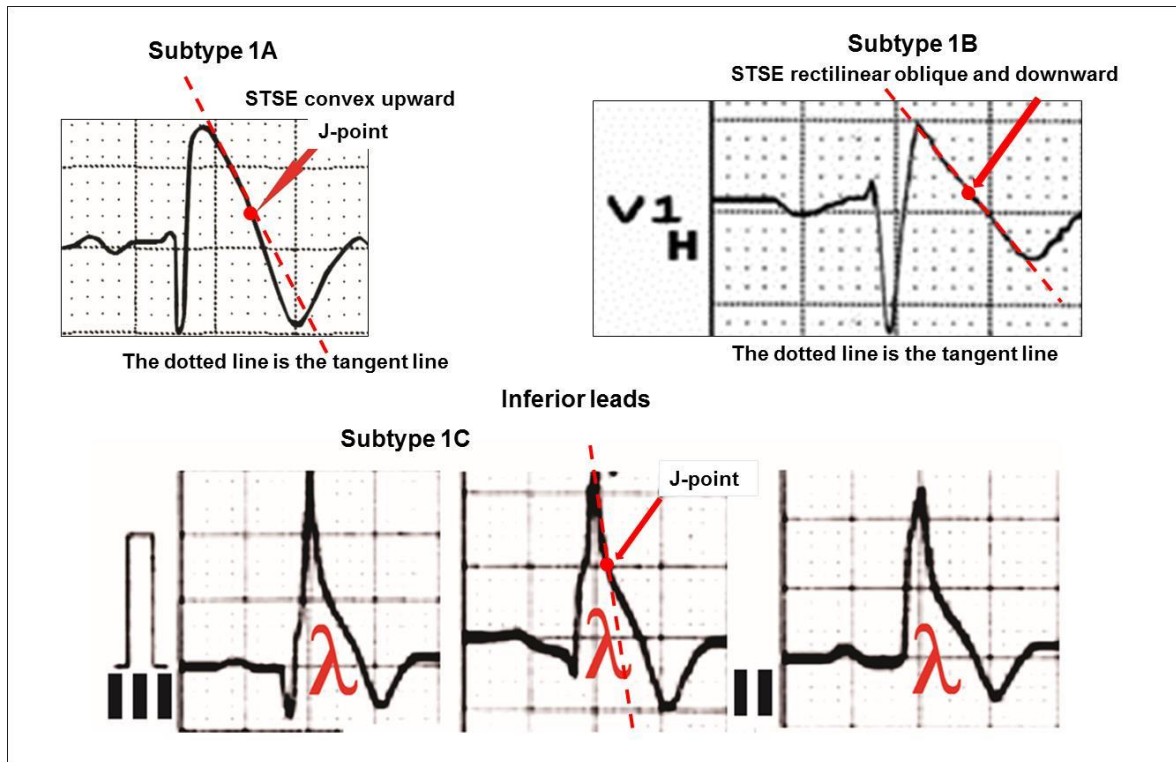
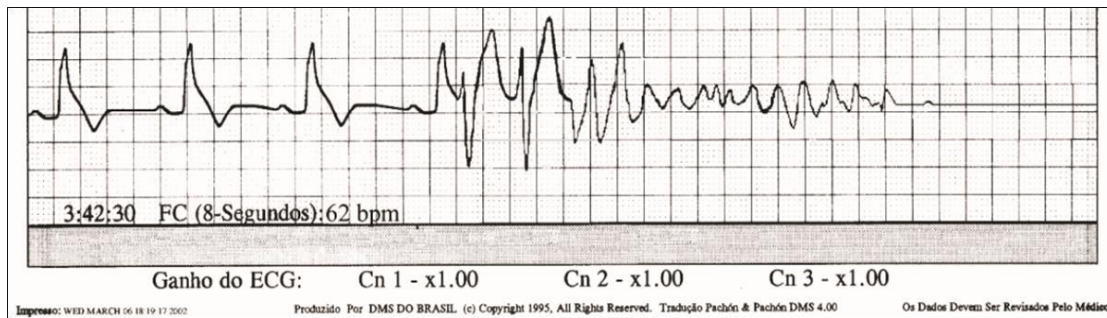


Figure x. Right precordial leads.

## Example of subtype 1C ECG Brugada pattern

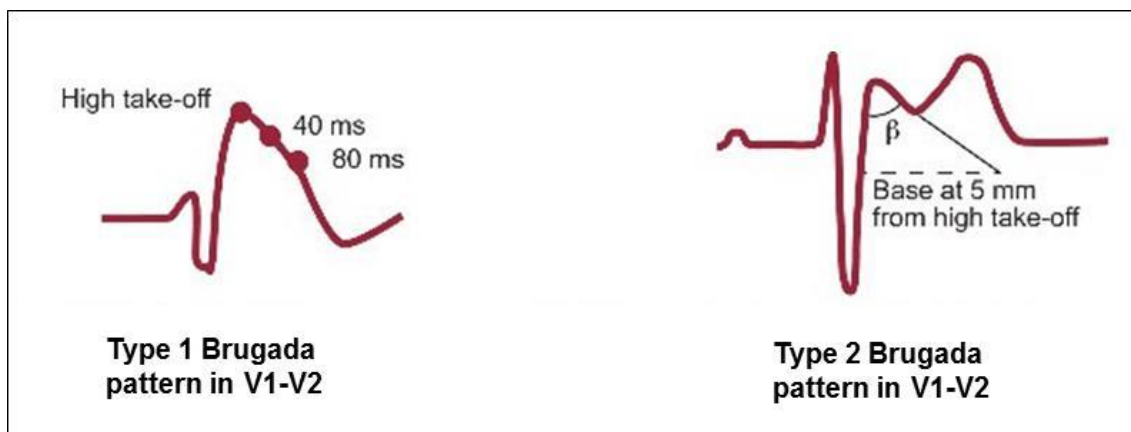


Figure x. The ECG shows persistent ST segment elevation in the inferior and apical leads, associated to concomitant reciprocal or mirror image in the anterior wall that was not modified with the use of sublingual nitrate in absence of hypothermia, electrolyte imbalance or ischemia <sup>92</sup>.



**Figure x.** Holter monitoring recorded the final event, manifest by PVT episode with initial short-coupling ventricular premature contractions (R on T) that ended quickly in VF and asystole. Pattern 1C of repolarization has been observed in acute myocardial infarction by Kukla et al <sup>93</sup>. These authors raised the hypothesis that the “Lambda-like ST” could be a new marker of risk of acute infarction with ST segment elevation.

In the new ECG criteria, only 2 ECG patterns are considered: pattern 1 identical to classic type 1 of other consensus (coved pattern) and pattern 2 that joins patterns 2 and 3 of the first consensus (saddle-back pattern) <sup>1</sup>.



**Figure x** Type 1 and 2 Brugada ECG pattern.

**Type 1 Brugada pattern in V1-V2:**

- At the end of QRS, there is ascending ST segment with a high take-off of at least 2 mm followed by a convex to the top or rectilinear downsloping ST segment. There are a few cases where high take-off is between 1 and 2 mm.
- There is no clear r' wave.
- The high take-off does not correspond to the J-point.

- At 40 ms of take-off, the decrease in amplitude of ST segment is 4 mm (it is much higher in RBBB and athletes).
- ST segment at high take-off > ST segment at 40 ms > ST segment at 80 ms
- ST segment is followed by negative and symmetrical T-wave.
- The duration of QRS in V1 is longer than in RBBB and longer than in V6 (mismatch).

### Type 2 Brugada pattern in V1-V2:

- High take-off that does not coincide with the J-point  $\geq 2$  mm.
- The descending arm of r' coincides with the beginning of ST segment.
- ST segment upslope is at least 0.5 mm.
- ST segment is followed by positive T wave in V2.
- The characteristics of the triangle formed by r' enables the different criteria to be defined that are useful for diagnosis: a) the duration of the base of the triangle formed by r' at 5 mm from the high take-off is greater than 3.5 mm, and b) the duration of QRS in Brugada type 2 syndrome is longer than in other cases with r' in V1, and there is a mismatch between V1 and V6.

### Type 2 Brugada pattern versus ordinary "innocent" incomplete RBBB

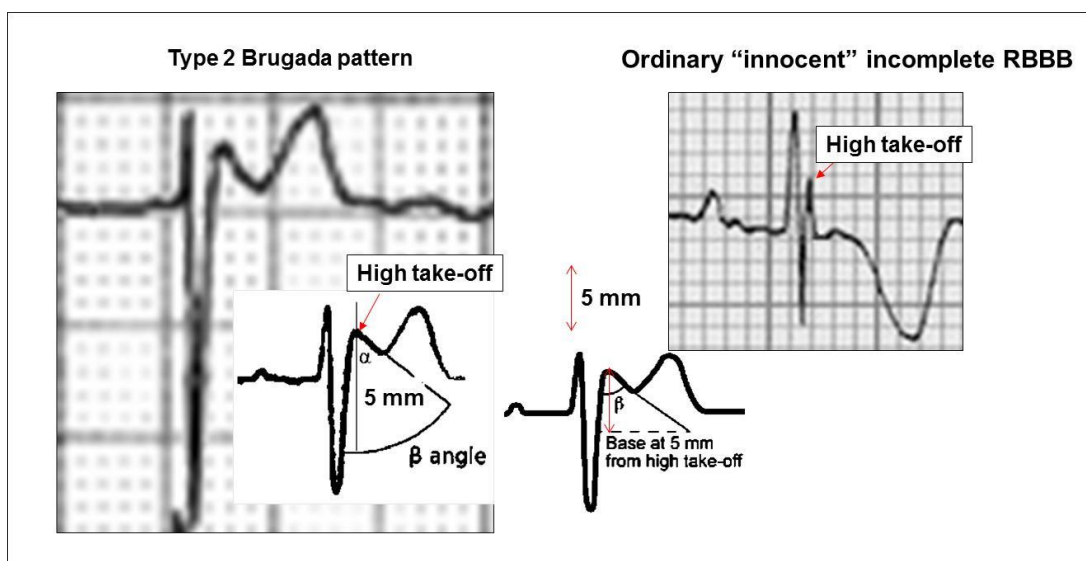


**Figure x.** Type 2 Brugada pattern versus ordinary “innocent” incomplete RBBB <sup>4 3</sup>.

<b><math>\beta</math> angle</b>	<b>&gt; 36°</b>	<b>Acute</b>
<b><math>\alpha</math> angle</b>	<b>Major</b>	<b>Minor</b>
<b>T-wave</b>	<b>Positive or plane</b>	<b>Negative</b>
<b>Duration of triangle base from the high take-off at 5 mm</b>	<b>Greater than 3.5 mm</b>	<b>Minimal</b>
<b>High take-off</b>	<b>Wide</b>	<b>Acute</b>

**Typical Brugada type 1 pattern after ajmaline injection (80 mg)**

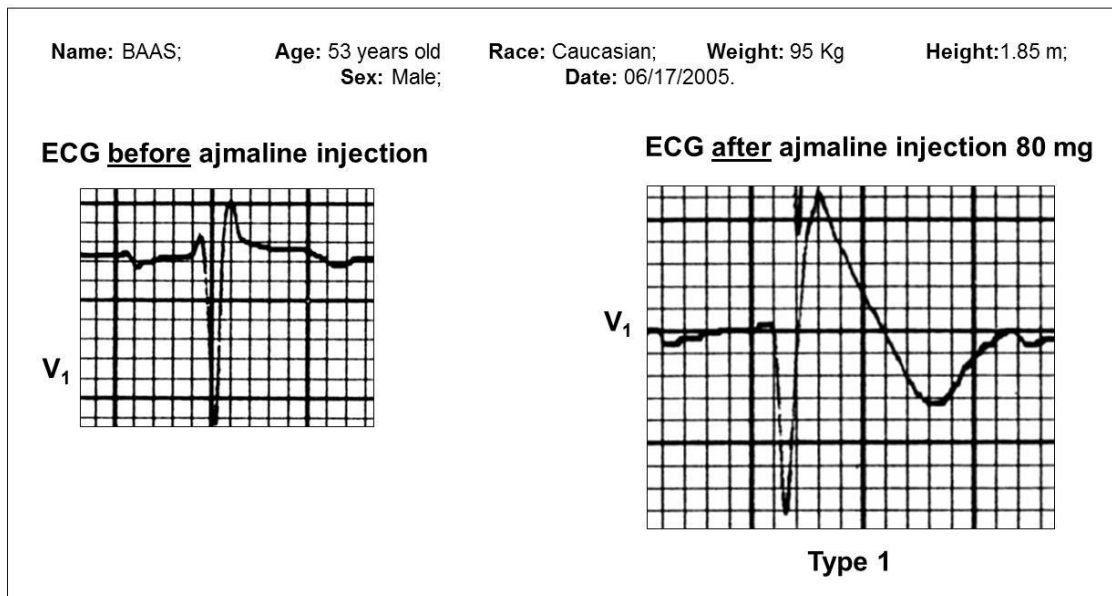


**Figure x.** ECG.

**Typical Brugada type 1 pattern after ajmaline injection (80 mg)**

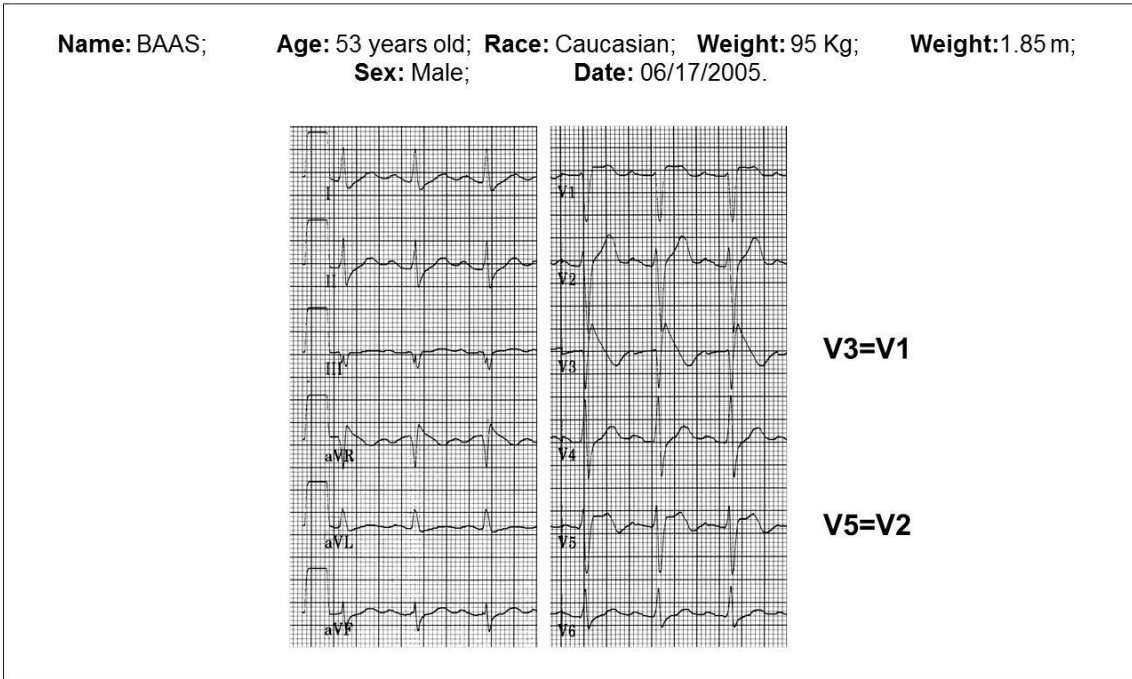


**Figure x.** Typical Brugada type 1 pattern after ajmaline injection (80 mg).

**Value of ECG and VCG in the diagnosis and prognosis of the Brugada syndrome**

**Signature ECG-change**

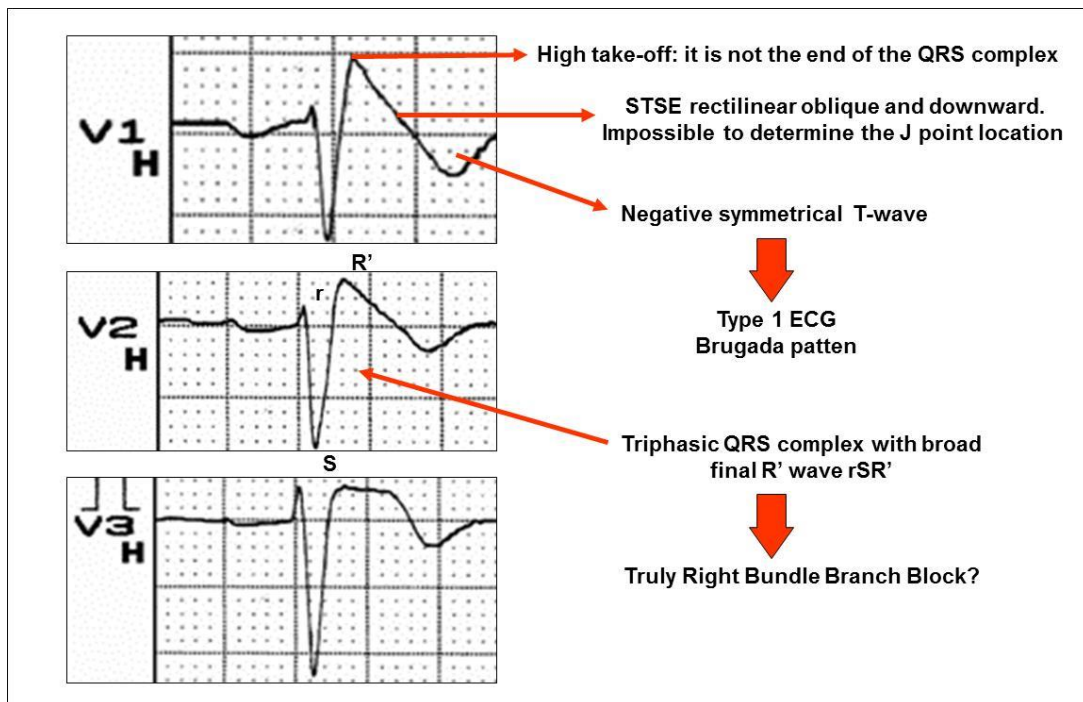


**Figure x.** Type 1 Brugada pattern: J point and ST segment elevation  $\geq 2$  mm, with upper convexity or descending oblique rectilinear followed by negative T wave in the right precordial leads (V1-V2 or from V1 through V3) and/or high right precordial leads V1H, V2H and V3H.

**ECG/VCG correlation in the horizontal plane TCD (Terminal Conduction Delay or Right End Conduction Delay(RECD)) in Type 1 BrS and truly RBBB**

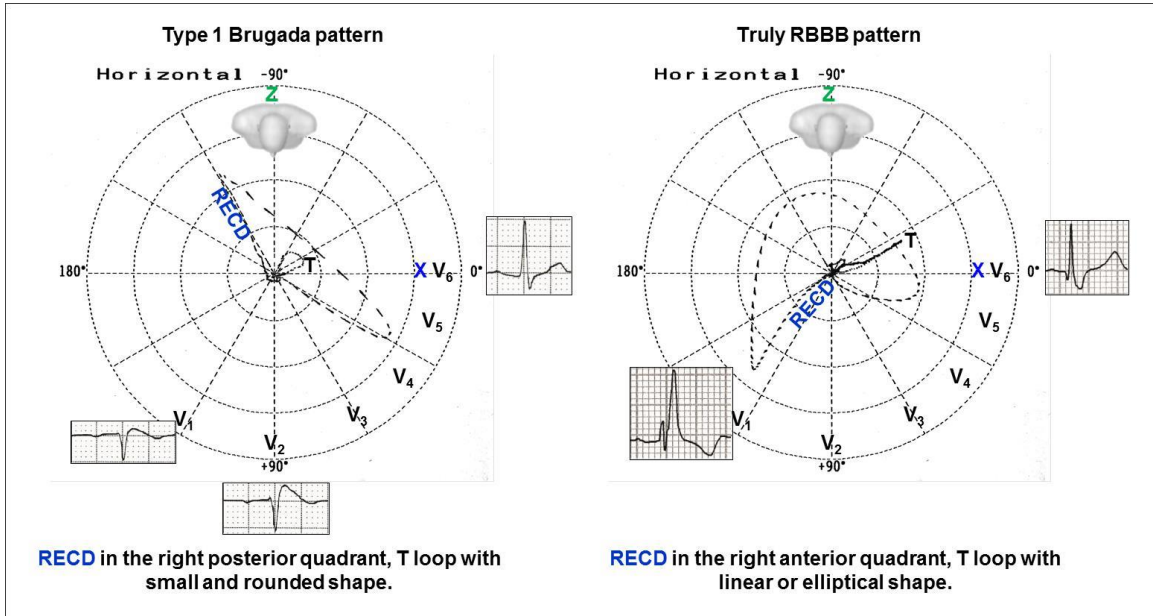


**Figure 87.** ECG/VCG correlation.

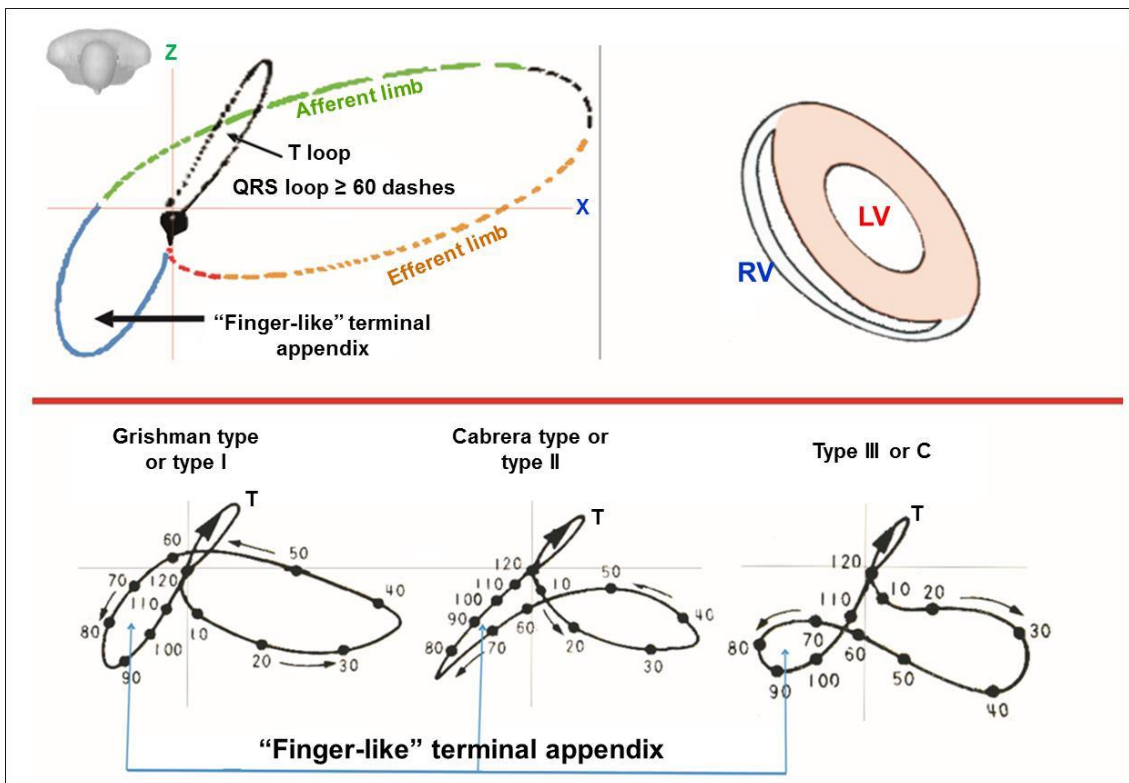


**Figure x.** Figure.

## Frontal plane

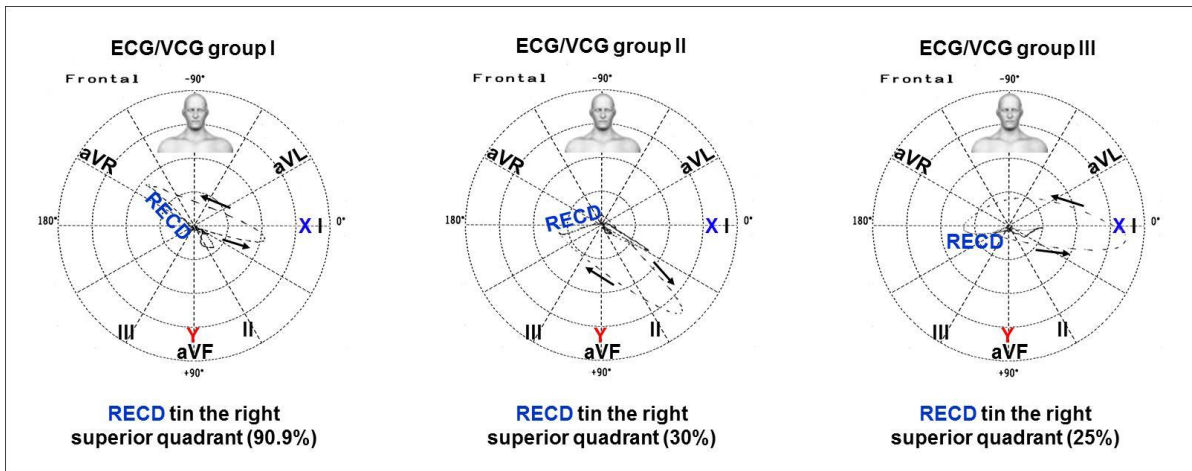


Figure 89. VCG.

## QRS loop types in the frontal plane

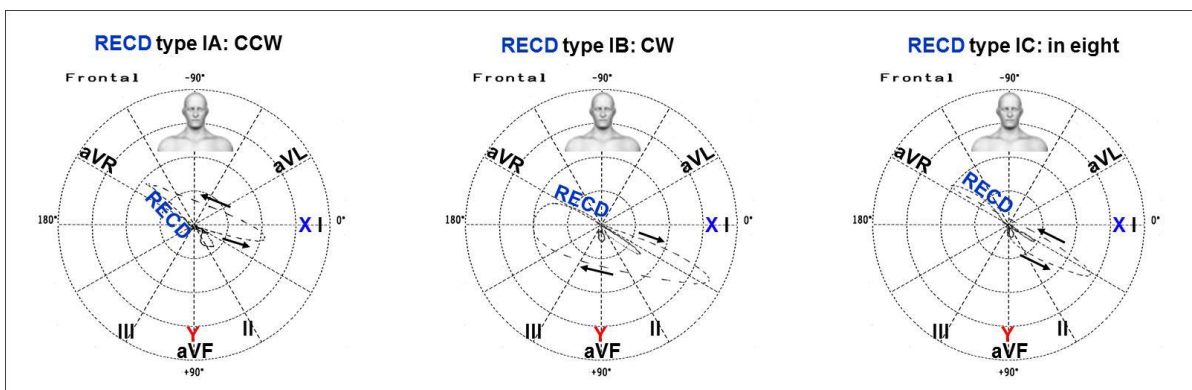
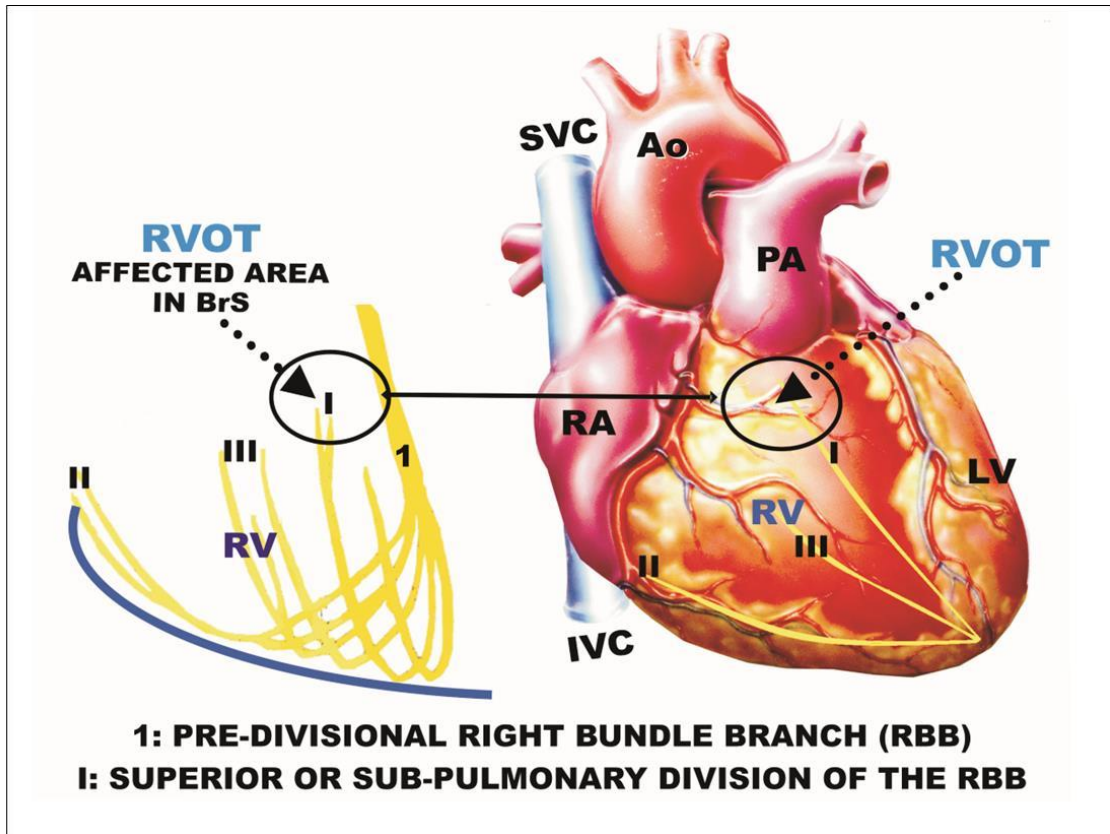


Figure x. The figure shows the three possible types of QRS loop rotations in BrS in the frontal plane. Type IA - QRS loop with counterclockwise rotation (CCW) and extreme superior QRS axis deviation: Right Superior Fascicular Block. >90% of the Brugada patients shows RECD in the right superior quadrant near aVR (RVOT).





**Figure x.** The figure shows the three hypothetical clusters of fibers (I, II and III) on the free wall of the right ventricle, and the partial superior right Hisian system affected in BrS: “Right Superior Fascicular Block” (depolarization mechanism).

**ECG/VCG differential diagnosis between right superior fascicular block (RSFB) and left anterior fascicular block (LAFB)**

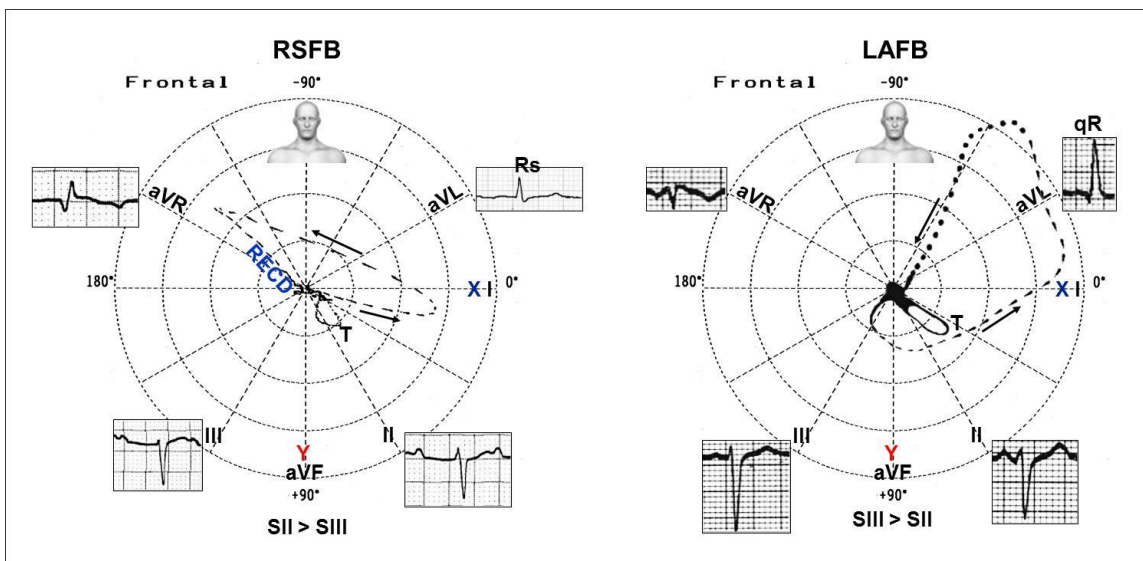


**Figure x.** ECG/VCG differential diagnosis between right superior fascicular block (RSFB) and left anterior fascicular block (LAFB).

	<b>LAFB</b>	<b>RSFB</b>
<b>Initial 10 ms vector of QRS loop</b>	Heading downward and to the right	Heading downward and to the left
<b>QRS morphology in I &amp; aVL</b>	qR pattern	Rs
<b>SII/SIII ratio</b>	SIII>SII	SII>SIII
<b>Location of end conduction delay (ECD)</b>	In the left superior quadrant when present	In the right superior quadrant <sup>94</sup>
<b>Prominent R wave in aVR (R-wave <math>\geq</math> 0.3 mV)</b>	Absent	It could be present and it is called aVR sign <sup>11</sup> .
<b>Morphology of QRS loop of vectorcardiogram in the horizontal plane</b>	Similar to normal	Similar to type-C right enlargement pattern: initial vector to the front and leftward, counterclockwise rotation and 20% or more of the area of the loop located in the right posterior quadrant in the horizontal plane <sup>95</sup>

Name: MK; Age: 38 y/o; Gender: Male; Ethnic Group: Asian; Weight: 68 kg; Height: 1.70 m

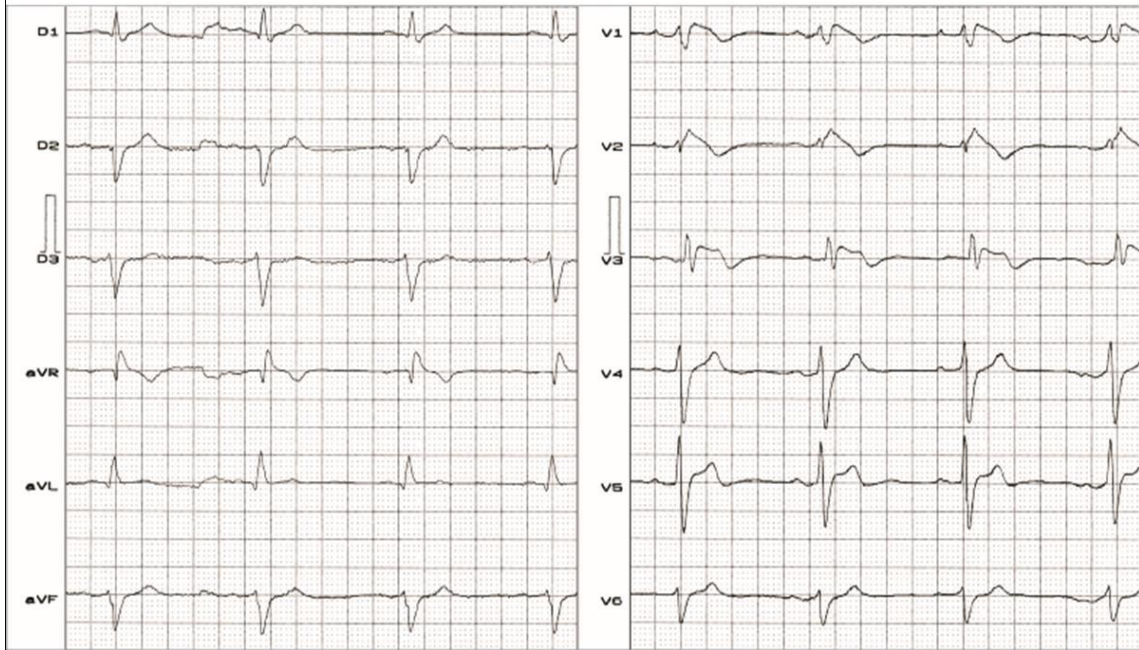


**Figure x.** Clinical diagnosis: Syncope. Positive familiar background of sudden death in young ( $\leq 35$  y/o) first-degree relative. Genetic research performed: negative. ECG diagnosis: Sinus bradycardia (HR  $< 60$  bpm), Brugada type 1 ECG pattern, prolonged QRS duration, aVR signal: final R wave of aVR lead  $> 3$  mm, fQRS in V1-V2. Extreme left axis deviation: Left anterior fascicular block? or Right superior fascicular block?

### ECG/VCG correlation

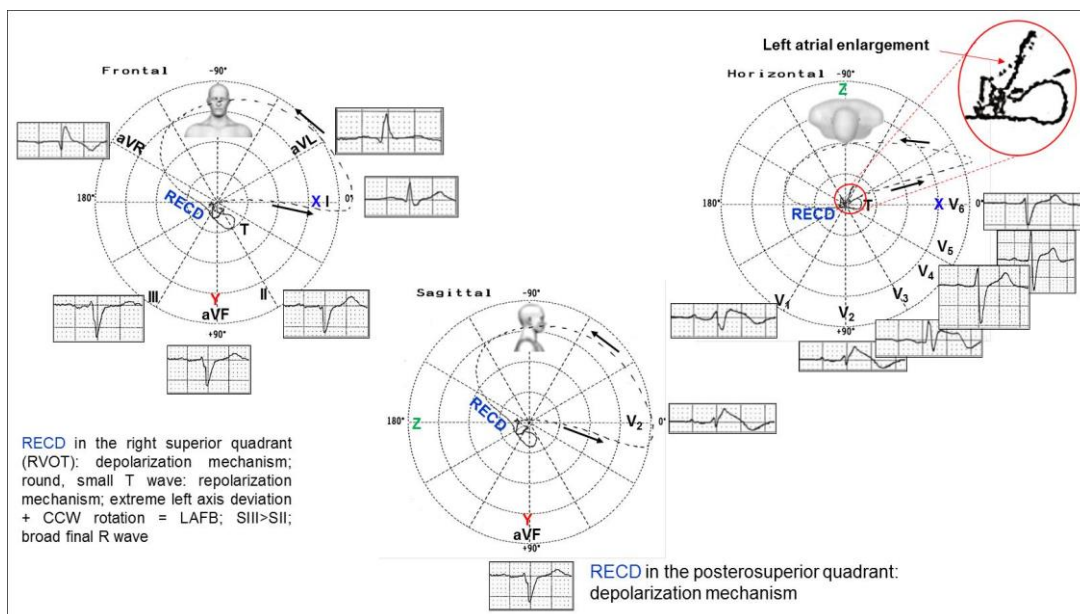


**Figure x.** ECG/VCG correlation.

**ECG with typical type 1 Brugada pattern and final part broadening by superior fascicle block of RBBB**

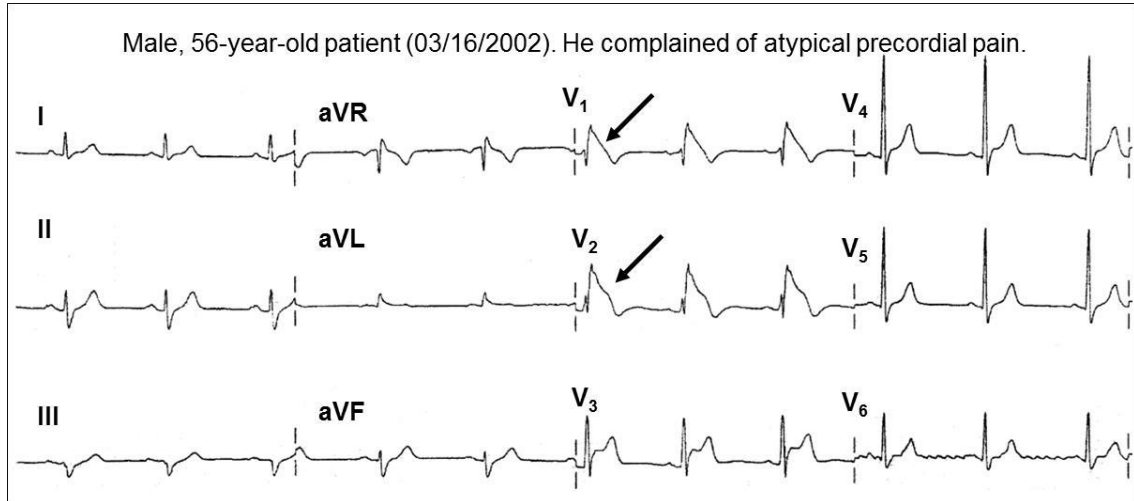


**Figure x.** Final part widening by the superior, anterosuperior or subpulmonary fascicle of the RBB, type I according to our classification. Extreme shift of SAQRS to the left in the left superior quadrant  $-45^\circ$ . ST segment and J point elevation with convex to the top morphology in V1 and V2 and saddle type in V3. aVR with D wave broadening: “crista delay” or RV outflow tract widening. S waves in left precordial leads V5-V6. SII >SIII. This information is very important for a differential diagnosis with left anterior fascicular block. Structural heart disease was not detected with noninvasive and invasive methods. Conclusion: ECG with typical Brugada type 1 pattern, and final part widening by superior fascicle block of RBB.

## ECG/VCG correlation of Brugada syndrome in the frontal and horizontal planes

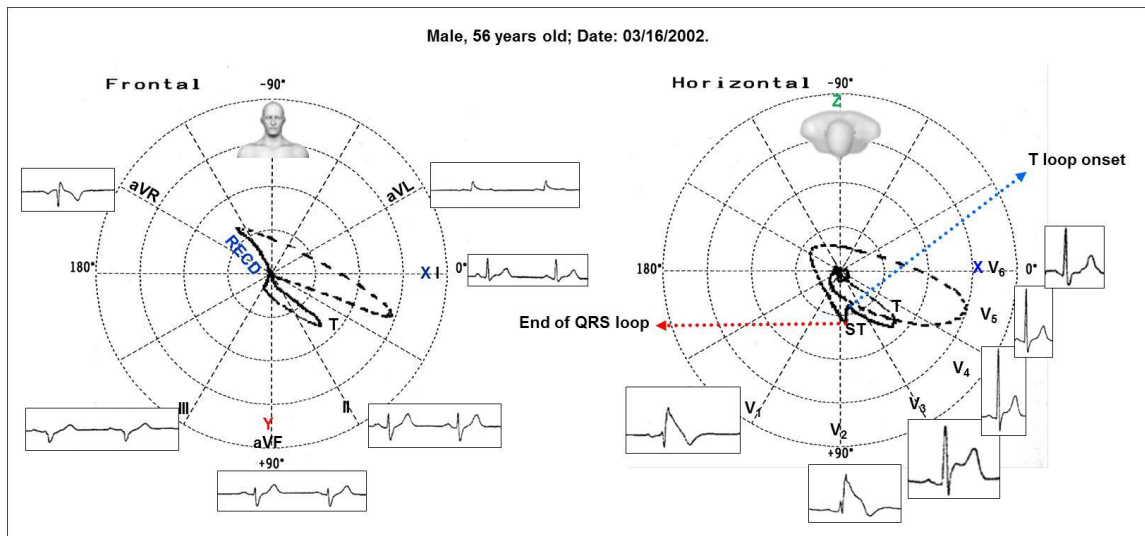


**Figure x.** The end of QRS loop does not coincide with T loop onset (as it occurs in normal conditions) since there is elevation both in the J point and the ST segment. Conclusion: it is the first VCG of Brugada syndrome shown in world literature. End conduction delay (ECD) by superior fascicle of the RBB. Type IA of our classification.

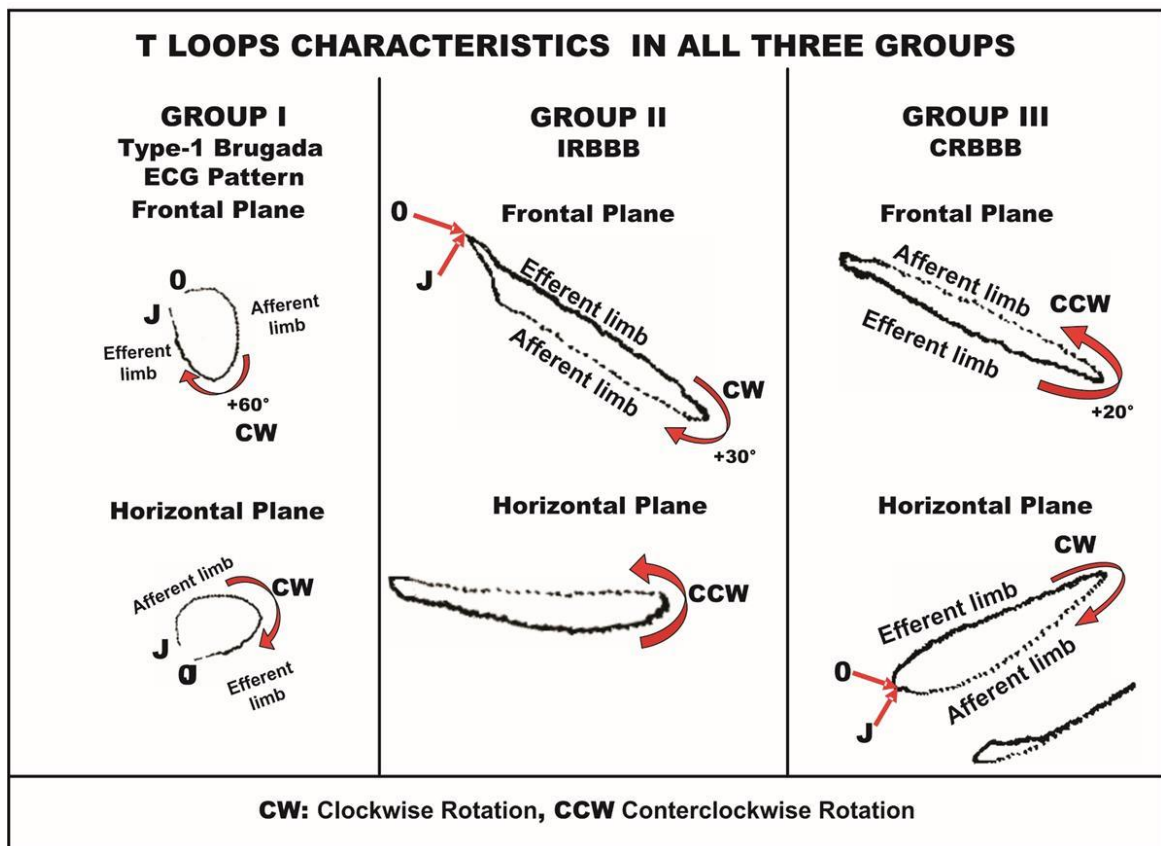


**Figure x.** T loops characteristics in all three groups.

**Localization of right precordial leads and accessory high parasternal leads <sup>96</sup>**

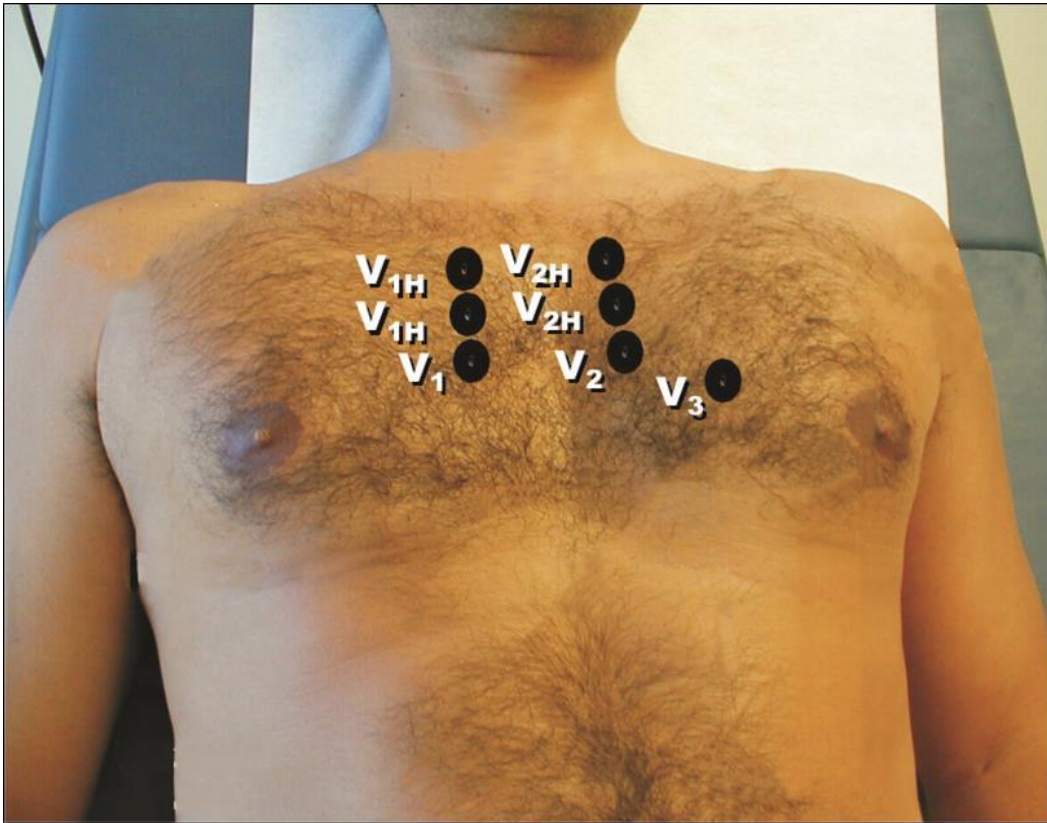


**Figure x.** V1 – over the 4th intercostal space, just to the right of the sternum; V2 – over the 4th intercostal space, just to the left of the sternum; V3 – midway between V2 and V4; V1H – over the 3rd or 2nd intercostal space, just to the right of the sternum; V2H – over the 3rd or 2nd intercostal space, just to the left of the sternum.

**Demonstration of transient spontaneous type 1 Brugada pattern with lower heart rate**

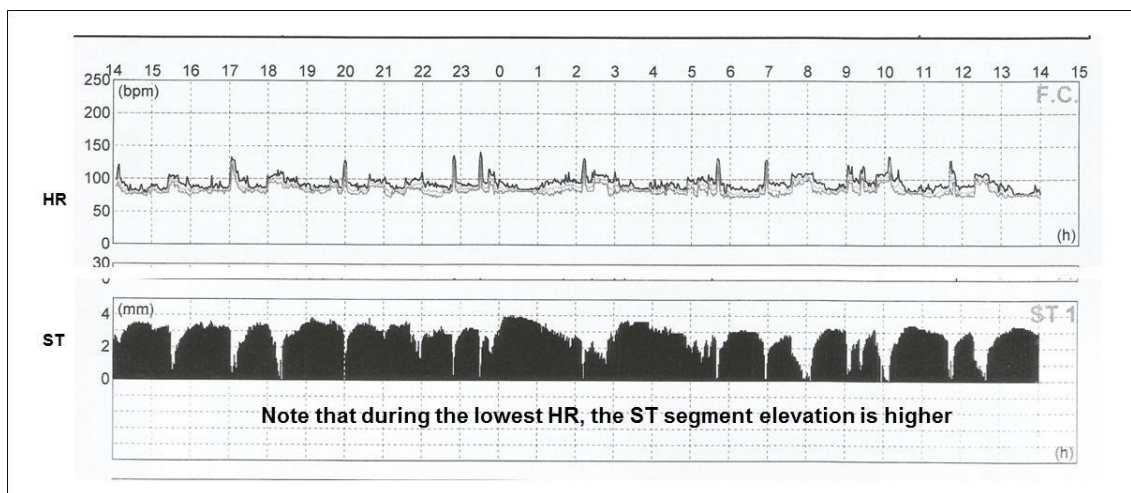


**Figure x.** Heart rate x Brugada pattern histogram.

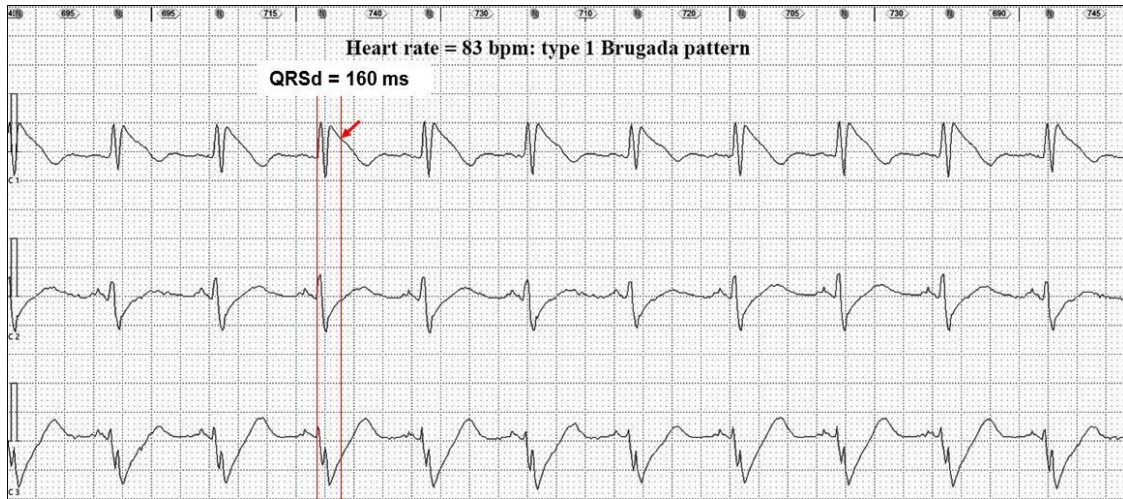


**Figure x.** Autonomic influences, such as high parasympathetic activity with lower heart rate, are triggers of arrhythmia and provide important mechanistic insights into the ionic and cellular mechanisms involved.

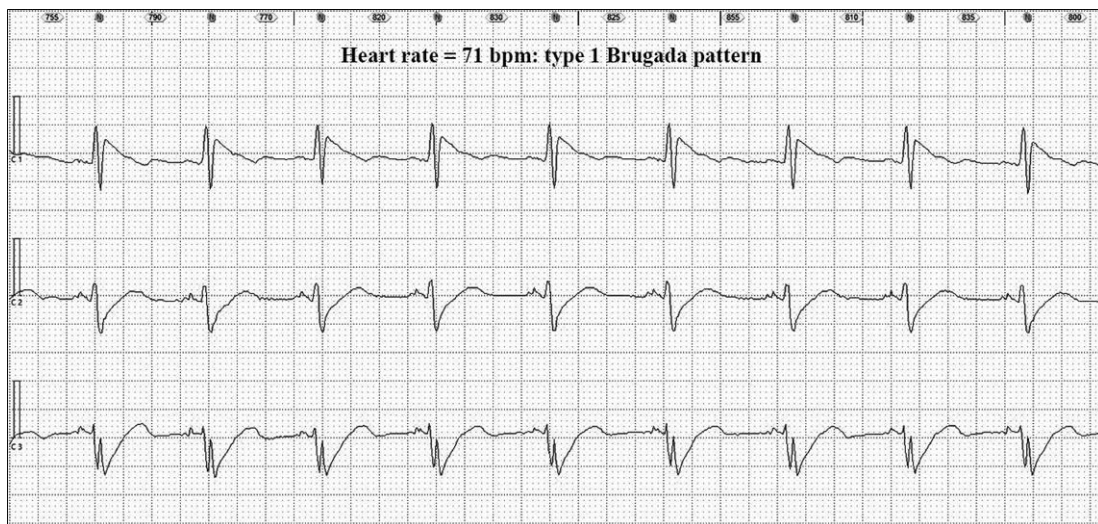


**Figure x.** ECG.

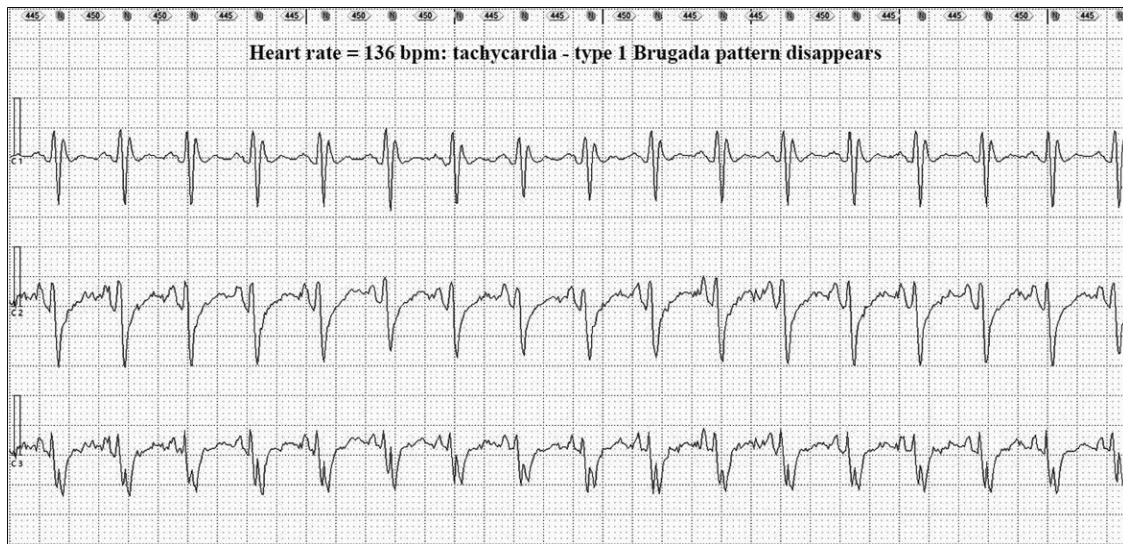


**Figure 1x.** 24h – Holter monitoring during tachycardia. Experimental studies suggest that BrS-linked SCN5A mutations reduce sodium current more at fast heart rates <sup>97, 98</sup>. Experiments in right ventricular tissue preparations indicate that tachycardia aggravates ST-segment elevation in BrS <sup>99, 100</sup>.

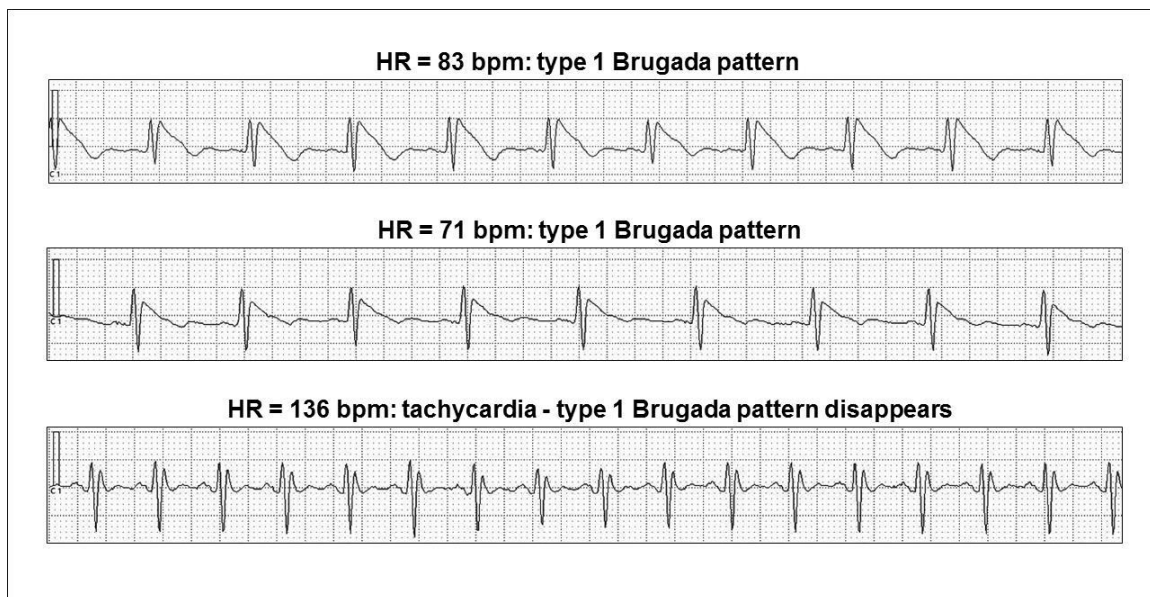


**Figure x.** ECG.



## ECG markers in identifying patients at risk in Brugada syndrome

1. Augmented P-wave duration in lead II, P-wave dispersion <sup>101</sup>.
2. PR prolongation consequence of HV split or HV prolongation <sup>21</sup>.
3. Presence of prominent final R wave on aVR lead R wave  $\geq 3$  mm or R/q  $\geq 0.75$  in lead aVR (aVR sign). Slow conduction at the RVOT may contribute to the induction of VF by PVS <sup>11</sup>.
4. The presence of a spontaneous type I ECG, history of syncope, ventricular effective refractory period  $<200$  ms, and QRS fragmentation seem useful to identify candidates for prophylactic ICD <sup>52</sup>.
5. Inferolateral early repolarization <sup>102</sup>.
6. Prolonged QRS duration measured from lead II or lead V2  $\geq 120$  ms <sup>27, 103</sup>.
7. QTc interval more than 460 ms in lead V2 wave <sup>22</sup> and QT-interval prolongation in right precordial leads <sup>30</sup>. Increase in QRS complex duration ( $>110^\circ$ ) in the right precordial leads, in absence of CRBBB: parietal block.
8.  $T_{\text{peak}} - T_{\text{end}}$  prolongation and  $T_{\text{peak}} - T_{\text{end}}$  dispersion <sup>31</sup>.
9. Dynamic alterations in the amplitude of the ST elevation wave <sup>22</sup>.
10. Loss of rate-dependent QT dynamics <sup>104</sup>.
11. The presence of horizontal (as opposed to rapidly ascending) ST segment after the J point <sup>24</sup>.
12. Augmentation of the ST segment elevation during the early recovery phase of exercise test <sup>33</sup>.
13. Deep negative T wave in lead V1.
14. The presence of atrial fibrillation <sup>105</sup>.
15. The presence of late potentials (LPs) <sup>106</sup>.

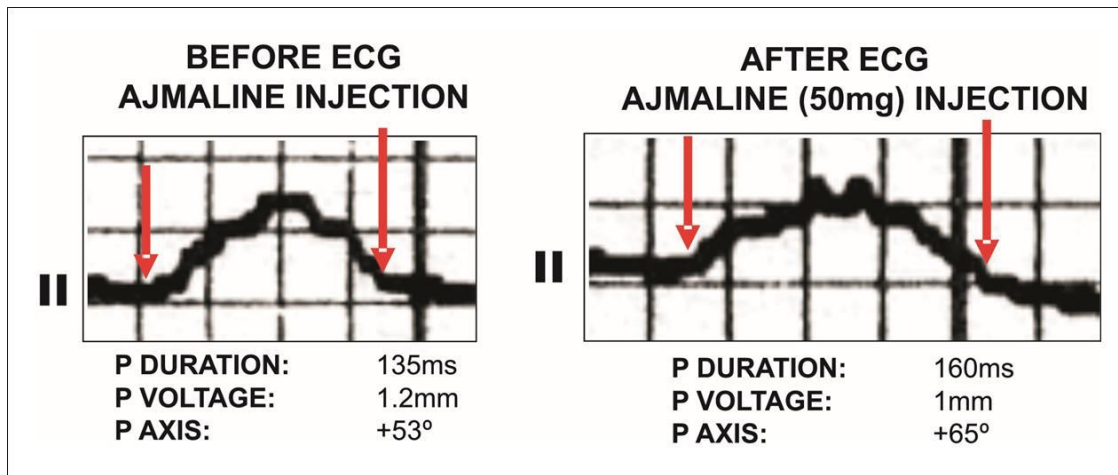


**Figure x.** The tracing shows the P wave in a patient with BrS and positive SNC5A mutation, performed before and immediately after ajmaline test (1 mg/kg). P wave duration (Pd) before the injection is prolonged (Pd=135 ms). After drug administration Pd wave increases more (Pd=162 ms). These atrial dromotropic disorders could be the substrate for reentrant atrial tachycardias such as AF.

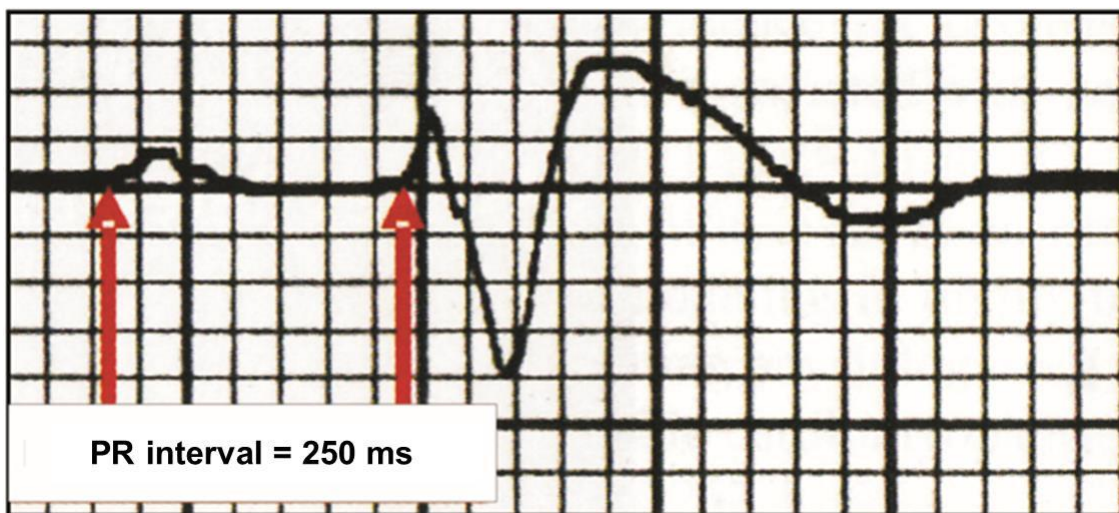


**Figure x.** The figure shows a tracing of a symptomatic patient with Brugada syndrome after intravenous ajmaline injection. First-degree atrioventricular block (PR interval = 216 ms) and Brugada type-1 ECG pattern in V1 lead (positive test). In BrS the PR interval of ECG and the His bundle electrogram in approximately 50% of the cases are prolonged, even reaching sometimes figures of 100 ms (Yokokawa 2007). This prolongation of the PR interval is observed predominantly in cases where the SCN5A gene mutation can be proven (carriers). The presence of a prolonged HV interval is possible in HBE by the existence of intra-His or infra-His block. PR prolongation consequence of HV split or HV prolongation is considered another ECG risk marker <sup>33</sup>.

**Terminal broad R wave of the QRS complex in lead aVR (Babai Bigi, Aslani et al. 2007)**

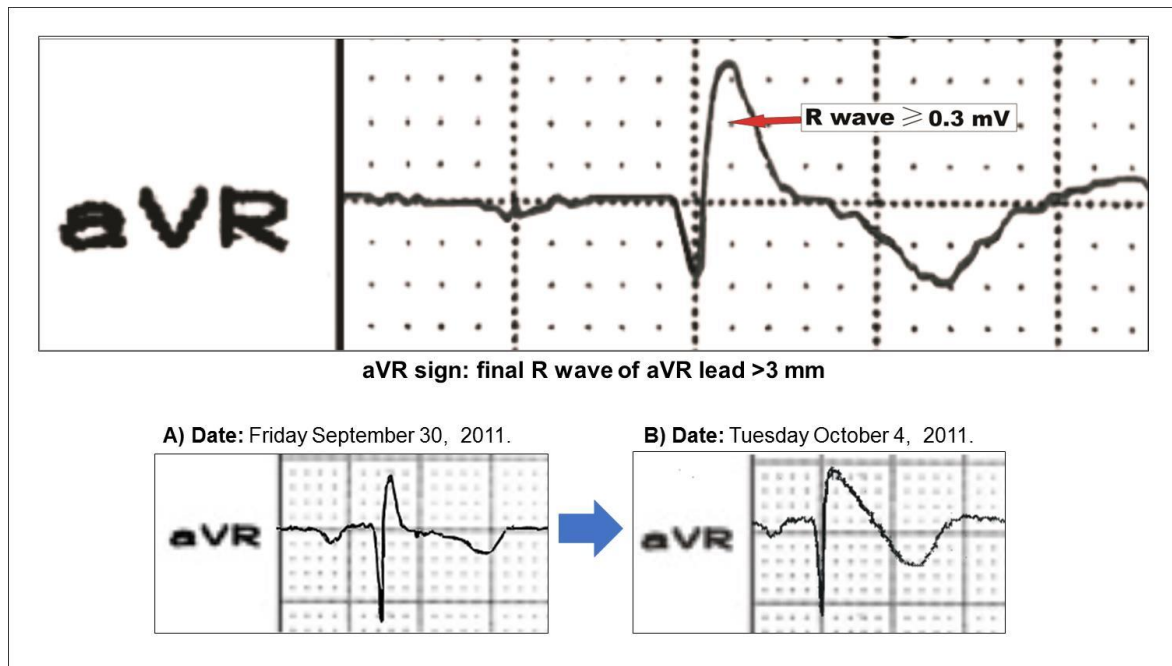


**Figure x.** The aVR sign: Presence of prominent final R wave on aVR lead; R wave  $\geq 3$  mm or R/q  $\geq 0.75$  in lead aVR (aVR sign). Slow conduction at the RVOT may contribute to the induction of VF by PVS.

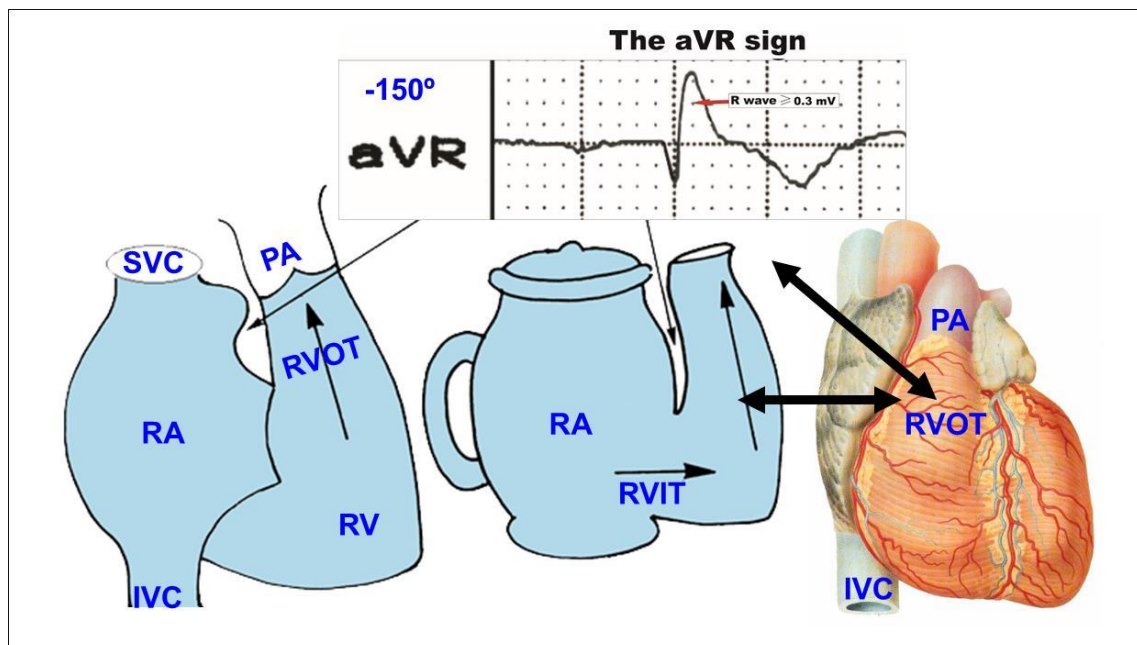


**Figure x.** The BrS affects predominantly the right ventricle in the right ventricle outflow tract (RVOT) epicardium <sup>107</sup>. The larger part of clinical evidence supports the presence of right end conduction delay (RECD) as part of the process of BrS pathophysiology in

the RVOT, as a consequence of structural abnormalities in the heart as part of BrS<sup>108</sup>. On the other hand, in the concealed forms of arrhythmogenic right ventricular cardiomyopathy/dysplasia (ARVC/D), the RECD pattern can also be observed showing type-1 ECG pattern. This pattern was shown many years ago by Guy Fontaine et al<sup>109</sup>.

### Fragmented QRS in Brugada Syndrome

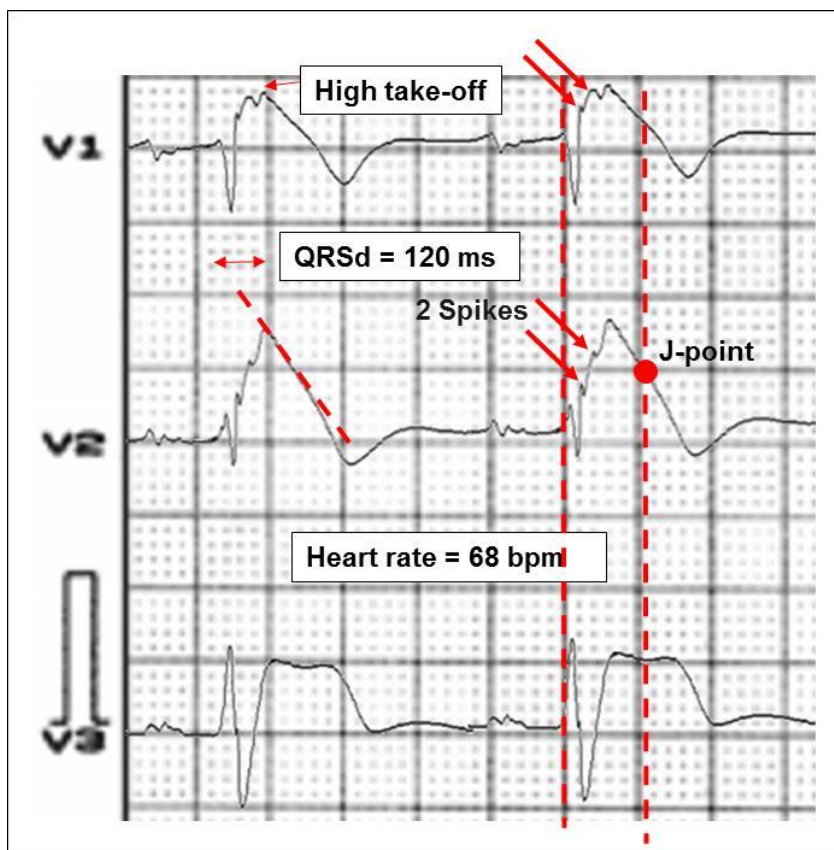


**Figure x.** Dotted lines show onset and termination of the QRS complex. Two spikes are observed at the upstroke of the S wave in leads V1 and V2. Fragmented wide QRS complex in a 35-year-old Asian male patient with BrS. f-QRS appears to be a marker for the substrate for spontaneous VF in BrS and predicts patients at high risk of syncope. It is a conduction abnormality within the QRS complex<sup>110</sup>.

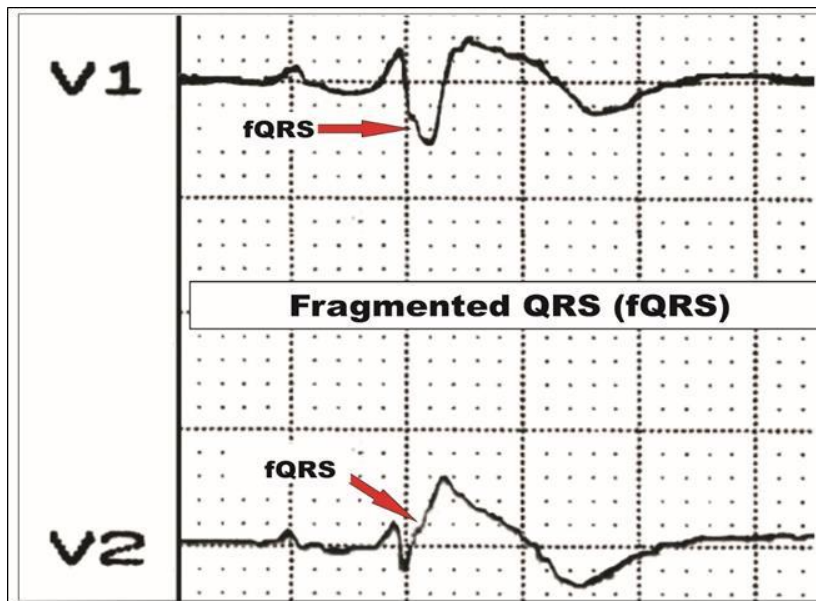


**Figure x.** Presence of a “notch” within a non-wide QRS complex in two adjacent leads (V1-V2.): f-QRS. It is a non-invasive marker of events <sup>111</sup> (Das 2009).

**Entities where fQRS is used as a non-invasive marker of events <sup>111</sup> (Das 2009)**

- Coronary artery disease <sup>112</sup> where it represents a conduction delay of the stimulus and is associated to an increase in mortality and arrhythmic events in these patients.
- Non-ischemic cardiomyopathies <sup>112</sup>. In non-ischemic dilated cardiomyopathy with narrow QRS to predict dyssynchrony <sup>113</sup>
- Arrhythmogenic right ventricular cardiomyopathy/dysplasia (ARVC/D) <sup>114</sup>
- Cardiac sarcoidosis <sup>115</sup>
- Congenital heart diseases (<sup>116</sup>
- Brugada syndrome <sup>117</sup>
- Acquired long QT syndrome <sup>118</sup>

The existence of fQRS plays an important role in the appearance of Torsades de Pointes (TdP) in patients with acquired long QT interval.

## Coexisting early repolarization pattern and Brugada syndrome: recognition of potentially overlapping entities

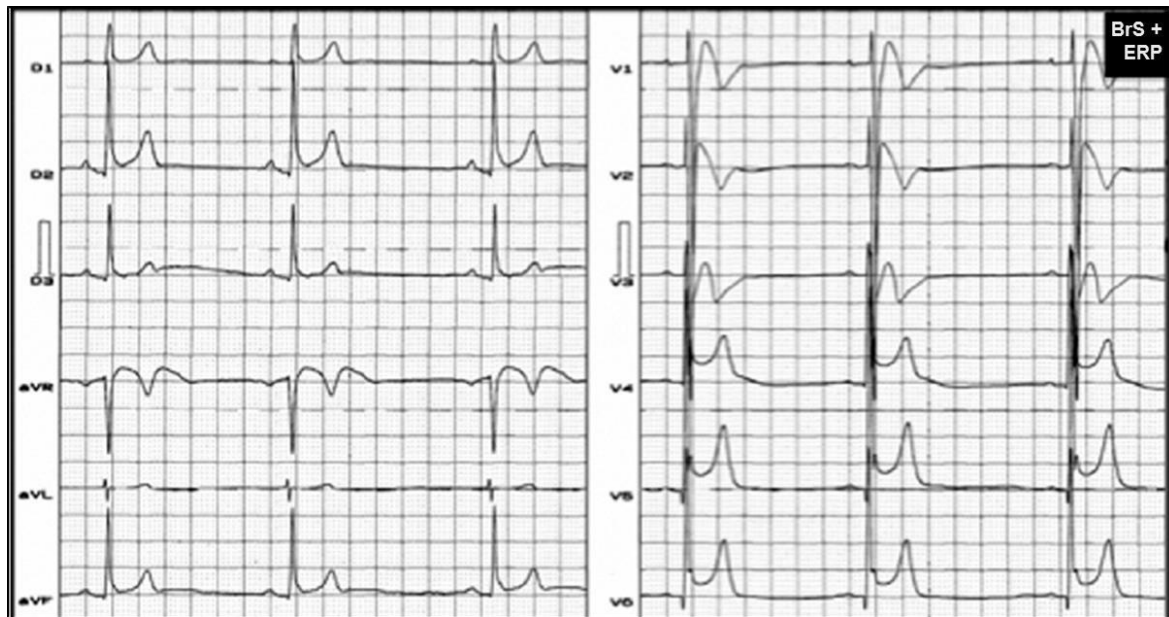


**Figure 110.** Coexistence ECG that shows concomitant early repolarization pattern in inferior lateral leads associated with type 1 Brugada pattern in young soccer player. Caucasian man <sup>119</sup>.

**J-wave syndromes including BrS and ERS is associated with life-threatening ventricular arrhythmias <sup>120</sup>**

### Similarities between BrS and ERS.

#### Male predominance

1. Occurrence of the first event predominantly at the middle age
2. Ventricular arrhythmias triggered by short-coupled PVCs during slower heart rates
3. Response to  $\beta$ -agonists, quinidine and phosphodiesterase III inhibitors
4. Prominent  $I_{to}$  activity
5. Shared mutations of the genes.

On the other hand, there are also some differences including:

1. Hyperthermia causing augmented J waves in BrS by inactivation of  $I_{Na}$  and recovery of  $I_{to}$ , hypothermia causing augmented J waves in early ERS by slower  $I_{Ca}$  and higher  $I_{to}$  activity
2. Right ventricular outflow tract involvement in BrS and inferolateral left ventricular involvement in ERS
3. Higher occurrence of late potentials and atrial fibrillation in BrS
4. Increased J wave manifestation with sodium channel blockers in BrS in contrast to decreased J waves in ERS.
5. BrS ECG pattern could be masked by therapeutic hypothermia.
6. When unipolar left ventricular epicardial electrograms used during provocation with sodium channel blockers, J waves increase whereas reduced J waves on the surface electrogram due to widening of QRS <sup>121</sup>.

### Typical ECG of Brugada Syndrome

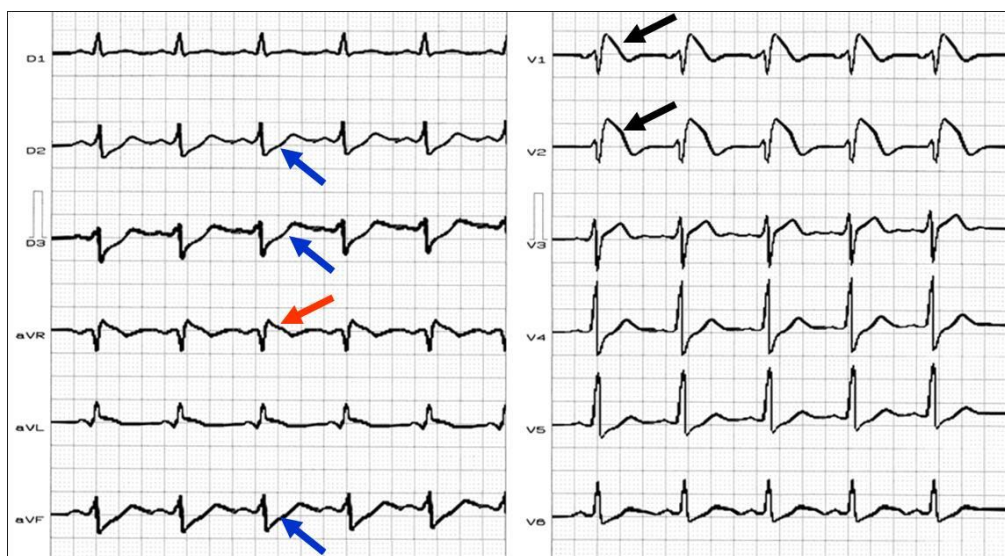


**Figure x.** J point and ST segment elevation, convex to the top, ST segment in right precordial leads from V1 through V2 (black arrows): Brugada sign or idiopathic J wave. Unipolar aVR lead that heads toward the RV epicardium above the outflow tract, which shows subtle ST segment and J point elevation (red arrows). Inferior leads show reciprocal or mirror images (blue arrows).

**Prolonged QRS duration measured from lead II or lead V2  $\geq 120$  ms (Junttila, Brugada et al. 2008, Junttila, Gonzalez et al. 2008).**

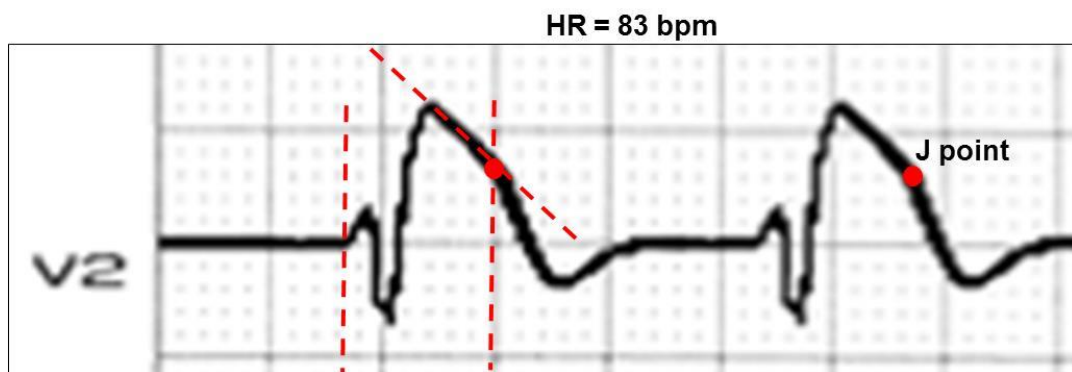


**Figure 112.** Vertical dotted lines show onset and termination of the QRS complex in V2. In this case QRSd = 165 ms. It is an ECG marker of events.



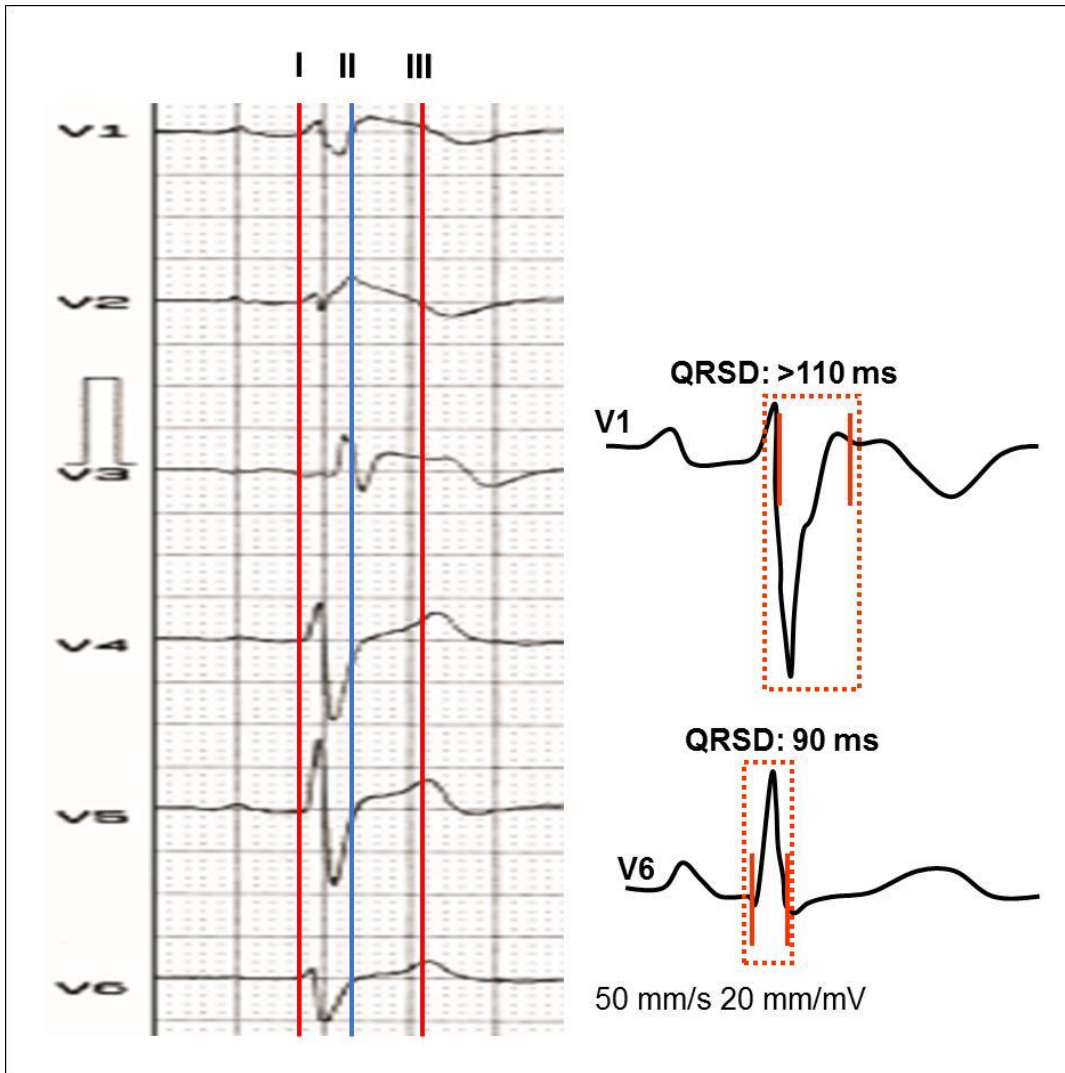


**Figure x.** Increase in QRS complex duration (>110°) in right precordial leads, in absence of CRBBB: parietal block; I: Onset of the QRS complex; II: Termination of the QRS complex from V4-V6; III: Termination of the QRS complex from V1-V3. QRSD of  $V1+V2+V3 / V4, V5, V6 > 1.2$ . This feature is considered typical of ARVC/D, but it is also observed in BrS leads <sup>30</sup>.

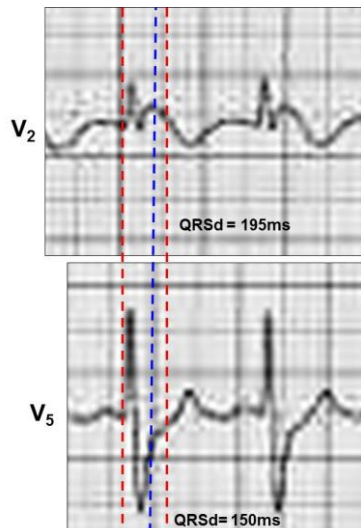


**Figure x.** Pitzalis et al<sup>30</sup> identified the selective prolongation of QT interval duration in the right precordial leads (V1 to V3) in comparison to the left ones (V4 to V6). As the QT interval is made up by ventricular depolarization (QRS) plus ventricular repolarization (ST/T). We think that this selective prolongation represents a certain degree of parietal block in the RVOT, as the one observed in ARVC/D. If the QT interval is prolonged only from V1 to V3, being normal or lesser from V4 to V6, it is clear that this increase may be due to prolongation of ventricular depolarization (QRS complex) and/or by ST/T prolongation (repolarization). If we admit that in BrS there is some degree of branch block, clearly the QT interval prolongation is due partly to this. The QTc interval constitutes the classical measurement for ventricular repolarization; however, this parameter includes ventricular depolarization (QRS), and therefore represents the so-called electric systole, which includes depolarization (QRS) and ventricular repolarization (ST/T = JT interval).

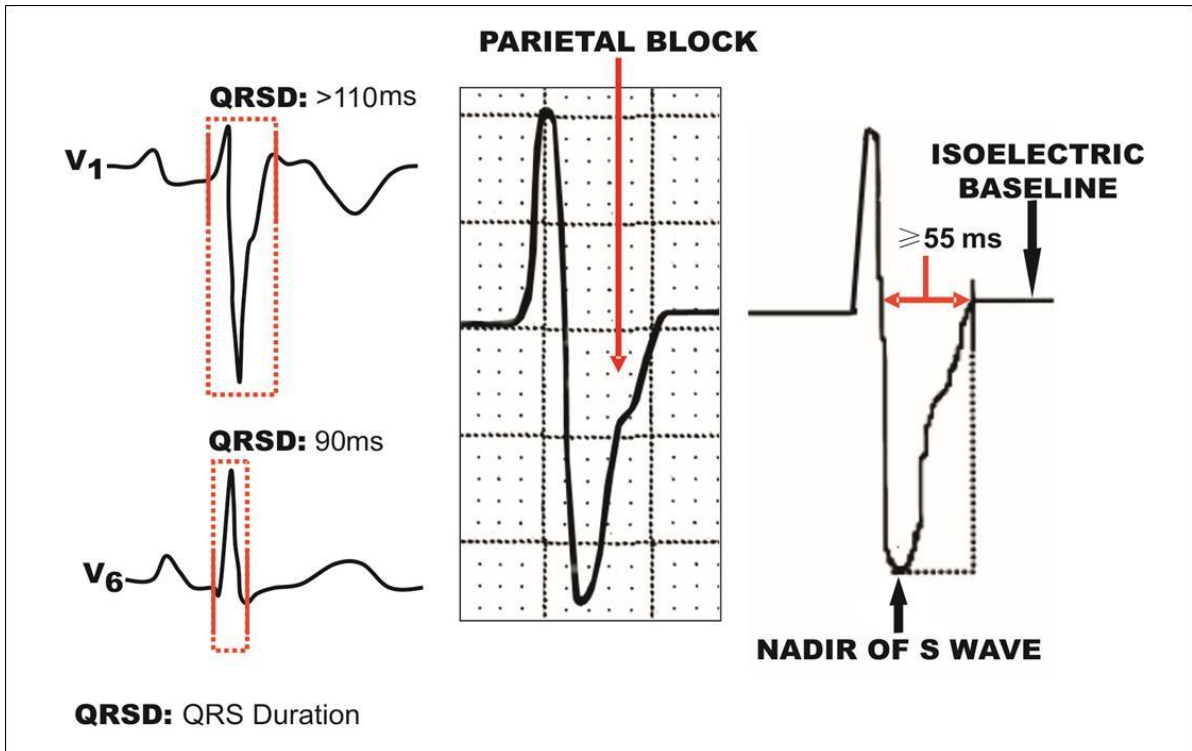


**Figure x.** Pitzalis et al <sup>30</sup> identified the selective prolongation of QT interval duration in the right precordial leads (V1 to V3) in comparison to the left ones (V4 to V6). As the QT interval is made up by ventricular depolarization (QRS) plus ventricular repolarization (ST/T) we think that this selective prolongation represents a certain degree of parietal block in the RVOT, as the one observed in ARVC/D.

### **$T_{\text{peak}} - T_{\text{end}}$ prolongation and $T_{\text{peak}} - T_{\text{end}}$ dispersion**

The normal value of  $T_{\text{peak}}/T_{\text{end}}$  interval (Tpe) is 94 ms in men and 92 in women when measured in the  $V_5$  lead. Tpe prolongation to values  $\geq 120$  ms is associated to a greater number of events in patients carriers of BrS

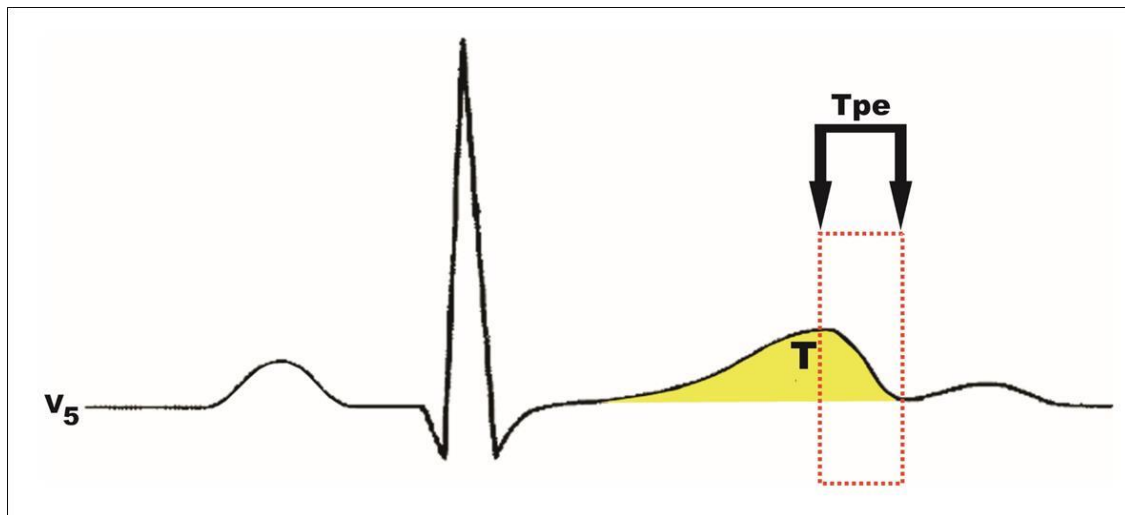


**Figure x.** Interval elapsed from the apex to the end of T wave ( $T_{\text{peak}}-T_{\text{end}}$  interval or Tpe). Tpe may correspond to transmural dispersion of repolarization and consequently, the amplification of this interval is associated to malignant ventricular arrhythmias.

Bigi et al. <sup>122</sup> studied the clinical predictors of AF in BrS. Of the 28 patients with Type 1 ST-segment elevation ECG pattern, 15 had paroxysmal AF. All of them had previous life-threatening cardiac events (8 had syncope, 2 had VF, 4 had polymorphic VT, and 1 had aborted SCD). Multiple regression analysis did not show any correlation between various parameters such as left atrial size, age, and P-wave dispersion. The authors concluded that the history of previous life threatening cardiac events is the strongest predictor of AF in Brugada syndrome.

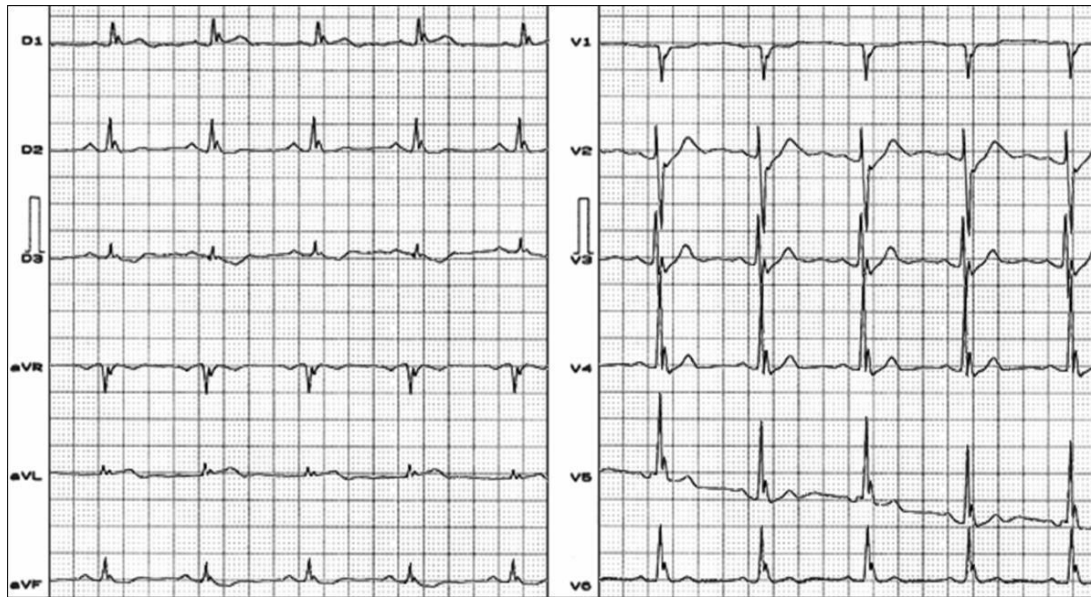


**Figure 1x.** Sinus rhythm J-wave in anterolateral and inferior leads without ST segment elevation.

**The patient during atrial fibrillation J wave in anterolateral leads without ST segment elevation and type 2 Brugada pattern in V2**

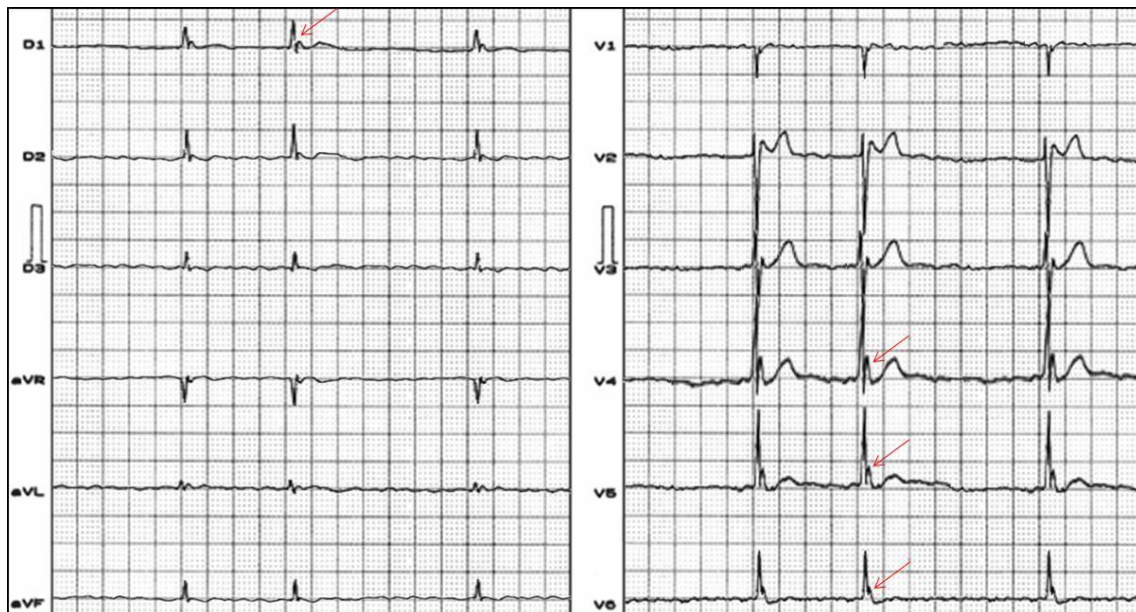


**Figure x.** ECG.

**We performed intravenous ajmaline test.**

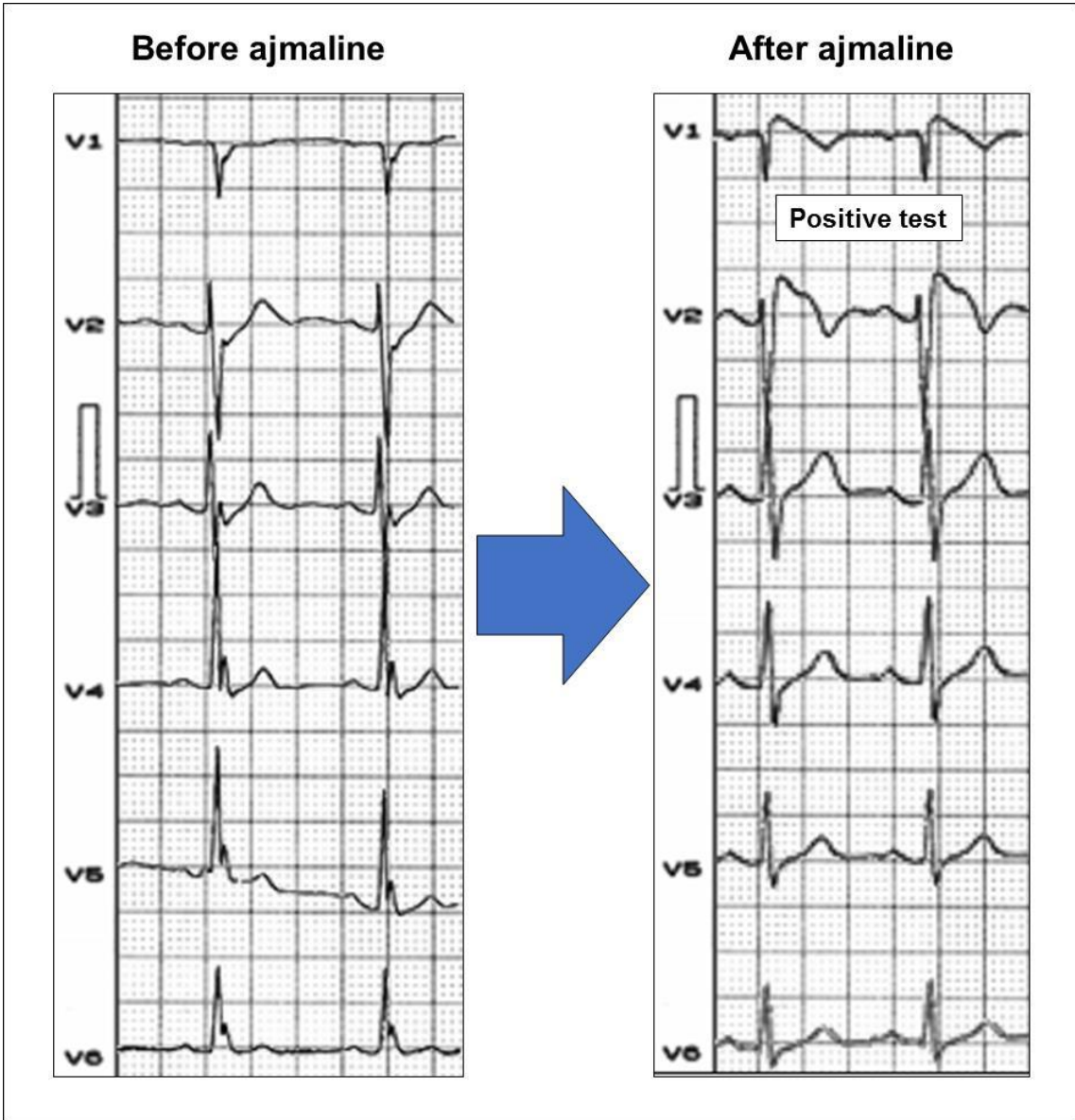
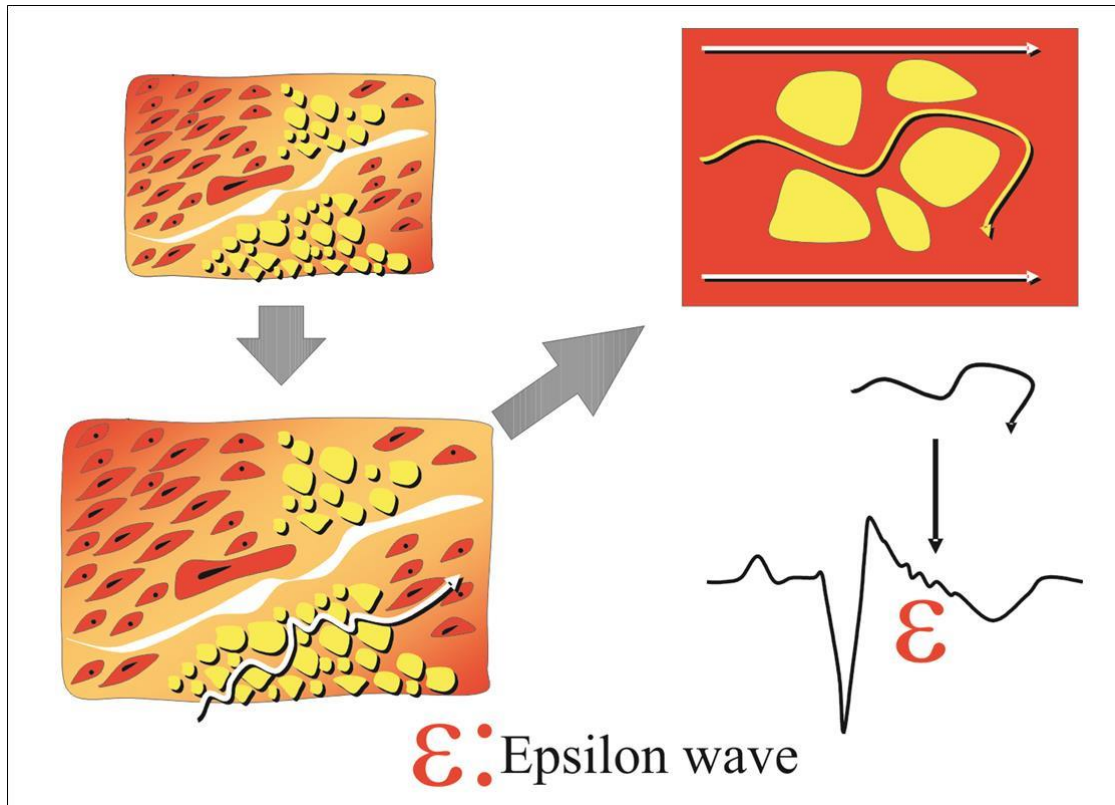
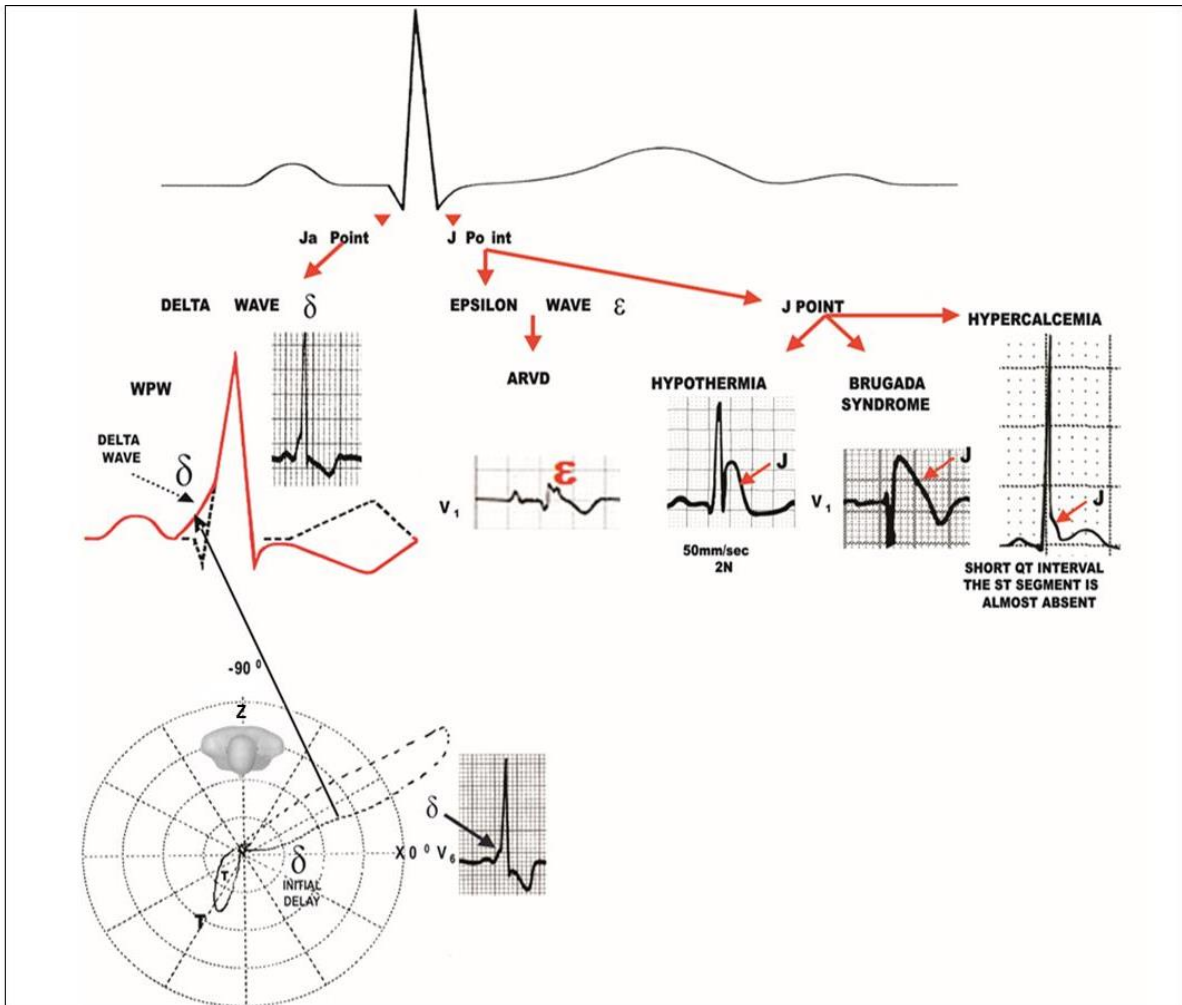


Figure x. ECG.



**Figure x.** Epsilon waves ( $\epsilon$ ) correspond to late potentials or low amplitude and short duration oscillations at the right ventricle free wall (dysplastic triangle) in patients with ARVC/D, and rarely in other entities, such as Brugada syndrome.



**Figure x.** In ECG, epsilon waves manifest as little notches or oscillations, varying in number (1, 2, 3, or more), located at the end of the QRS complex, at the J point or onset of the ST segment (there is no consensus about this) observed in the right precordial leads; however more rarely, they could be seen in the frontal plane leads, especially in the inferior leads.





**Figure x.** A signal-averaged ECG (SAECG) with abnormal LPs in a 60-year-old asymptomatic man and spontaneous type 1 Brugada ECG pattern. Total filtered QRSd = 137 ms. Duration of the high frequency low amplitude (HFLA) < 40  $\mu$ V. The root-mean-square voltage (RMS) in the terminal 40 ms of the QRS are 137 ms, 55 ms and 15  $\mu$ V, respectively (all three parameters are abnormal); The role of the standard time-domain SAECG in BrS is limited by, Inability to detect conduction abnormalities within the QRS complex; Uncertain value in patients with BBB, and The use of a single-lead ECG complex, which is derived from the XYZ orthogonal leads and does not contain any regional information.

**Malignant Early Repolarization Pathological J or malignant waves of idiopathic ventricular fibrillation associated with early repolarization pattern (ERP): the “Haïssaguerre pattern”**

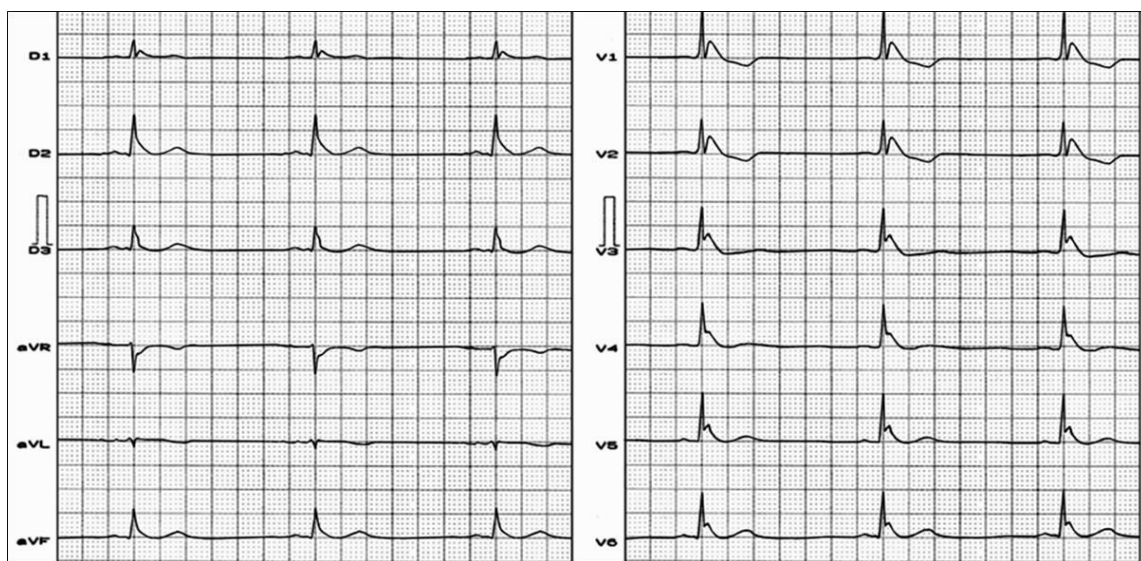


**Figure x.** Subtype 3 shows an ER pattern registered globally in the inferior, lateral and right precordial leads. This variant is associated with the highest level of risk for the

development of VF storms <sup>123</sup>. In subtype 3, the Brugada waves may be seen together with giant J waves in other ECG leads. Although the Brugada waves are not called ER, their underlying mechanism is identical to that of the ER patterns.

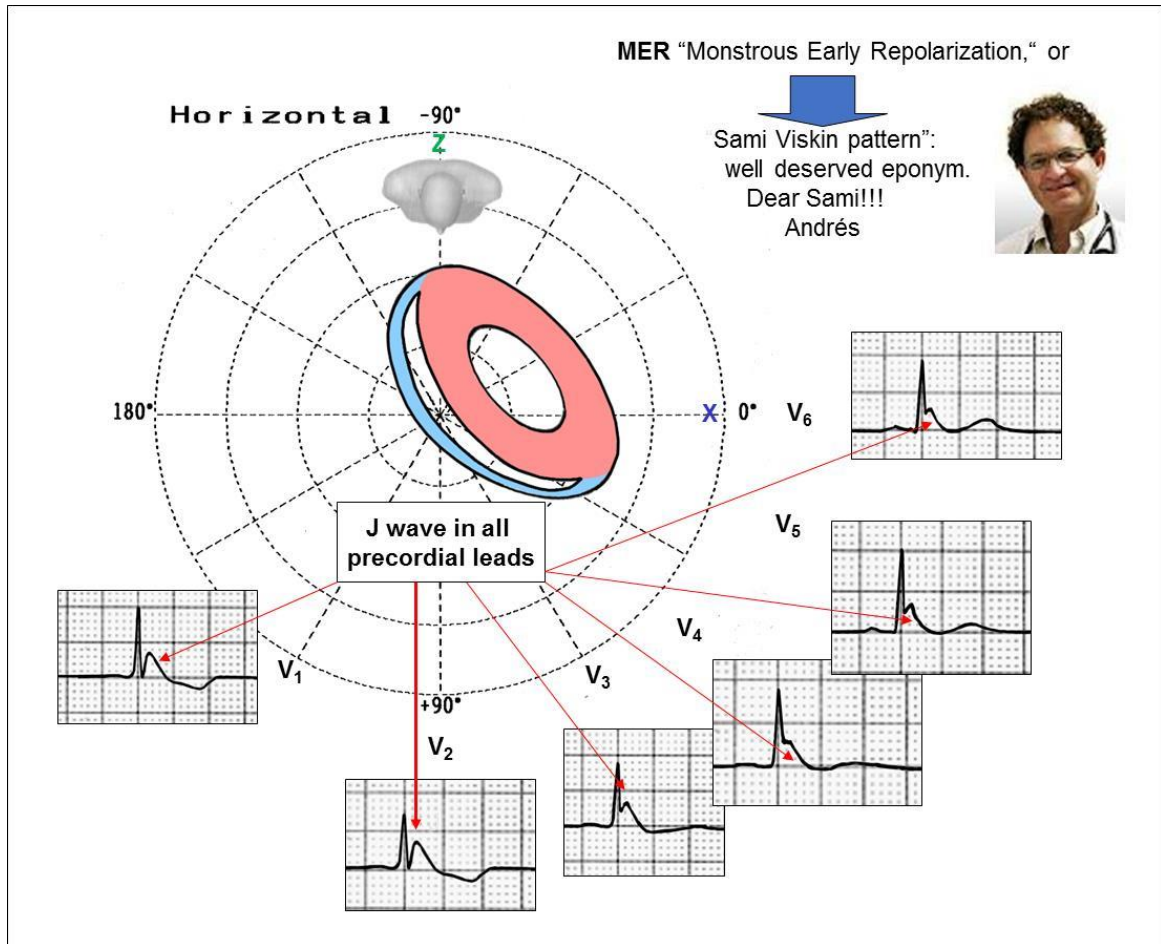


**Figure x.** Classical case of Type 3 Early Repolarization Syndrome (ERS) <sup>124 125</sup>.

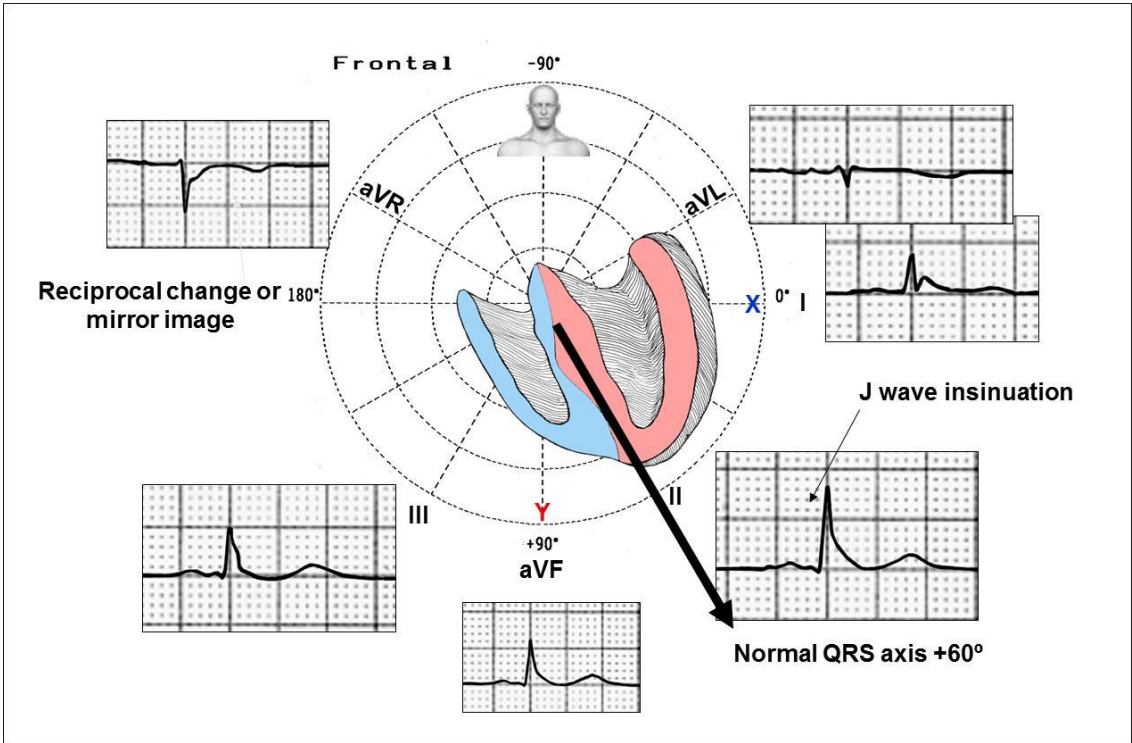


Figure x. ECG/FP.

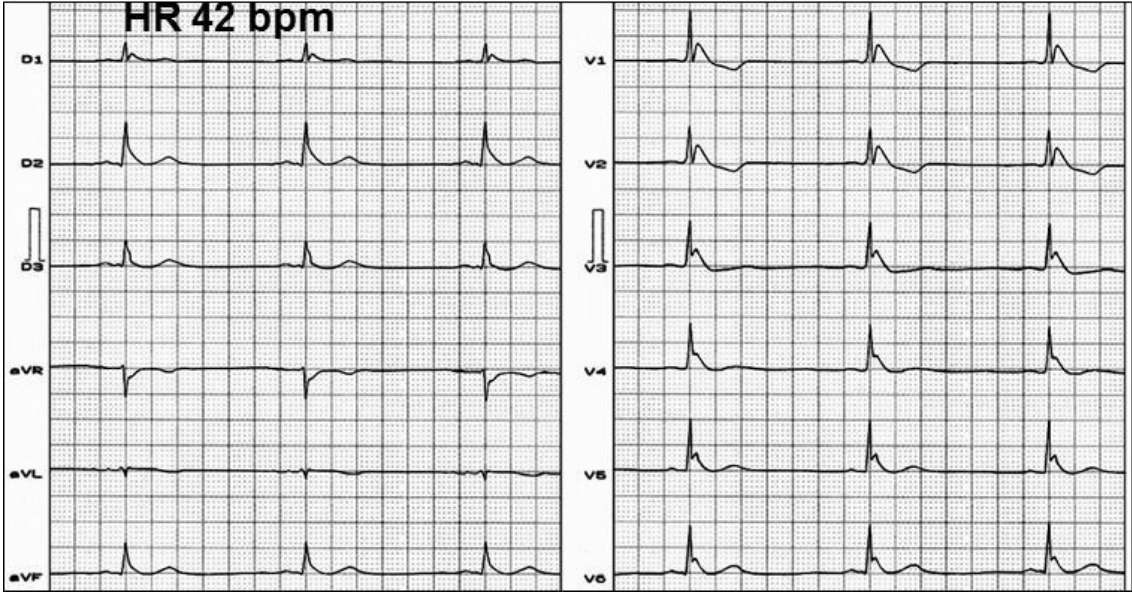
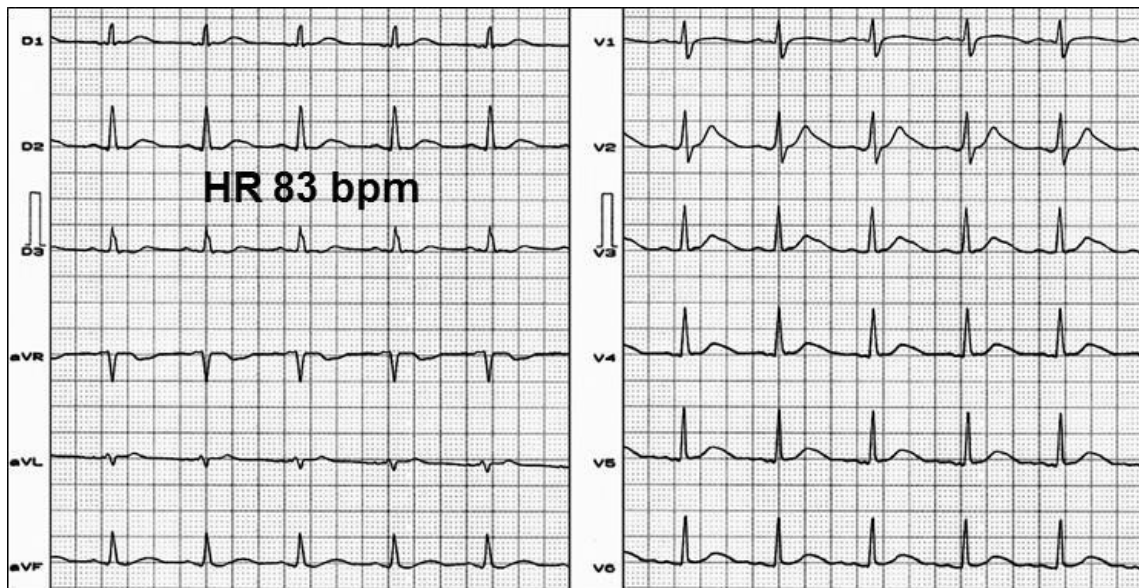


Figure x. Basal tracing. We observe J-wave across all precordial and inferior leads.



**Figure X.** ECG after two days after oral quinidine 1500 mg/day.

**Comments:** The drug reduces the magnitude of the Ito channel – mediator of phase 1 and consequently normalize the elevation of the ST segment. Additionally, it could improve repolarization due to its vagolytic effect (M2 muscarinic receptor block) and to the exacerbation of reflex sympathetic tone.

### **Brugada Phenocopies**

**“An environmental condition that imitates or copies one produced by a gene”**

In order to learn about the morphological classification of Brugada phenocopies, please visit the website: [www.brugadaphenocopy.com](http://www.brugadaphenocopy.com).

Brugada phenocopies are clinical entities that present with an ECG pattern identical to either the type 1 or type 2 Brugada patterns yet differ etiologically from true Brugada syndrome. The pattern presents in association with an identifiable condition and, upon resolution of that condition, the ECG pattern normalizes.

Brugada phenocopy is not due to a congenital sodium channel abnormality. Indeed, the defining feature of Brugada phenocopy is the absence of true congenital Brugada syndrome. Therefore a provocative test with a sodium channel blocking agent such as ajmaline, flecainide, or procainamide will not reproduce the ECG pattern <sup>126</sup>.

### **The Brugada ECG Pattern**

True congenital Brugada syndrome is characterized by two ECG patterns in the right precordial leads (V1-V3). These patterns involve ST elevations that produce either the type 1 “*coved*” or type 2 “*saddleback*” patterns <sup>1</sup>.

The typical type 1 pattern has a high take-off ST-segment elevation that is  $\geq 2$  mm followed by a downsloping concave or rectilinear ST-segment. The ST-segment in type 1 patterns is followed by a negative and symmetrical T wave,

### **Causes of Brugada Phenocopy**

Brugada phenocopies may be induced by a multitude of clinical circumstances that have been characterized into six distinct etiological categories <sup>126 127</sup>: metabolic conditions, mechanical compression, ischemia, myocardial and pericardial disease, ECG modulation, miscellaneous.

The number of reported cases of Brugada phenocopies has steadily increased since the proposal of the term and concordantly, the number of conditions known to cause Brugada phenocopies has also increased. To date, there have been 66 reported cases of Brugada phenocopy, 16 of which are confirmed, meeting all of the mandatory criteria for diagnosis.

Confirmed Type 1 Brugada phenocopies have been reported in the context of an acute inferior ST-segment elevation myocardial infarction with right ventricular involvement <sup>128, 129</sup>; hyperkalemia <sup>130</sup>; adrenal crisis <sup>131</sup>; concurrent hypokalemia and hyponatremia <sup>132</sup>; acute myocarditis due to hypereosinophilic syndrome <sup>133</sup>; concurrent hypernatremia, hypokalemia, and acidosis <sup>134</sup>; hypokalemia in the context of congenital hypokalemic periodic paralysis <sup>135</sup>; writhing of a reconstructed esophagus resulting in mechanical compression on the heart <sup>136</sup>; ketamine intoxication with concurrent acidosis <sup>137</sup>; and acute cannabis intoxication <sup>138</sup>. The remaining five confirmed Brugada phenocopies were type 2 and reported in the context of pectus excavatum resulting in mechanical mediastinal compression <sup>139</sup>; hyperkalemia <sup>140</sup>; acute pericarditis <sup>141</sup>; and electrocution <sup>142</sup>.

## **Recurrent Brugada Phenocopy**

In each of the previous 13 cases, Brugada phenocopy was observed in a single clinical event. However, there are currently two known cases of confirmed recurrent Brugada phenocopy, both in the context of hypokalemia. In 2010, Tsai et al <sup>143</sup> reported a case of Brugada phenocopy in the context of hypokalemia due to thyrotoxicosis. In a brief summary, the patient presented in 2005 with sudden-onset bilateral leg weakness following a large meal. The ECG demonstrated a type 2 Brugada ECG pattern and laboratory tests were significant for hypokalemia, hyperglycemia, low TRH and high free thyroxine.

With treatment and normalization of the potassium and glucose levels, the ECG resolved to a normal pattern. In 2008, this patient experienced a recurrent episode of flaccid paralysis following a heavy meal. The ECG demonstrated a type 1 Brugada ECG pattern and laboratory tests revealed hypokalemia, hyperglycemia, low TSH and normal thyroxine. Correction of the hyperglycemia and hypokalemia yet again resulted in resolution of the Brugada ECG pattern.

In 2013, a second case report demonstrated the clinical reproducibility of Brugada phenocopy. Genaro et al <sup>144</sup> reported the case of a man who presented to the Emergency Department with a 15-day history of diarrhea. An ECG demonstrated a type 1 Brugada ECG pattern in the setting of severe hypokalemia and acidosis. Upon correction of the metabolic abnormalities, the ECG pattern resolved. While in hospital, recurrent episodes of diarrhea resulted in hypokalemia without acidosis and an ECG demonstrated the return of the Type 1 Brugada ECG pattern. The ECG pattern resolved once again after IV.

## **Diagnosis of Brugada Phenocopy**

The diagnostic criteria for Brugada phenocopies are (I-V are mandatory) <sup>128, 129 126</sup>  
<sup>127</sup>:

An ECG pattern that has a type-1 or type-2 Brugada morphology

- I. The patient has an underlying condition that is identifiable
- II. The ECG pattern resolves upon resolution of the underlying condition
- III. There is a low clinical pretest probability of true Brugada syndrome determined by a lack of symptoms, medical history, and family history

- IV. The results of provocative testing with a sodium channel blocker such as ajmaline, flecainide, or procainamide are negative
- V. Provocative testing is not mandatory if surgical RVOT manipulation has occurred within the last 96 hours.
- VI. The results of genetic testing are negative (desirable but not mandatory because the SCN5A mutation is identifiable in only 20% to 30% of probands affected by true BrS).
- VII. Correction of hypokalemia.

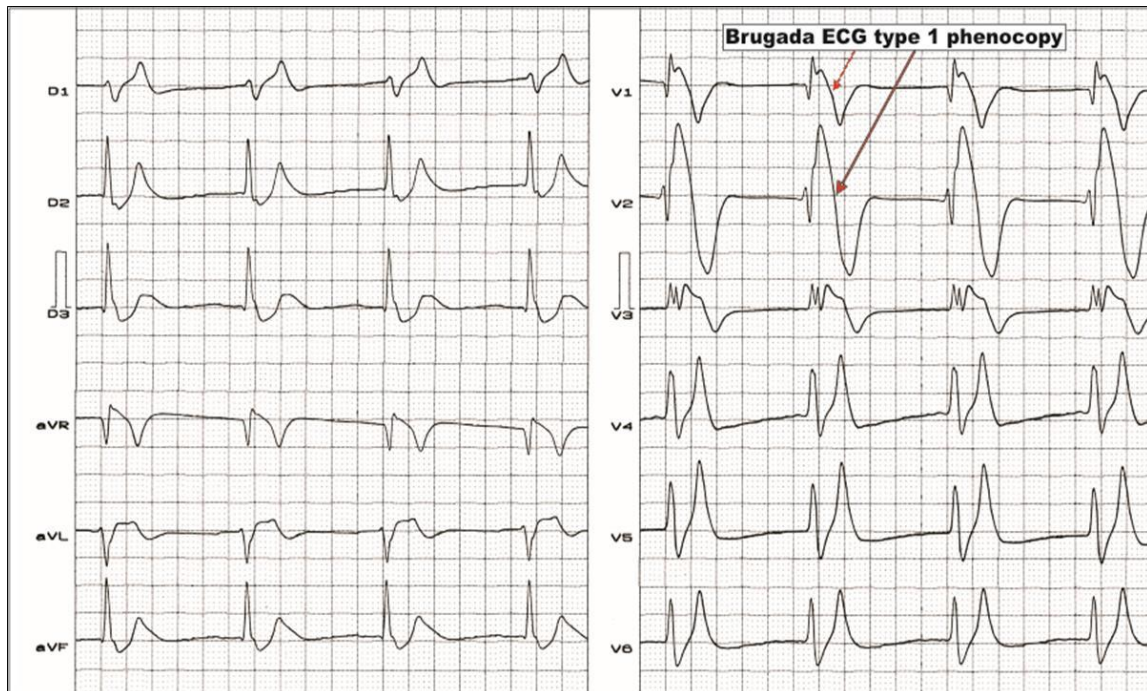


**Figure X.** Clinical diagnosis: terminal renal insufficiency. Severe hyperkalemia:  $K^+$  8.7 mEq/L. This sign is known as dialyzable injury current. ECG diagnosis: very likely, junctional with P waves near the J point, HR: 54 bpm, QRSd: 160 ms, ST segment elevation from V1 to V3 and I, aVL and aVR. V1 to V3 display ST segment upwardly convex pattern, similar to Brugada syndrome or Brugada phenocopy<sup>145</sup>, typical T waves in “tent”, pointed, and with a narrow base.

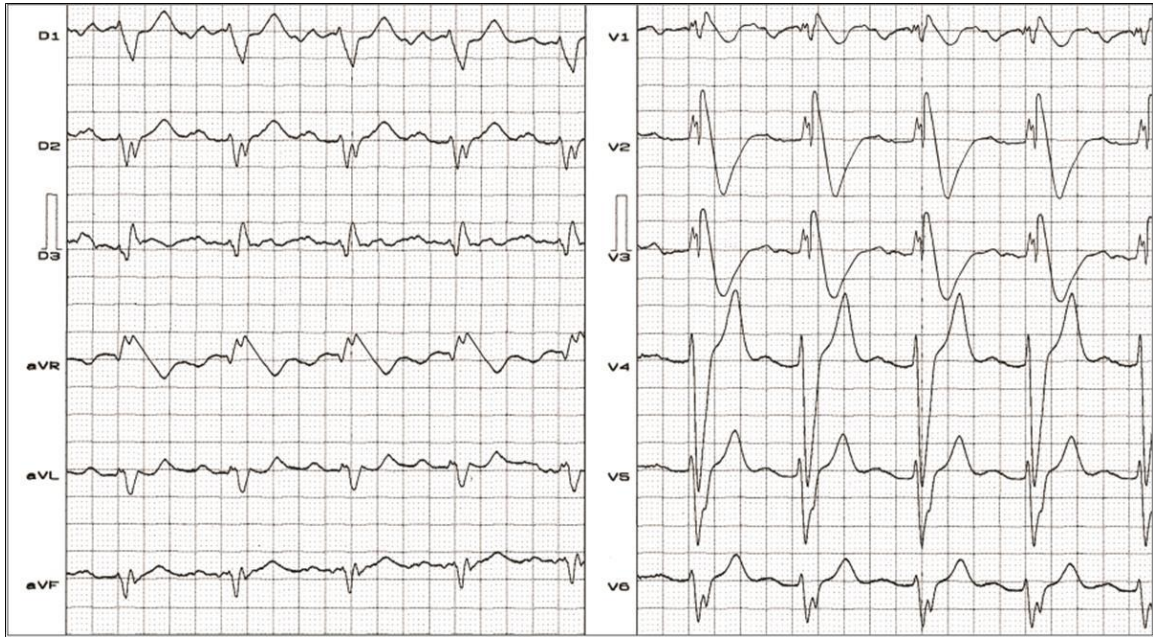


**Figure X.** ECG diagnosis: Left atrial enlargement, PR interval prolongation or first-degree AV block secondary to augmentation of effective refractory periods of atrioventricular node ( $>AH$  interval), His-Purkinje system ( $>HV$  interval), nonspecific intraventricular conduction disturbance, (marked abnormal ventricular activation pattern (bizarre): does not satisfy the criteria of either LBBB or RBBB), long QT interval with normal JT interval and Brugada type 1 ECG phenocopy: ST segment elevation convex to the top followed by negative T waves from V1 to V3. Induced Brugada-type 1 ECG pattern, is a sign for imminent malignant arrhythmias. Brugada phenocopy secondary to accidental plasma concentrations of propafenone in the toxic range.

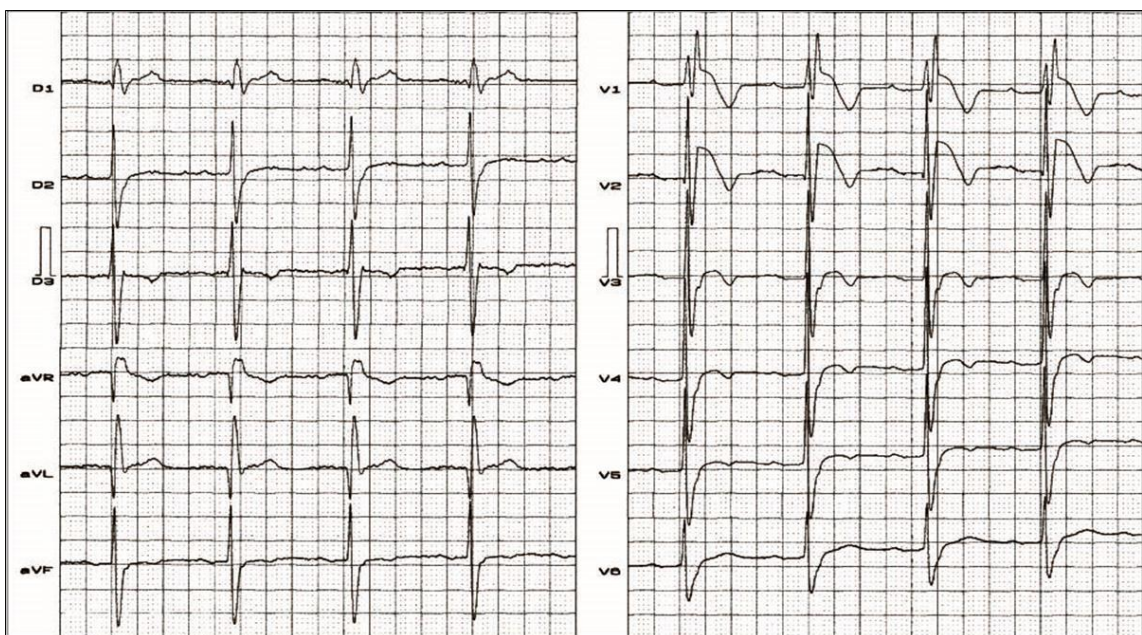




**Figure X.** Clinical diagnosis: myotonic muscular dystrophy (Steinert's disease) / type 2 diabetes mellitus / high blood pressure. Brugada syndrome? Brugada phenocopy? ECG diagnosis: sinus rhythm, HR: 55 bpm, PR interval: 250 ms (first-degree AV block), QRS duration: 165 ms,  $\hat{S}\hat{A}QRS$ : near  $-40^\circ$ : Complete RBBB + left anterior fascicular block (LAFB), probable trifascicular block. J point and ST segment elevation  $\geq 2$  mm in V1 and V2 followed by a negative T wave: Brugada ECG type 1 phenocopy.

**ECG/VCG correlation in the frontal plane**

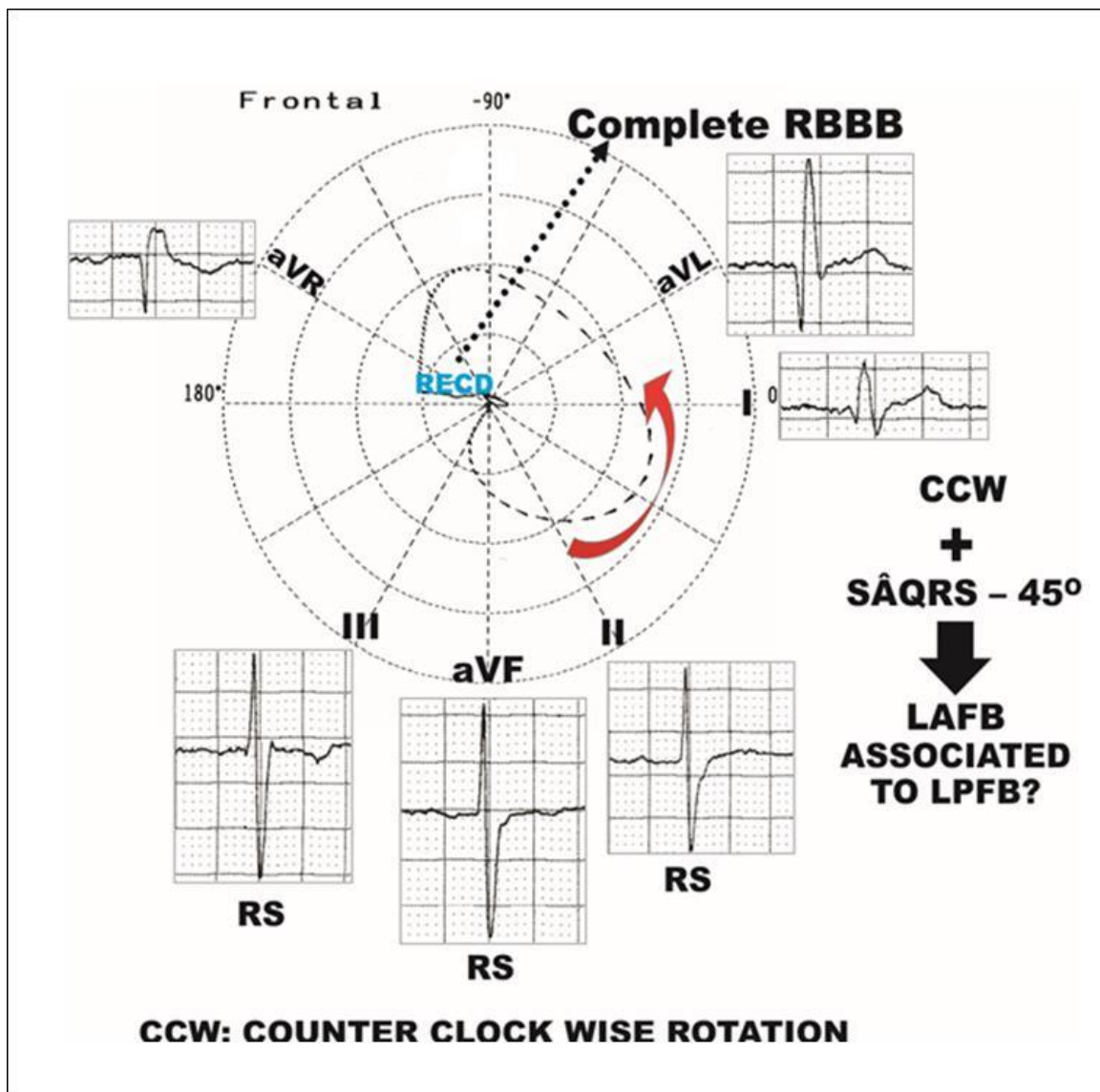


**Figure X.** In classical LAFB, the inferior leads II, III and aVF, show rS pattern. In this case, the voltage of R waves in the inferior leads is greater, originating RS pattern in these leads. Additionally, QRS loop morphology is rounded and not elliptical as in typical LPFB. Both facts (RS pattern and rounded shape) suggest some degree of associated

LPFB. This suspicion is reinforced by the presence of first degree AV block, which may be pointing dromotropic difficulty in the left posterior fascicle.

**ECG/VCG correlation in the horizontal plane**

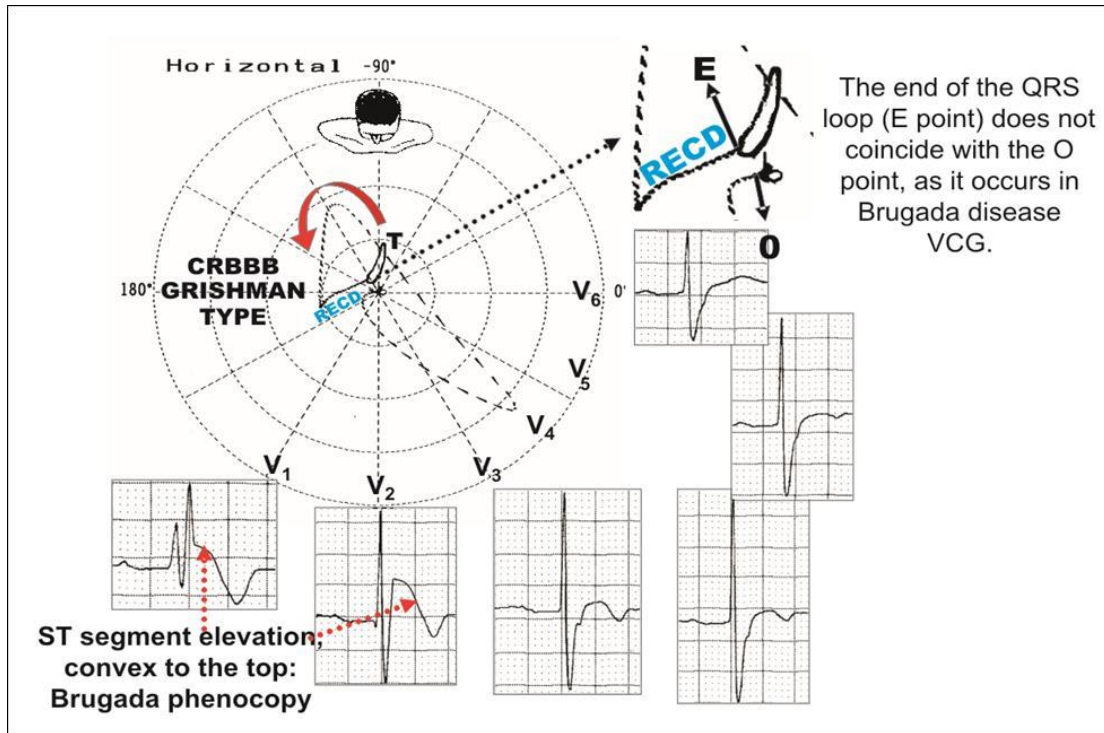


**Figure X.** Clinical diagnosis: Myotonic Muscular Dystrophy (Steinert's Disease). ECG/VCG diagnosis: Complete RBBB Grishman type or Kennedy type I (afferent limb of QRS loop behind the X orthogonal line). J point and ST segment elevation  $\geq 2$  mm convex to the top and followed by a negative T wave in the right precordial leads: Brugada phenocopy <sup>146 147</sup>.

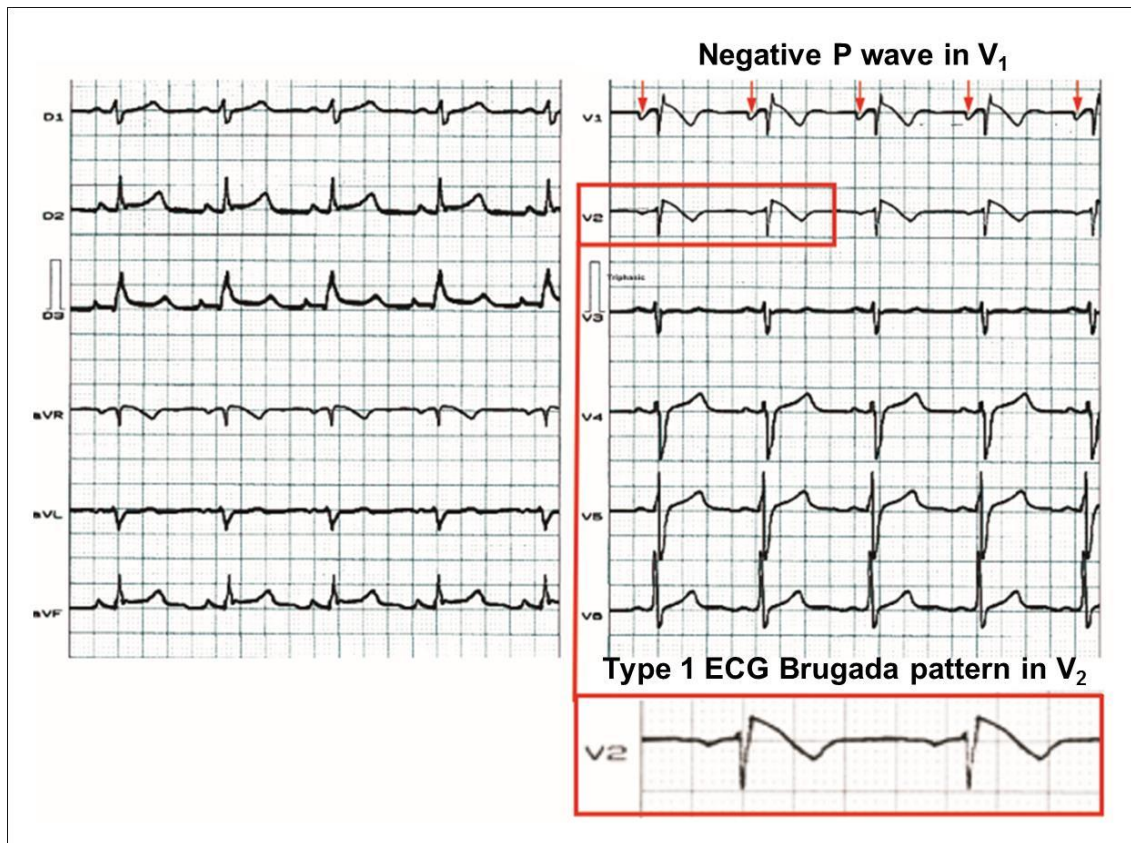


**Figure X.** ECG of a 18 y/o male patient with pectus excavatum<sup>148</sup> and Brugada type 1 ECG pattern: Brugada phenocopy.

### Bruganda syndrome and sports eligibility

An open and still undefined challenge is that of fitness for competitive sports in patients with the Brugada sign. The limitation of physical activity in these patients has been the main cornerstone of preventive therapy for decades. However, the low incidence of sudden cardiac death in these subjects has gradually loosened this concept of prevention. Today, the new Italian COCIS protocols [1] and the European guidelines on the subject open up the possibility of carrying out competitive sports in some of these subjects.

From these guidelines we can draw the following indications:

Eligibility can be granted:

- in asymptomatic subjects with type 2 or 3 pattern in the absence of a family history of juvenile sudden death;
- in subjects with drug-induced type 1 without risk factors.

Eligibility may be reasonable in asymptomatic subjects with a spontaneous type 1 pattern, with no family history of sudden death or other minor risk factors and who have a negative EPS.

Eligibility should be denied:

- in subjects symptomatic of arrhythmic syncope with spontaneous or drug-induced type 1 pattern;
- in subjects with familial sudden death and with a spontaneous or drug-induced type 1 pattern.

The basis of this more open attitude that characterises the COCIS 2019 guidelines [[Cardiological protocols on determining eligibility for competitive sports 1995. Organizational Cardiological Committee on Eligibility for Sports \(COCIS\)](#)]. [Article in Italian]. *G Ital Cardiol.* 1996; 26:949-83.] derives from the following considerations. Malignant arrhythmias in BrS typically appear at rest during bradycardia phases and, so far, there is no evidence that sport increases the risk of sudden death. It is hypothesized that the addition of a training-induced vagal tone may promote nocturnal arrhythmias. However, to date, there is still no evidence.

The European Association of Preventive Cardiology (EAPC) is also very open on the subject and even goes so far as to say that patients with symptomatic Brugada syndrome (syncope and/or sudden resuscitated cardiac death), after ICD implantation, if they are asymptomatic for at least three months and observing the necessary precautions, can practise all sports, even competitive ones, after a decision-making process shared between doctor and athlete. Unlike the more open positions previously mentioned, the ESC guidelines have remained overly cautious in the indication for sporting activity in these patients, without being unbalanced [[Pelliccia A, Sharma S, Gati S, Bäck M, Börjesson](#)

M, Caselli S, Collet JP, Corrado D, Drezner JA, Halle M, Hansen D, Heidbuchel H, Myers J, Niebauer J, Papadakis M, Piepoli MF, Prescott E, Roos-Hesselink JW, Graham Stuart A, Taylor RS, Thompson PD, Tiberi M, Vanhees L, Wilhelm M; ESC Scientific Document Group. 2020 ESC Guidelines on sports cardiology and exercise in patients with cardiovascular disease. *Eur Heart J.* 2021;42:17-96.].

The American Heart Association and the American College of Cardiology have not yet updated their guidelines. They date back to 2015 and conclude that Brugada athletes should be excluded from all competitive sports until a thorough evaluation by a cardiologist expert in arrhythmias has been completed, and the athlete and his family are well informed of the non-competitive risk [Ackerman MJ, Zipes DP, Kovacs RJ, Maron BJ; American Heart Association Electrocardiography and Arrhythmias Committee of Council on Clinical Cardiology, Council on Cardiovascular Disease in Young, Council on Cardiovascular and Stroke Nursing, Council on Functional Genomics and Translational Biology, and American College of Cardiology. Eligibility and Disqualification Recommendations for Competitive Athletes With Cardiovascular Abnormalities: Task Force 10: The Cardiac Channelopathies: A Scientific Statement From the American Heart Association and American College of Cardiology. *Circulation.* 2015;132:e326-9.].

## **REFERENCES**

1. Bayes de Luna A, Brugada J, Baranchuk A, *et al.* Current electrocardiographic criteria for diagnosis of Brugada pattern: a consensus report. *J Electrocardiol.* 2012;45:433-442.
2. Peritz DC, Chung EH. Criteria for evaluating rSr' patterns due to high precordial ECG lead placement accurately confirm absence of a Brugada ECG pattern. *J Electrocardiol.* 2016;49:182-186.

3. Ohkubo K, Watanabe I, Okumura Y, *et al.* A new criteria differentiating type 2 and 3 Brugada patterns from ordinary incomplete right bundle branch block. *Int Heart J.* 2011;52:159-163.
4. Chevallier S, Forclaz A, Tenkorang J, *et al.* New electrocardiographic criteria for discriminating between Brugada types 2 and 3 patterns and incomplete right bundle branch block. *J Am Coll Cardiol.* 2011;58:2290-2298.
5. Serra G, Baranchuk A, Bayes-De-Luna A, *et al.* New electrocardiographic criteria to differentiate the Type-2 Brugada pattern from electrocardiogram of healthy athletes with r'-wave in leads V1/V2. *Europace.* 2014;16:1639-1645.
6. Serra G, Baranchuk A, Bayes-De-Luna A, *et al.* Base of the triangle to determine a Brugada electrocardiogram pattern. *Europace.* 2015;17:505.
7. Crea P, Rivetti L, Bitto R, *et al.* Diagnosis of type 2 Brugada pattern: insights from a pilot survey. *Minerva Cardioangiol.* 2020.
8. Sciarra L, Moriya M, Robles AG, *et al.* Type 2 Brugada pattern: more doubts than certainties. *Minerva Cardioangiol.* 2020.
9. Priori SG, Wilde AA, Horie M, *et al.* Executive summary: HRS/EHRA/APHRs expert consensus statement on the diagnosis and management of patients with inherited primary arrhythmia syndromes. *Europace.* 2013;15:1389-1406.
10. Calo L, Giustetto C, Martino A, *et al.* A New Electrocardiographic Marker of Sudden Death in Brugada Syndrome: The S-Wave in Lead I. *J Am Coll Cardiol.* 2016;67:1427-1440.
11. Babai Bigi MA, Aslani A, Shahrzad S. aVR sign as a risk factor for life-threatening arrhythmic events in patients with Brugada syndrome. *Heart Rhythm.* 2007;4:1009-1012.
12. Rattanawong P, Riangwiwat T, Prasitlunkum N, *et al.* Baseline fragmented QRS increases the risk of major arrhythmic events in Brugada syndrome: Systematic review and meta-analysis. *Ann Noninvasive Electrocardiol.* 2018;23:e12507.
13. Kataoka N, Mizumaki K, Nakatani Y, *et al.* Paced QRS fragmentation is associated with spontaneous ventricular fibrillation in patients with Brugada syndrome. *Heart Rhythm.* 2016;13:1497-1503.
14. Francis J, Antzelevitch C. Atrial fibrillation and Brugada syndrome. *J Am Coll Cardiol.* 2008;51:1149-1153.
15. Migliore F, Testolina M, Zorzi A, *et al.* First-degree atrioventricular block on basal electrocardiogram predicts future arrhythmic events in patients with Brugada

syndrome: a long-term follow-up study from the Veneto region of Northeastern Italy. *Europace*. 2019;21:322-331.

16. Pranata R, Yonas E, Chintya V, *et al.* Association between PR Interval, First-degree atrioventricular block and major arrhythmic events in patients with Brugada syndrome - Systematic review and meta-analysis. *J Arrhythm*. 2019;35:584-590.
17. Aro AL. First-degree atrioventricular block: risk marker or innocent finding? *Heart*. 2016;102:655-656.
18. Kamakura T, Sacher F, Katayama K, *et al.* High-risk atrioventricular block in Brugada syndrome patients with a history of syncope. *J Cardiovasc Electrophysiol*. 2021;32:772-781.
19. Ragab AAY, Houck CA, van der Does L, *et al.* Usefulness of the R-Wave Sign as a Predictor for Ventricular Tachyarrhythmia in Patients With Brugada Syndrome. *Am J Cardiol*. 2017;120:428-434.
20. Pérez-Riera AR, Yanowitz F, Barbosa-Barros R, *et al.* Electrocardiographic “Northwest QRS Axis” in the Brugada Syndrome: A Potential Marker to Predict Poor Outcome. *J Am Coll Cardiol Case Rep*. 2020 2:2230-2234.
21. Miyamoto A, Hayashi H, Makiyama T, *et al.* Risk determinants in individuals with a spontaneous type 1 Brugada ECG. *Circ J*. 2011;75:844-851.
22. Take Y, Morita H, Wu J, *et al.* Spontaneous electrocardiogram alterations predict ventricular fibrillation in Brugada syndrome. *Heart Rhythm*. 2011;8:1014-1021.
23. Kawata H, Morita H, Yamada Y, *et al.* Prognostic significance of early repolarization in inferolateral leads in Brugada patients with documented ventricular fibrillation: a novel risk factor for Brugada syndrome with ventricular fibrillation. *Heart Rhythm*. 2013;10:1161-1168.
24. Takagi M, Aonuma K, Sekiguchi Y, *et al.* The prognostic value of early repolarization (J wave) and ST-segment morphology after J wave in Brugada syndrome: multicenter study in Japan. *Heart Rhythm*. 2013;10:533-539.
25. Conte G, de Asmundis C, Sieira J, *et al.* Prevalence and Clinical Impact of Early Repolarization Pattern and QRS-Fragmentation in High-Risk Patients With Brugada Syndrome. *Circ J*. 2016;80:2109-2116.
26. Tokioka K, Kusano KF, Morita H, *et al.* Electrocardiographic parameters and fatal arrhythmic events in patients with Brugada syndrome: combination of depolarization and repolarization abnormalities. *J Am Coll Cardiol*. 2014;63:2131-2138.

27. Junttila MJ, Brugada P, Hong K, *et al.* Differences in 12-lead electrocardiogram between symptomatic and asymptomatic Brugada syndrome patients. *J Cardiovasc Electrophysiol.* 2008;19:380-383.
28. Ohkubo K, Watanabe I, Okumura Y, *et al.* Prolonged QRS duration in lead V2 and risk of life-threatening ventricular Arrhythmia in patients with Brugada syndrome. *Int Heart J.* 2011;52:98-102.
29. Nagase S, Kamakura T, Kataoka N, *et al.* Low-Voltage Type 1 ECG Is Associated With Fatal Ventricular Tachyarrhythmia in Brugada Syndrome. *J Am Heart Assoc.* 2018;7:e009713.
30. Pitzalis MV, Anaclerio M, Iacoviello M, *et al.* QT-interval prolongation in right precordial leads: an additional electrocardiographic hallmark of Brugada syndrome. *J Am Coll Cardiol.* 2003;42:1632-1637.
31. Castro Hevia J, Antzelevitch C, Tornes Barzaga F, *et al.* Tpeak-Tend and Tpeak-Tend dispersion as risk factors for ventricular tachycardia/ventricular fibrillation in patients with the Brugada syndrome. *J Am Coll Cardiol.* 2006;47:1828-1834.
32. Naseef A, Behr ER, Batchvarov VN. Electrocardiographic methods for diagnosis and risk stratification in the Brugada syndrome. *J Saudi Heart Assoc.* 2015;27:96-108.
33. Makimoto H, Nakagawa E, Takaki H, *et al.* Augmented ST-segment elevation during recovery from exercise predicts cardiac events in patients with Brugada syndrome. *J Am Coll Cardiol.* 2010;56:1576-1584.
34. Yoshioka K, Amino M, Zareba W, *et al.* Identification of high-risk Brugada syndrome patients by combined analysis of late potential and T-wave amplitude variability on ambulatory electrocardiograms. *Circ J.* 2013;77:610-618.
35. Garcia-Fuertes D, Villanueva-Fernandez E, Crespin-Crespin M, *et al.* Type 1 Brugada Pattern Unmasked During the Recovery Period of an Exercise Stress Test. *Arq Bras Cardiol.* 2016;106:447-449.
36. Morita H, Fukushima-Kusano K, Nagase S, *et al.* Sinus node function in patients with Brugada-type ECG. *Circ J.* 2004;68:473-476.
37. Batchvarov VN, Govindan M, Camm AJ, *et al.* Brugada-like changes in the peripheral leads during diagnostic ajmaline test in patients with suspected Brugada syndrome. *Pacing Clin Electrophysiol.* 2009;32:695-703.
38. Bonakdar H, Haghjoo M, Sadr-Ameli MA. Brugada syndrome manifested by the typical electrocardiographic pattern both in the right precordial and the high lateral leads. *Indian Pacing Electrophysiol J.* 2008;8:137-140.



39. Chinushi M, Izumi D, Furushima H, *et al.* Multiple premature beats triggered ventricular arrhythmias during pilsicainide infusion in a patient with inferior ST-segment elevation. *Pacing Clin Electrophysiol.* 2006;29:1445-1448.
40. Kalla H, Yan GX, Marinchak R. Ventricular fibrillation in a patient with prominent J (Osborn) waves and ST segment elevation in the inferior electrocardiographic leads: a Brugada syndrome variant? *J Cardiovasc Electrophysiol.* 2000;11:95-98.
41. Rollin A, Sacher F, Gourraud JB, *et al.* Prevalence, characteristics, and prognosis role of type 1 ST elevation in the peripheral ECG leads in patients with Brugada syndrome. *Heart Rhythm.* 2013;10:1012-1018.
42. Takagi M, Aihara N, Takaki H, *et al.* Clinical characteristics of patients with spontaneous or inducible ventricular fibrillation without apparent heart disease presenting with J wave and ST segment elevation in inferior leads. *J Cardiovasc Electrophysiol.* 2000;11:844-848.
43. van den Berg MP, Wiesfeld AC. Brugada syndrome with ST-segment elevation in the lateral leads. *J Cardiovasc Electrophysiol.* 2006;17:1035.
44. Honarbakhsh S, Providencia R, Garcia-Hernandez J, *et al.* A Primary Prevention Clinical Risk Score Model for Patients With Brugada Syndrome (BRUGADA-RISK). *JACC Clin Electrophysiol.* 2021;7:210-222.
45. Deliniere A, Baranchuk A, Gai J, *et al.* Prediction of ventricular arrhythmias in patients with a spontaneous Brugada type 1 pattern: the key is in the electrocardiogram. *Europace.* 2019;21:1400-1409.
46. Pablo Florez J, Garcia D, Valverde I, *et al.* Role of syncope in predicting adverse outcomes in patients with suspected Brugada syndrome undergoing standardized flecainide testing. *Europace.* 2018;20:f64-f71.
47. Letsas KP, Efremidis M, Gavrielatos G, *et al.* Neurally mediated susceptibility in individuals with Brugada-type ECG pattern. *Pacing Clin Electrophysiol.* 2008;31:418-421.
48. Garcia Iglesias D, Roqueni Gutierrez N, De Cos FJ, *et al.* Analysis of the High-Frequency Content in Human QRS Complexes by the Continuous Wavelet Transform: An Automatized Analysis for the Prediction of Sudden Cardiac Death. *Sensors (Basel).* 2018;18.

49. Garcia-Iglesias D, de Cos FJ, Romero FJ, *et al.* Spectral Analysis of the QT Interval Increases the Prediction Accuracy of Clinical Variables in Brugada Syndrome. *J Clin Med.* 2019;8.
50. Gehi AK, Duong TD, Metz LD, *et al.* Risk stratification of individuals with the Brugada electrocardiogram: a meta-analysis. *J Cardiovasc Electrophysiol.* 2006;17:577-583.
51. Paul M, Gerss J, Schulze-Bahr E, *et al.* Role of programmed ventricular stimulation in patients with Brugada syndrome: a meta-analysis of worldwide published data. *Eur Heart J.* 2007;28:2126-2133.
52. Priori SG, Gasparini M, Napolitano C, *et al.* Risk stratification in Brugada syndrome: results of the PRELUDE (PRogrammed ELectrical stimUlation preDICTive valuE) registry. *J Am Coll Cardiol.* 2012;59:37-45.
53. Shinohara T, Takagi M, Kamakura T, *et al.* Risk stratification in asymptomatic patients with Brugada syndrome: Utility of multiple risk factor combination rather than programmed electrical stimulation. *J Cardiovasc Electrophysiol.* 2021;32:507-514.
54. Chen Q, Kirsch GE, Zhang D, *et al.* Genetic basis and molecular mechanism for idiopathic ventricular fibrillation. *Nature.* 1998;392:293-296.
55. Amin AS, Boink GJ, Atrafi F, *et al.* Facilitatory and inhibitory effects of SCN5A mutations on atrial fibrillation in Brugada syndrome. *Europace.* 2011;13:968-975.
56. Han D, Tan H, Sun C, *et al.* Dysfunctional Nav1.5 channels due to SCN5A mutations. *Exp Biol Med (Maywood).* 2018;243:852-863.
57. Bezzina C, Veldkamp MW, van Den Berg MP, *et al.* A single Na(+) channel mutation causing both long-QT and Brugada syndromes. *Circ Res.* 1999;85:1206-1213.
58. Remme CA, Wilde AA, Bezzina CR. Cardiac sodium channel overlap syndromes: different faces of SCN5A mutations. *Trends Cardiovasc Med.* 2008;18:78-87.
59. Wilde AAM, Amin AS. Clinical Spectrum of SCN5A Mutations: Long QT Syndrome, Brugada Syndrome, and Cardiomyopathy. *JACC Clin Electrophysiol.* 2018;4:569-579.
60. Robyns T, Nuyens D, Vandenberg B, *et al.* Genotype-phenotype relationship and risk stratification in loss-of-function SCN5A mutation carriers. *Ann Noninvasive Electrocardiol.* 2018;23:e12548.
61. Amin AS, Reckman YJ, Arbelo E, *et al.* SCN5A mutation type and topology are associated with the risk of ventricular arrhythmia by sodium channel blockers. *Int J Cardiol.* 2018;266:128-132.

62. London B, Michalec M, Mehdi H, *et al.* Mutation in glycerol-3-phosphate dehydrogenase 1 like gene (GPD1-L) decreases cardiac Na<sup>+</sup> current and causes inherited arrhythmias. *Circulation*. 2007;116:2260-2268.
63. Antzelevitch C, Pollevick GD, Cordeiro JM, *et al.* Loss-of-function mutations in the cardiac calcium channel underlie a new clinical entity characterized by ST-segment elevation, short QT intervals, and sudden cardiac death. *Circulation*. 2007;115:442-449.
64. Beziau DM, Barc J, O'Hara T, *et al.* Complex Brugada syndrome inheritance in a family harbouring compound SCN5A and CACNA1C mutations. *Basic Res Cardiol*. 2014;109:446.
65. Chernyavskaya Y, Ebert AM, Milligan E, *et al.* Voltage-gated calcium channel CACNB2 (beta2.1) protein is required in the heart for control of cell proliferation and heart tube integrity. *Dev Dyn*. 2012;241:648-662.
66. Tada T, Kusano KF, Nagase S, *et al.* Clinical significance of macroscopic T-wave alternans after sodium channel blocker administration in patients with Brugada syndrome. *J Cardiovasc Electrophysiol*. 2008;19:56-61.
67. Watanabe H, Darbar D, Kaiser DW, *et al.* Mutations in sodium channel beta1- and beta2-subunits associated with atrial fibrillation. *Circ Arrhythm Electrophysiol*. 2009;2:268-275.
68. Delpon E, Cordeiro JM, Nunez L, *et al.* Functional effects of KCNE3 mutation and its role in the development of Brugada syndrome. *Circ Arrhythm Electrophysiol*. 2008;1:209-218.
69. Hu D, Barajas-Martinez H, Burashnikov E, *et al.* A mutation in the beta 3 subunit of the cardiac sodium channel associated with Brugada ECG phenotype. *Circ Cardiovasc Genet*. 2009;2:270-278.
70. Ueda K, Hirano Y, Higashiuesato Y, *et al.* Role of HCN4 channel in preventing ventricular arrhythmia. *J Hum Genet*. 2009;54:115-121.
71. Giudicessi JR, Ye D, Tester DJ, *et al.* Transient outward current (I<sub>to</sub>) gain-of-function mutations in the KCND3-encoded Kv4.3 potassium channel and Brugada syndrome. *Heart Rhythm*. 2011;8:1024-1032.
72. Olesen MS, Jensen NF, Holst AG, *et al.* A novel nonsense variant in Nav1.5 cofactor MOG1 eliminates its sodium current increasing effect and may increase the risk of arrhythmias. *Can J Cardiol*. 2011;27:523 e517-523.
73. Campuzano O, Berne P, Selga E, *et al.* Brugada syndrome and p.E61X\_RANGRF. *Cardiol J*. 2014;21:121-127.

74. Ishikawa T, Sato A, Marcou CA, *et al.* A novel disease gene for Brugada syndrome: sarcolemmal membrane-associated protein gene mutations impair intracellular trafficking of hNav1.5. *Circ Arrhythm Electrophysiol.* 2012;5:1098-1107.
75. Barajas-Martinez H, Hu D, Ferrer T, *et al.* Molecular genetic and functional association of Brugada and early repolarization syndromes with S422L missense mutation in KCNJ8. *Heart Rhythm.* 2012;9:548-555.
76. Hu D, Barajas-Martinez H, Terzic A, *et al.* ABCC9 is a novel Brugada and early repolarization syndrome susceptibility gene. *Int J Cardiol.* 2014;171:431-442.
77. Riuro H, Beltran-Alvarez P, Tarradas A, *et al.* A missense mutation in the sodium channel beta2 subunit reveals SCN2B as a new candidate gene for Brugada syndrome. *Hum Mutat.* 2013;34:961-966.
78. Huang L, Tang S, Peng L, *et al.* Molecular Autopsy of Desmosomal Protein Plakophilin-2 in Sudden Unexplained Nocturnal Death Syndrome. *J Forensic Sci.* 2016;61:687-691.
79. Cerrone M, Delmar M. Desmosomes and the sodium channel complex: implications for arrhythmogenic cardiomyopathy and Brugada syndrome. *Trends Cardiovasc Med.* 2014;24:184-190.
80. Papavassiliu T, Wolpert C, Fluchter S, *et al.* Magnetic resonance imaging findings in patients with Brugada syndrome. *J Cardiovasc Electrophysiol.* 2004;15:1133-1138.
81. Cerrone M, Noorman M, Lin X, *et al.* Sodium current deficit and arrhythmogenesis in a murine model of plakophilin-2 haploinsufficiency. *Cardiovasc Res.* 2012;95:460-468.
82. Nademanee K, Raju H, de Noronha SV, *et al.* Fibrosis, Connexin-43, and Conduction Abnormalities in the Brugada Syndrome. *J Am Coll Cardiol.* 2015;66:1976-1986.
83. Hennessey JA, Marcou CA, Wang C, *et al.* FGF12 is a candidate Brugada syndrome locus. *Heart Rhythm.* 2013;10:1886-1894.
84. Hu D, Barajas-Martinez H, Pfeiffer R, *et al.* Mutations in SCN10A are responsible for a large fraction of cases of Brugada syndrome. *J Am Coll Cardiol.* 2014;64:66-79.
85. Behr ER, Savio-Galimberti E, Barc J, *et al.* Role of common and rare variants in SCN10A: results from the Brugada syndrome QRS locus gene discovery collaborative study. *Cardiovasc Res.* 2015;106:520-529.
86. Raatikainen MJ, Arnar DO, Merkely B, *et al.* Access to and clinical use of cardiac implantable electronic devices and interventional electrophysiological procedures in the

European Society of Cardiology Countries: 2016 Report from the European Heart Rhythm Association. *Europace*. 2016;18 Suppl 3:iii1-iii79.

87. Bezzina CR, Barc J, Mizusawa Y, *et al*. Common variants at SCN5A-SCN10A and HEY2 are associated with Brugada syndrome, a rare disease with high risk of sudden cardiac death. *Nat Genet*. 2013;45:1044-1049.
88. Boczek NJ, Ye D, Johnson EK, *et al*. Characterization of SEMA3A-encoded semaphorin as a naturally occurring Kv4.3 protein inhibitor and its contribution to Brugada syndrome. *Circ Res*. 2014;115:460-469.
89. Antzelevitch C. Brugada syndrome: clinical, genetic, molecular, cellular and ionic aspects. *Expert Rev Cardiovasc Ther*. 2003;1:177-185.
90. Wilde AA, Antzelevitch C, Borggrefe M, *et al*. Proposed diagnostic criteria for the Brugada syndrome. *Eur Heart J*. 2002;23:1648-1654.
91. Wilde AA, Antzelevitch C, Borggrefe M, *et al*. Proposed diagnostic criteria for the Brugada syndrome: consensus report. *Circulation*. 2002;106:2514-2519.
92. Riera AR, Ferreira C, Schapachnik E, *et al*. Brugada syndrome with atypical ECG: downsloping ST-segment elevation in inferior leads. *J Electrocardiol*. 2004;37:101-104.
93. Kukla P, Jastrzebski M, Baciór B, *et al*. [Variant Brugada syndrome--mild ST segment elevation in inferior leads and aborted sudden cardiac death]. *Kardiol Pol*. 2007;65:1494-1498.
94. Pastore CA, Moffa PJ, Spiritus MO, *et al*. [Fascicular blocks of the right branch. Standardization of vectorelectrocardiographic findings]. *Arq Bras Cardiol*. 1983;41:161-166.
95. Luna Filho B, Bocanegra JA, Pfeferman A, *et al*. [Fascicular block of the His bundle: critical approach for its identification]. *Arq Bras Cardiol*. 1989;53:261-265.
96. Butz T, Vogt J, Vielhauer C, *et al*. Detection of a type 1 Brugada ECG by ECG recording at a higher intercostal space of leads V(1) and V (2). *Herz*. 2010;35:112.
97. Casini S, Tan HL, Bhuiyan ZA, *et al*. Characterization of a novel SCN5A mutation associated with Brugada syndrome reveals involvement of DIIS4-S5 linker in slow inactivation. *Cardiovasc Res*. 2007;76:418-429.
98. Veldkamp MW, Viswanathan PC, Bezzina C, *et al*. Two distinct congenital arrhythmias evoked by a multidysfunctional Na(+) channel. *Circ Res*. 2000;86:E91-97.
99. Morita H, Zipes DP, Morita ST, *et al*. Temperature modulation of ventricular arrhythmogenicity in a canine tissue model of Brugada syndrome. *Heart Rhythm*. 2007;4:188-197.

100. Morita H, Zipes DP, Morita ST, *et al.* Differences in arrhythmogenicity between the canine right ventricular outflow tract and anteroinferior right ventricle in a model of Brugada syndrome. *Heart Rhythm.* 2007;4:66-74.
101. Letsas KP, Weber R, Astheimer K, *et al.* Predictors of atrial tachyarrhythmias in subjects with type 1 ECG pattern of Brugada syndrome. *Pacing Clin Electrophysiol.* 2009;32:500-505.
102. Kamakura S, Ohe T, Nakazawa K, *et al.* Long-term prognosis of probands with Brugada-pattern ST-elevation in leads V1-V3. *Circ Arrhythm Electrophysiol.* 2009;2:495-503.
103. Junttila MJ, Gonzalez M, Lizotte E, *et al.* Induced Brugada-type electrocardiogram, a sign for imminent malignant arrhythmias. *Circulation.* 2008;117:1890-1893.
104. Sangawa M, Morita H, Nakatsu T, *et al.* Abnormal transmural repolarization process in patients with Brugada syndrome. *Heart Rhythm.* 2009;6:1163-1169.
105. Kusano KF, Taniyama M, Nakamura K, *et al.* Atrial fibrillation in patients with Brugada syndrome relationships of gene mutation, electrophysiology, and clinical backgrounds. *J Am Coll Cardiol.* 2008;51:1169-1175.
106. Ikeda T, Sakurada H, Sakabe K, *et al.* Assessment of noninvasive markers in identifying patients at risk in the Brugada syndrome: insight into risk stratification. *J Am Coll Cardiol.* 2001;37:1628-1634.
107. Doi A, Takagi M, Maeda K, *et al.* Conduction delay in right ventricle as a marker for identifying high-risk patients with Brugada syndrome. *J Cardiovasc Electrophysiol.* 2010;21:688-696.
108. Coronel R, Casini S, Koopmann TT, *et al.* Right ventricular fibrosis and conduction delay in a patient with clinical signs of Brugada syndrome: a combined electrophysiological, genetic, histopathologic, and computational study. *Circulation.* 2005;112:2769-2777.
109. Hayashi H, Sumiyoshi M, Yasuda M, *et al.* Prevalence of the Brugada-type electrocardiogram and incidence of Brugada syndrome in patients with sick sinus syndrome. *Circ J.* 2010;74:271-277.
110. Morita H, Kusano KF, Miura D, *et al.* Fragmented QRS as a marker of conduction abnormality and a predictor of prognosis of Brugada syndrome. *Circulation.* 2008;118:1697-1704.

111. Das MK, Zipes DP. Fragmented QRS: a predictor of mortality and sudden cardiac death. *Heart Rhythm*. 2009;6:S8-14.
112. Das MK, El Masry H. Fragmented QRS and other depolarization abnormalities as a predictor of mortality and sudden cardiac death. *Curr Opin Cardiol*. 2010;25:59-64.
113. Tigen K, Karaahmet T, Gurel E, *et al*. The utility of fragmented QRS complexes to predict significant intraventricular dyssynchrony in nonischemic dilated cardiomyopathy patients with a narrow QRS interval. *Can J Cardiol*. 2009;25:517-522.
114. Peters S, Trummel M, Koehler B. QRS fragmentation in standard ECG as a diagnostic marker of arrhythmogenic right ventricular dysplasia-cardiomyopathy. *Heart Rhythm*. 2008;5:1417-1421.
115. Homsy M, Alsayed L, Safadi B, *et al*. Fragmented QRS complexes on 12-lead ECG: a marker of cardiac sarcoidosis as detected by gadolinium cardiac magnetic resonance imaging. *Ann Noninvasive Electrocardiol*. 2009;14:319-326.
116. Moss AJ. Fragmented QRS: the new high-risk kid on the block in acquired long QT syndrome. *Heart Rhythm*. 2010;7:1815-1816.
117. Cheema A, Khalid A, Wimmer A, *et al*. Fragmented QRS and mortality risk in patients with left ventricular dysfunction. *Circ Arrhythm Electrophysiol*. 2010;3:339-344.
118. Yuce M, Davutoglu V, Ozbala B, *et al*. Fragmented QRS is predictive of myocardial dysfunction, pulmonary hypertension and severity in mitral stenosis. *Tohoku J Exp Med*. 2010;220:279-283.
119. McIntyre WF, Perez-Riera AR, Femenia F, *et al*. Coexisting early repolarization pattern and Brugada syndrome: recognition of potentially overlapping entities. *J Electrocardiol*. 2012;45:195-198.
120. Calvo D, Florez JP, Valverde I, *et al*. Surveillance after cardiac arrest in patients with Brugada syndrome without an implantable defibrillator: An alarm effect of the previous syncope. *Int J Cardiol*. 2016;218:69-74.
121. Nakagawa K, Nagase S, Morita H, *et al*. Left ventricular epicardial electrogram recordings in idiopathic ventricular fibrillation with inferior and lateral early repolarization. *Heart Rhythm*. 2014;11:314-317.
122. Bigi MA, Aslani A, Shahrzad S. Clinical predictors of atrial fibrillation in Brugada syndrome. *Europace*. 2007;9:947-950.
123. Nam GB, Kim YH, Antzelevitch C. Augmentation of J waves and electrical storms in patients with early repolarization. *N Engl J Med*. 2008;358:2078-2079.

124. Yan GX, Antzelevitch C. Cellular basis for the electrocardiographic J wave. *Circulation*. 1996;93:372-379.
125. Antzelevitch C. Modulation of transmural repolarization. *Ann N Y Acad Sci*. 2005;1047:314-323.
126. Baranchuk A, Nguyen T, Ryu MH, *et al*. Brugada phenocopy: new terminology and proposed classification. *Ann Noninvasive Electrocardiol*. 2012;17:299-314.
127. Anselm DD, Evans JM, Baranchuk A. Brugada phenocopy: A new electrocardiogram phenomenon. *World J Cardiol*. 2014;6:81-86.
128. Anselm DD, Baranchuk A. Brugada Phenocopy in the context of pulmonary embolism. *Int J Cardiol*. 2013;168:560.
129. Anselm DD, Baranchuk A. Brugada phenocopy: redefinition and updated classification. *Am J Cardiol*. 2013;111:453.
130. Recasens L, Merono O, Ribas N. Hyperkalemia mimicking a pattern of Brugada syndrome. *Rev Esp Cardiol (Engl Ed)*. 2013;66:309.
131. Dogan M, Ertem AG, Cimen T, *et al*. Type-1 Brugada-like ECG pattern induced by adrenal crisis. *Herz*. 2015;40:304-306.
132. Mok NS, Tong CK, Yuen HC. Concomitant-acquired Long QT and Brugada syndromes associated with indapamide-induced hypokalemia and hyponatremia. *Pacing Clin Electrophysiol*. 2008;31:772-775.
133. Nayyar S, Nair M. Brugada pattern in toxic myocarditis due to severe aluminum phosphide poisoning. *Pacing Clin Electrophysiol*. 2009;32:e16-17.
134. Kovacic JC, Kuchar DL. Brugada pattern electrocardiographic changes associated with profound electrolyte disturbance. *Pacing Clin Electrophysiol*. 2004;27:1020-1023.
135. Gazzoni GF, Borges AP, Bergoli LC, *et al*. Brugada-like electrocardiographic changes induced by hypokalemia. *Arq Bras Cardiol*. 2013;100:e35-37.
136. Kaneko Y, Nakajima T, Irie T, *et al*. Brugada-type ST-elevation associated with writhing of a reconstructed esophagus. *Intern Med*. 2013;52:2287-2288.
137. Rollin A, Maury P, Guilbeau-Frugier C, *et al*. Transient ST elevation after ketamine intoxication: a new cause of acquired brugada ECG pattern. *J Cardiovasc Electrophysiol*. 2011;22:91-94.
138. Daccarett M, Freih M, Machado C. Acute cannabis intoxication mimicking brugada-like ST segment abnormalities. *Int J Cardiol*. 2007;119:235-236.



139. Awad SF, Barbosa-Barros R, Belem Lde S, *et al.* Brugada phenocopy in a patient with pectus excavatum: systematic review of the ECG manifestations associated with pectus excavatum. *Ann Noninvasive Electrocardiol.* 2013;18:415-420.
140. Ortega-Carnicer J, Benezet J, Ruiz-Lorenzo F, *et al.* Transient Brugada-type electrocardiographic abnormalities in renal failure reversed by dialysis. *Resuscitation.* 2002;55:215-219.
141. Ozeke O, Selcuk MT, Topaloglu S, *et al.* Brugada-like early repolarisation pattern associated with acute pericarditis. *Emerg Med J.* 2006;23:e64.
142. Wang JG, McIntyre WF, Kong W, *et al.* Electrocution-induced Brugada phenocopy. *Int J Cardiol.* 2012;160:e35-37.
143. Tsai CF, Wu DJ, Lin MC, *et al.* A Brugada-pattern electrocardiogram and thyrotoxic periodic paralysis. *Ann Intern Med.* 2010;153:848-849.
144. Genaro NR, Anselm DD, Cervino N, *et al.* Brugada phenocopy clinical reproducibility demonstrated by recurrent hypokalemia. *Ann Noninvasive Electrocardiol.* 2014;19:387-390.
145. Riera AR, Uchida AH, Schapachnik E, *et al.* Propofol infusion syndrome and Brugada syndrome electrocardiographic phenocopy. *Cardiol J.* 2010;17:130-135.
146. Nguyen T, Smythe J, Baranchuk A. Rhabdomyoma of the interventricular septum presenting as a Brugada phenocopy. *Cardiol Young.* 2011;21:591-594.
147. Arce M, Riera AR, Femenia F, *et al.* Brugada electrocardiographic phenocopy in a patient with chronic Chagasic cardiomyopathy. *Cardiol J.* 2010;17:525-527.
148. Kataoka H. Electrocardiographic patterns of the Brugada syndrome in 2 young patients with pectus excavatum. *J Electrocardiol.* 2002;35:169-171.